CHRONOPOTENTIOMETRY IN ACETONITRILE; OXIDATION OF SUBSTITUTED ACETATES AND SUBSTITUTED FERROCENES

Thesis by

Charles Dyer Russell

In Partial Fulfillment of the Requirements

For the Degree of

Doctor of Philosophy

California Institute of Technology

Pasadena, California

1963

ACKNOWLEDGEMENTS

The author wishes to express his gratitude to Professor Fred C. Anson for his encouragement and assistance. A debt of gratitude is also owed many other faculty members and graduate students of the California Institute of Technology, none of whom has ever refused the author assistance or advice when needed.

Financial support by the National Science Foundation, the California Institute of Technology, and the Sloan Foundation is certainly appreciated.

Material contribution has been made to this thesis in the form of chromatographic analyses performed by R. G. Rinker and Y. L. Wang for Part II, and computer programming by J. M. Peterson and R. S. Deverill for the Appendix. D. Hall has contributed much to Part III both in the experimental work and in its interpretation.

ABSTRACT

Chronopotentiometry was used to study electrode reactions in acetonitrile solutions. Evidence is presented for the formation of an oxide film on platinum electrodes in acetonitrile by reaction with traces of moisture. Oxygen dissolved in acetonitrile solutions of tetraethylammonium perchlorate is reduced to peroxide at the platinum electrode, although it is not reduced in solutions of alkali perchlorates. The potential-limiting background reactions in tetraethylammonium perchlorate solutions were investigated by current-reverse chronopotentiometry.

Oxidation of acetate ion in acetonitrile gave 91±6% current yield of carbon dioxide and 77±3% ethane. Acetic acid does not react below the anodic background potential. Oxidation of substituted acetates was studied chronopotentiometrically but traces of moisture in the solution were found to react simultaneously at the electrode and seriously interfere. Water is not oxidized below the background potential in the absence of carboxylate ion.

Oxidation potentials for a series of substituted ferrocenes were measured chronopotentiometrically and evidence was found for a new type of neighboring-group interaction between the iron in ferrocinium ion and oxygen, nitrogen, or halogen in the ring position. The same substitutuents did not interact in the alpha position.

A computer program was written for the calculation of kinetic data from totally irreversible chronopotentiometric waves and used to evaluate graphical methods previously proposed. New graphical and algebraic methods were also evaluated. These methods were applied to the determination of rate constants for the reduction of iodate ion at mercury in aqueous sodium hydroxide solution.

TABLE OF CONTENTS

PART I

CHRONOPOTENTIOMETRY IN ACETONITRILE

General Introduction

The first chronopotentiometric studies in acetonitrile were the analytical determination of anthracene by Voorhies and Furman (1) and Geske's studies of the oxidation of tropilidene and tetraphenylborate (2). These were followed by the work of Kuwana, Bublitz and Hoh (3) and of Hoh, McEwen and Kleinberg (4) on substituent effects in the oxidation of metallocene compounds.

Part I of this thesis deals with three reactions of general interest in acetonitrile electrochemistry, dealing with solutions which contain only supporting electrolyte and dissolved atmospheric oxygen: oxidation of platinum electrode surfaces, reduction of dissolved oxygen, and the potential-limiting cathodic and anodic reactions. Consideration was restricted to a single electrode material, platinum, and a single supporting electrolyte, tetraethylammonium perchlorate. Part II deals with the chronopotentiometric waves for the oxidation of substituted acetates. Part III is an extension and revision of the cited work on the oxidation of metallocenes. An appendix discusses methods for the interpretation of totally irreversible chronopotentiometric waves in the light of results from a least-squares treatment by digital computer.

Further introductory information is given in each section, pertaining to the topic at hand. General reviews of chronopotentiometry are given by Delahay (5) and by Rouse (6).

Experimental

Reagents. Acetonitrile. Matheson, Coleman and Bell Practical Grade acetonitrile was distilled three times from phosphorus pentoxide and a final time from Mallinckrodt anhydrous potassium carbonate. Its acetic acid content was less than 0.0003 M (determined by titration with aqueous NaOH) and its water content was roughly 0.03 M (as determined by the infrared absorption at 1.9 microns).

Tetraethylammonium perchlorate. Tetraethylammonium perchlorate was prepared by the method of Kolthoff and Coetzee (7) and recrystallized from water five times.

Nitrogen. Linde High Purity Dry Nitrogen was used without further purification.

Electrolysis cell. The electrolysis cell is illustrated in Figure I-1. Working and auxiliary electrode compartments were separated by a fine porosity sintered-glass disk. The shape of the working electrode compartment was designed to promote linear diffusion and current flow perpendicular to the electrode surface and consequently a uniform current density over the surface (8). The underside of the working electrode was sealed over with glass and connection was made by a spot-welded platinum lead wire passing through the glass. The lead wire was insulated by a length of Teflon spaghetti sealed to the glass with epoxy resin. The reference electrode was connected with the working electrode compartment in a manner which minimized ohmic drop. The electrode area was calculated as 0.529 cm^2 from the transition time for the reduction of 0.004 M $K_3 Fe(CN)_6$, 1.00 M KCl in water (3). The potentiostatically determined value of $7.63 \times 10^{-6} cm^2/sec$ for the diffusion coefficient of ferricyanide ion which

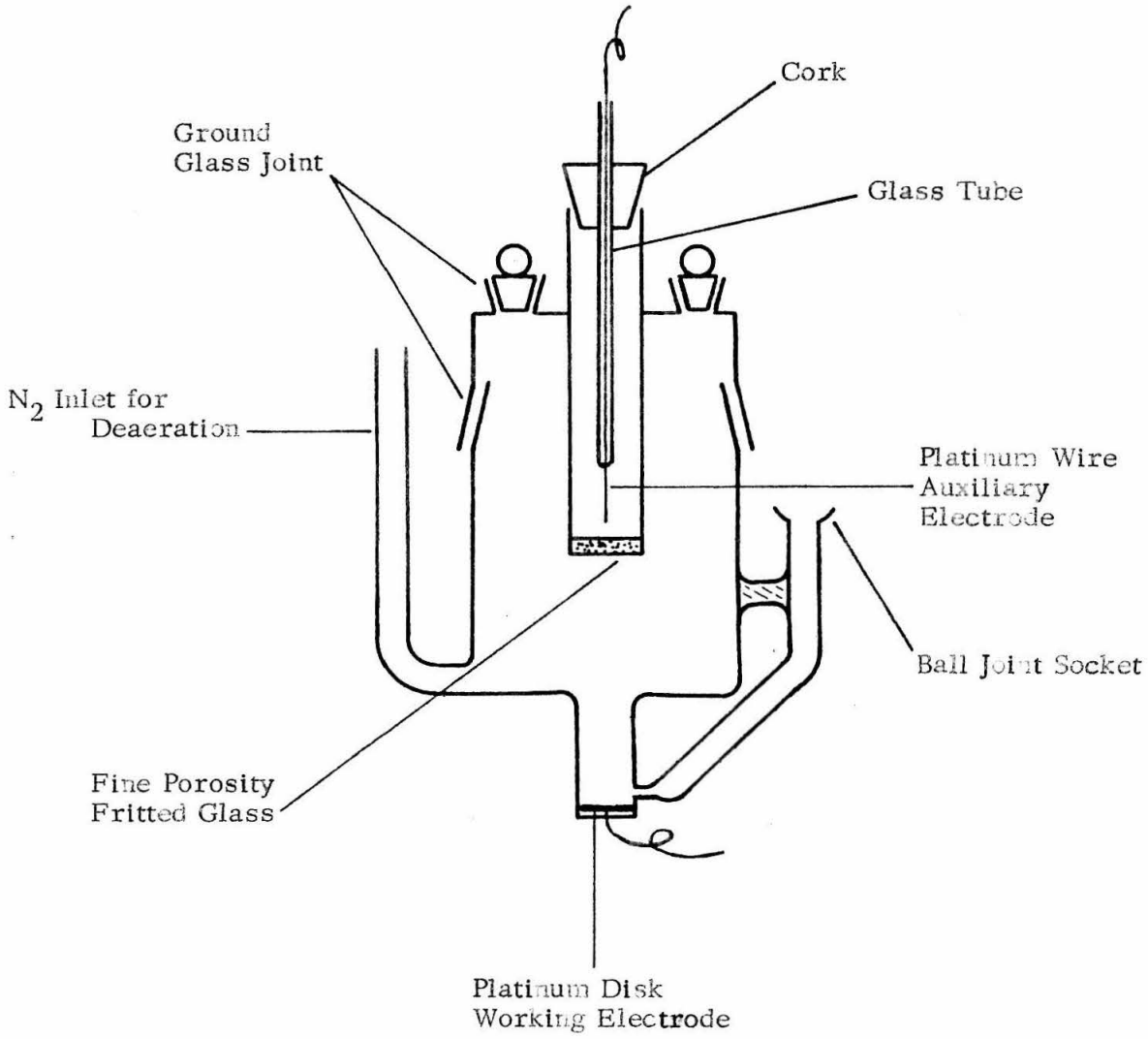

FIG. I-1

CHRONOPOTENTIOMETRIC CELL

von Stackelberg, Pilgram, and Toome (9) reported for solutions of this composition was used in the calculation.

Reference electrodes. Two reference electrodes were used, both of which are illustrated in Figure I-2. The Ag/0.01 M $AgNO_3$, 0.2 M $(C_2H_5)_4NClO_4$ in CH_3CN reference electrode was used for most measurements. All voltages are given with reference to this electrode unless otherwise specified. The silver-silver ion couple has been recommended by a number of authors as a primary potential reference in acetonitrile (10, 11, 12). Tetraethylammonium perchlorate was added to eliminate the liquid-junction potential between the reference electrode and the solution in the cell; this will have affected the electrode potential somewhat but it ensured reproducibility of the potential measurements. Leakage from the silver nitrate reference electrode was very low, amounting to no more than a half drop per hour. It was cleaned, dried and refilled with fresh silver nitrate solution each day.

The Hg/Hg_2SO_4, K_2SO_4 (sat. aq.) electrode did not function as well in acetonitrile solutions, its potential drifting about ± 0.02 V. It was used to compare potentials for oxide film formation on the electrode surface in water and in acetonitrile.

Electronic circuitry. Oscillographic measurements were made using the transistor current source of Figure I-3. Its circuit was suggested by Professor C. A. Mead of the California Institute of Technology. It delivered a preset controlled current of 0 to 50 ma in a pulse of preset duration, followed by a second pulse of independently adjusted current (0 to 50 ma) and duration with opposite polarity. The duration of the pulses was limited only by the size of the variable capacitors used; 600 μf was necessary for a 10-sec. pulse. The rise time was

REFERENCE ELECTRODES

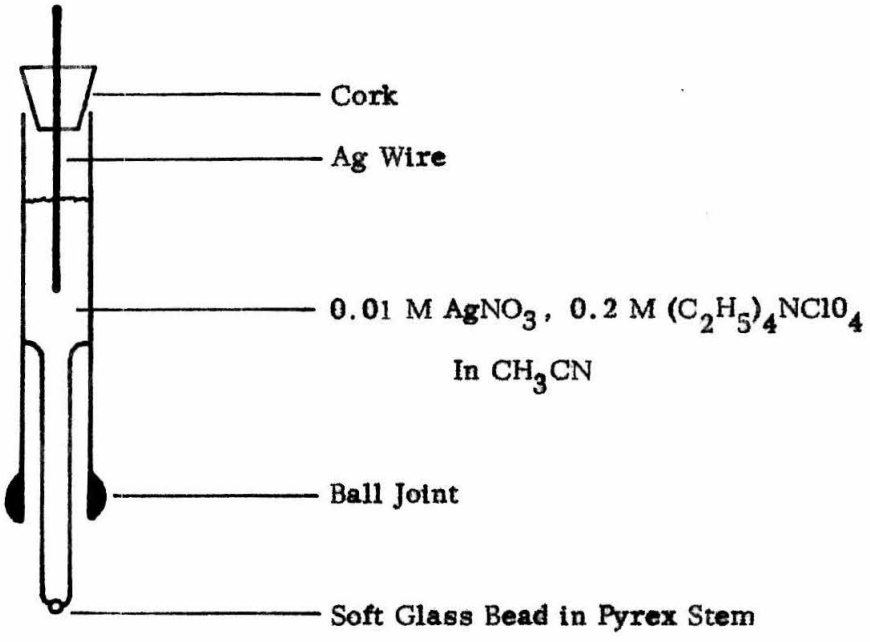

SILVER NITRATE REFERENCE ELECTRODE

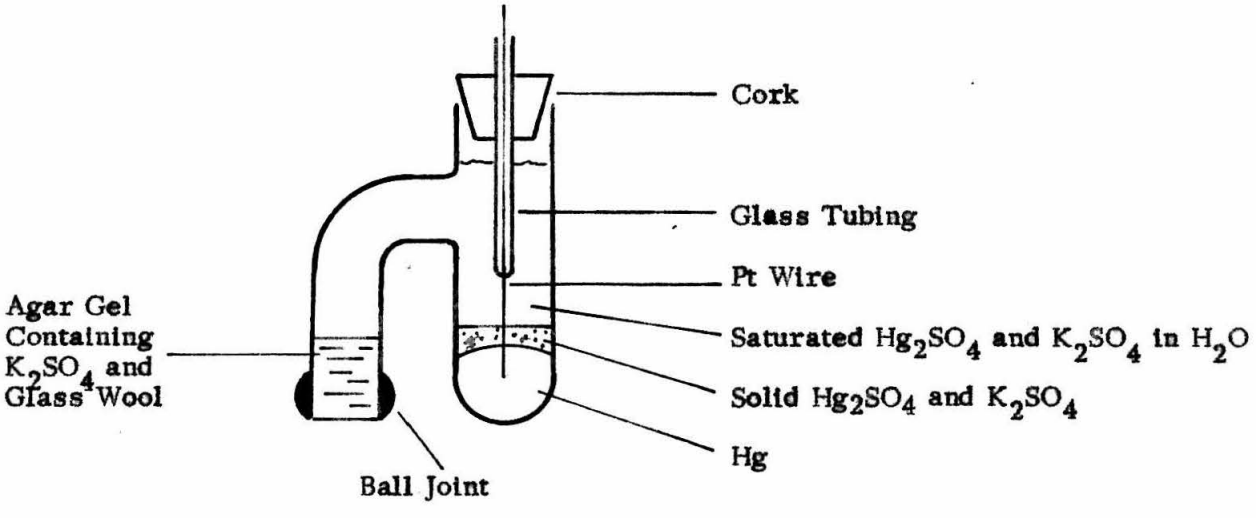

MERCUROUS SULFATE REFERENCE ELECTRODE

FIG. I-2

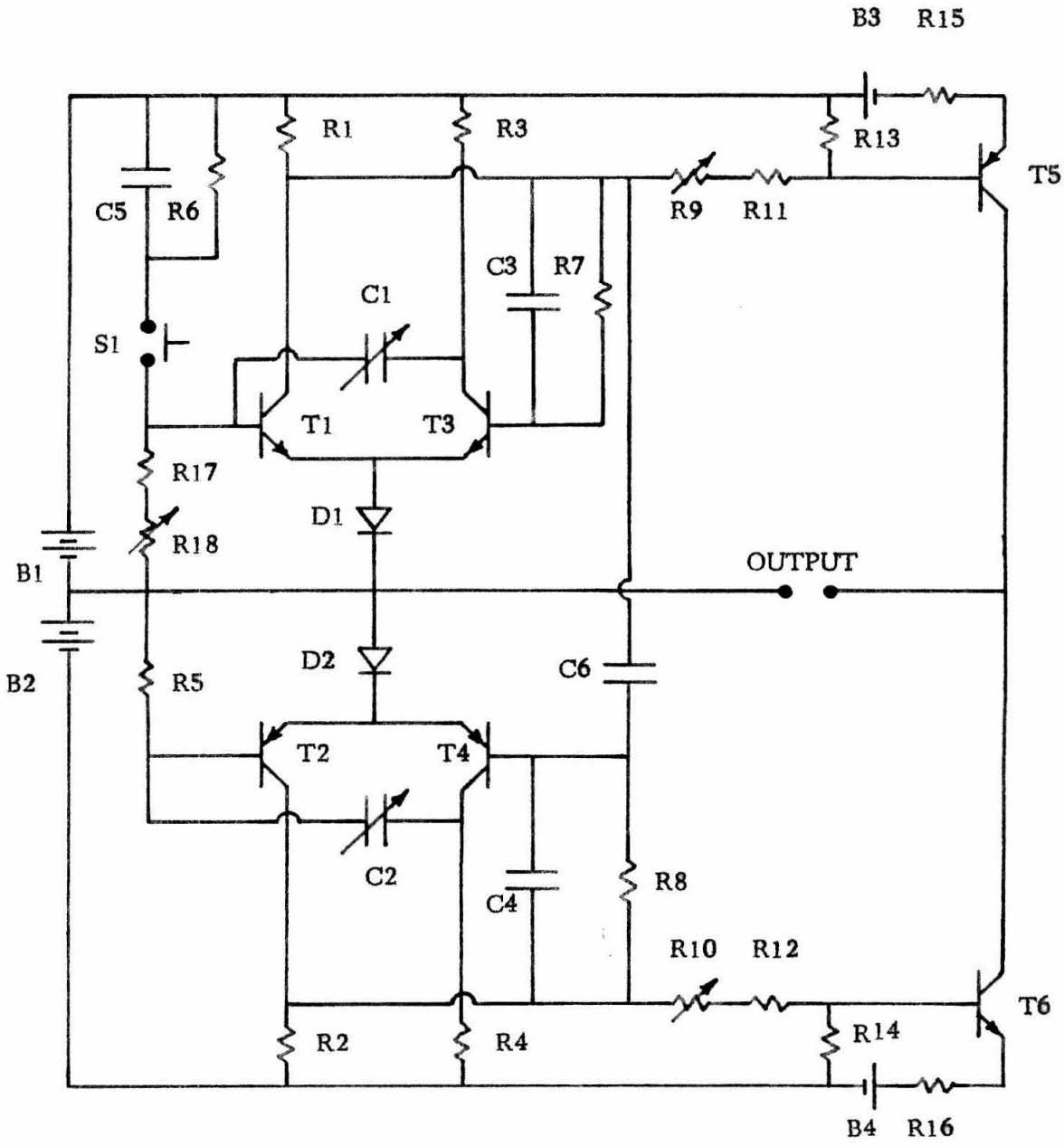

FIG. I-3

CONTROLLED CURRENT SOURCE

TABLE I-1

COMPONENTS FOR CONTROLLED CURRENT SOURCE

Batteries	
B1, B2	22-1/2 V
B3, B4	1.34 V (mercury cell)
Capacitors	
C1, C2	External decade capacitor (see text)
C3, C4	50 μμf
C5, C6	350 μμf
Diodes	
D1, D2	1N1084 (silicon)
Resistors	
R1-R5	4.7K
R6	22 M
R7, R8	22 K
R9, R10	10 K variable
R11-R14	1 K
R15, R16	100 Ω
R17	500 Ω
R18	5 K variable
Switches	
S1	Pushbutton
Transistors	
T1-T4	Germanium switching transistors. Obsolete models donated by the International Business Machines Corporation were used.
T5	2N1131
T6	2N342

less than 10 microseconds and the leakage current was less than 1/50 microamp. The current was controlled to within 2% over the duration of a pulse and over a range of output voltages from 0 to 10 V; at current outputs below 10 ma the current was controlled to within 1%. It should be pointed out that both the rise time and the current control could be improved by making some substitutions among the transistors, although this was unnecessary for the present study.

A Tektronix Type 531A oscilloscope with Type D vertical amplifier or a Type 536 oscilloscope with Type D vertical amplifier and Type T Time-Base Generator was used with a Polaroid Land camera to record the oscillograms.

A Heathkit Model PS-3 variable power supply was used in series with a variable resistor as the current source for the remaining measurements. The chronopotentiograms were recorded on a Moseley Model 3S Autograf X-Y-time recorder connected to the reference electrode through a follower amplifier of the DeFord type (13) constructed with George A. Philbrick Company plug-in amplifiers.

Procedure: All measurements were performed at $25.0 \pm 0.1^{\circ}$ C. The ohmic drop between working and reference electrodes was measured using a method described by Anson (14) and due correction made to the measured potentials. The ohmic drop corresponded to a 40-ohm transfer coefficient (ohmic drop/cell current) when the cell was filled with 0.2M Et_4NClO_4 in CH_3CN.

Oxidation of Platinum Electrode Surfaces

It has been well established that platinum surfaces acquire a film of platinum oxides or chemisorbed oxygen upon strong chemical or electrochemical oxidizing treatment. For brevity this film will be called the "oxide film" without any

implication regarding the nature of the platinum-oxygen bond. The oxide film formed by anodizing a platinum electrode in aqueous solution to the point of oxygen evolution or by treating the electrode with such chemical oxidants as aqueous ceric ion or divalent silver is approximately a monolayer thick (15, 16, 17). Chronopotentiometric waves are observed both for its formation and its reduction, but the wave for its formation is poorly defined with no sharp inflection marking the transition time. Both waves are very irreversible.

A similar behavior of the platinum electrode might be expected in nonaqueous solution if traces of moisture are present — and very little moisture is necessary to form a monolayer oxide film. This is found to be the case in acetonitrile. Popov and Geske (18) have observed the formation of oxide films on rotating platinum electrodes in "anhydrous" acetonitrile. Their results are confirmed by the chronopotentiometric measurements reported here. Conway and Dzieciuch (19) discovered that an anodic film was formed on platinum electrodes in solutions of potassium formate in formic acid and of potassium trifluoroacetate in trifluoroacetic acid. They ascribed the film to the formation of platinum carboxylates on the electrode surface, but the evidence they present does not rule out the possibility that this is an oxide film.

Figure I-4 shows chronopotentiometric waves for a platinum electrode immersed in acetonitrile containing 0.2 M tetraethylammonium perchlorate and about 0.03 M H_2O. Curve 1 corresponds to the oxidation of the electrode surface and Curve 2, a repetition using the already oxidized electrode, shows little additional oxidation. Curve 3 shows the reduction, at one fourth the current density, of the oxide film formed in Curve 1. Curve 4, using the electrode reduced by recording Curve 3, shows that the oxide film has been completely

OXIDE FILM WAVES

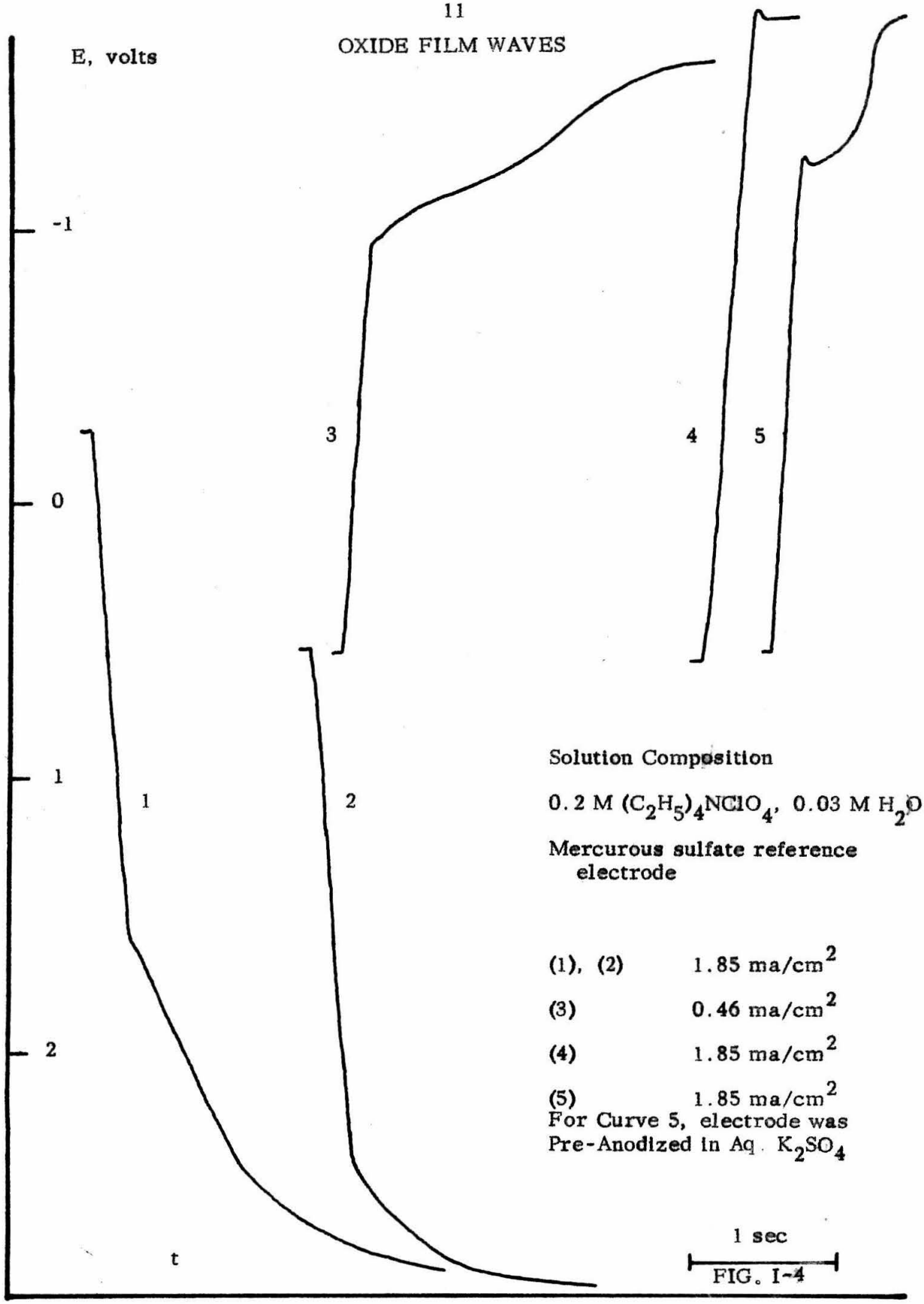

FIG. I-4

stripped from the surface. This behavior closely parallels that of a platinum electrode in aqueous solution (fig. I-5) and results from the reaction of the electrode with water present in the acetonitrile.

As may be seen from Figure I-4, the charge consumed in the anodic wave (2 mcoul/cm^2) is appreciably greater than that consumed in the cathodic wave (0.8 mcoul/cm^2). This same phenomenon has been observed in aqueous solution and has been attributed to the oxidation of water to oxygen concurrently with the oxidation of the electrode surface (17). An alternative explanation (16) is that the oxide film is reduced at least partly to hydrogen peroxide instead of water, causing the current consumed to be as little as half that used in the anodic process. This agrees reasonably with the charge magnitudes observed. No cathodic wave was observed for a solution of hydrogen peroxide in acetonitrile containing tetraethylammonium perchlorate supporting electrolyte, so that hydrogen peroxide would not be reduced if once formed. It does not seem likely that an oxygen-oxygen bond would be formed in the reduction of a normal metallic oxide so that the question of whether water or hydrogen peroxide is produced is bound up with the question of whether the oxygen present on the electrode surface retains the oxygen-oxygen bond. No means of distinguishing these two possibilities has yet been devised, although it may be possible to detect hydrogen peroxide generated at the electrode surface by current-reverse chronopotentiometry.

The potential for oxidation of the platinum surface is +0.5 V. vs. the Hg/Hg_2SO_4, K_2SO_4 (sat. aqueous) reference electrode (SMS) in aqueous K_2SO_4 and +2.4 V. vs. SMS in acetonitrile containing 0.2 M tetraethylammonium perchlorate. The potential for the reduction of the oxide film is -0.8 V. vs. SMS in aqueous K_2SO_4 and -1.3 V. vs. SMS in acetonitrile. A higher overpotential is

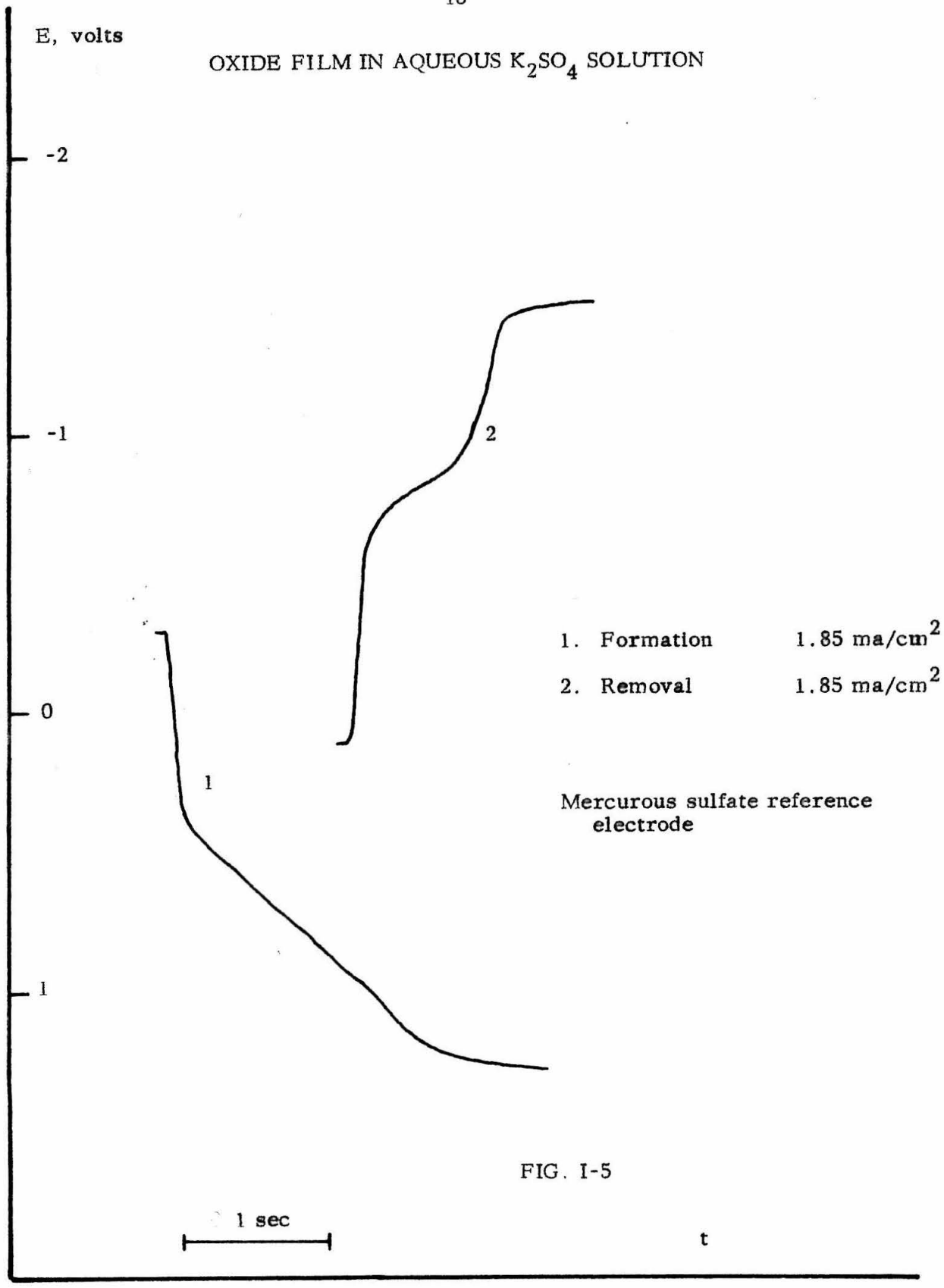
E, volts
OXIDE FILM IN AQUEOUS K_2SO_4 SOLUTION
-2
-1
0
1
2
1
1. Formation 1.85 ma/cm^2
2. Removal 1.85 ma/cm^2
Mercurous sulfate reference electrode
1 sec
t

FIG. I-5

expected for the formation and reduction of the film in acetonitrile; water participates in the electrode reaction as a proton or oxide donor and its concentration is far less in the acetonitrile solution than in aqueous solution. Furthermore, the apparent irreversibility of the reaction is increased by the fact that the solution is unbuffered, and since a greater range of hydrogen ion activity is accessible in acetonitrile (autoprotolysis constant $10^{-19.5}$) (20) the effect should be more pronounced.

The amount of oxide reduced in Curve 3 of Figure I-4 corresponds to 0.8 mcoul/cm^2; in Curve 2 of Figure I-5, 1.6 mcoul/cm^2. Laitinen and Enke (17) have estimated the charge corresponding to a monolayer to be 0.5 mcoul/cm^2 and report gas-absorption measurements on a platinum surface which indicate little difference (12%) between its geometric area and its true area. The oxide film can thus be regarded at least approximately as a monolayer. In acetonitrile solution, unlike aqueous solution, the electrode is not completely oxidized by raising the electrode briefly to the background potential, as attested by the figures for the charge consumed in the cathodic wave. Prolonged anodization increased the amount of oxide.

For purposes of comparison a platinum electrode was oxidized by anodic treatment in aqueous potassium sulfate solution, oven-dried at 130°, and transferred to a 0.2 M solution of tetraethylammonium perchlorate in acetonitrile. The cathodic stripping curve is shown as Curve 5 in Figure I-4. It presents substantially the same appearance as the curve for the reduction of the oxide film formed in acetonitrile except that it is somewhat longer in accordance with the above discussion. The charge consumed was 1.2 mcoul/cm^2. Some loss of oxide occurred while drying. It was noted in the course of this experiment that oven-drying

the electrode at 130° C. is sufficient in itself to cause the formation of a small amount of oxide on the electrode surface, presumably by direct reaction with atmospheric oxygen. If the electrode is oxidized and then freshly reduced before drying the amount of oxide formed is appreciably greater.

Figure I-6 shows stripping curves for an electrode which has been oxidized in acetonitrile at various controlled potentials. It is seen that no distinct potential exists at which the oxide forms, but its formation begins at about + 1.4 V vs. SMS. An anodic wave was obtained by reversing the current before the transition time (fig. I-7). This probably represents the re-oxidation of the electrode surface in the presence of hydroxyl ion generated in the cathodic process.

Reduction of Dissolved Oxygen.

We found that dissolved oxygen exhibits a well-formed one-step cathodic chronopotentiometric wave at a platinum electrode in acetonitrile solutions of tetraethylammonium perchlorate. Popov and Geske (18) reported, however, that dissolved oxygen is not reduced at the rotating platinum electrode in lithium perchlorate solution. Coetzee and Kolthoff (7) studied the reduction of oxygen at the dropping-mercury electrode in acetonitrile solutions of sodium perchlorate, potassium thiocyanate, and tetraethylammonium perchlorate. They found that reduction occurred in two steps, presumably successive reduction to hydrogen peroxide and water. The half-wave potential and diffusion current for the second wave were sharply influenced by the concentration and composition of the supporting electrolyte.

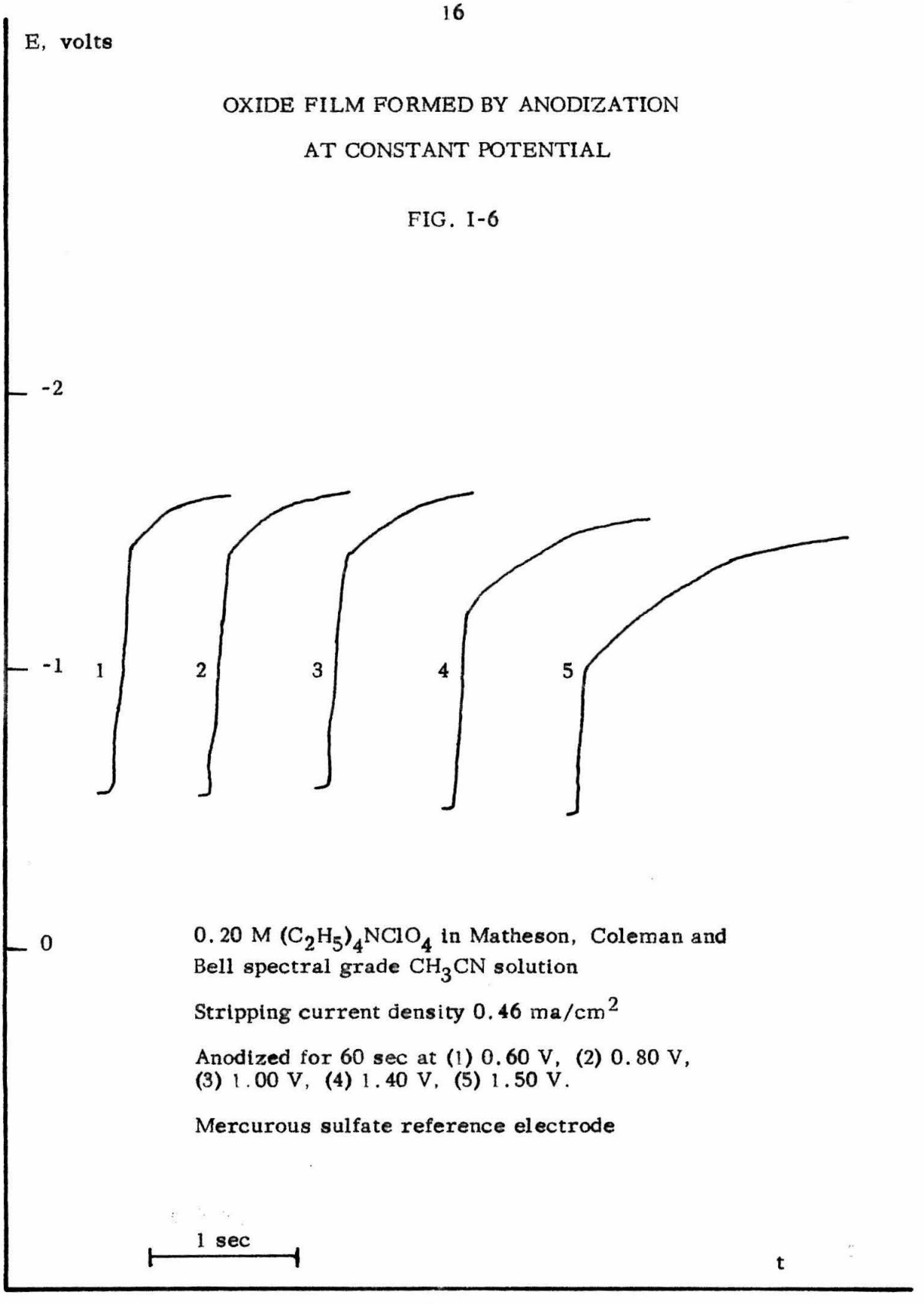

OXIDE FILM FORMED BY ANODIZATION

AT CONSTANT POTENTIAL

FIG. I-6

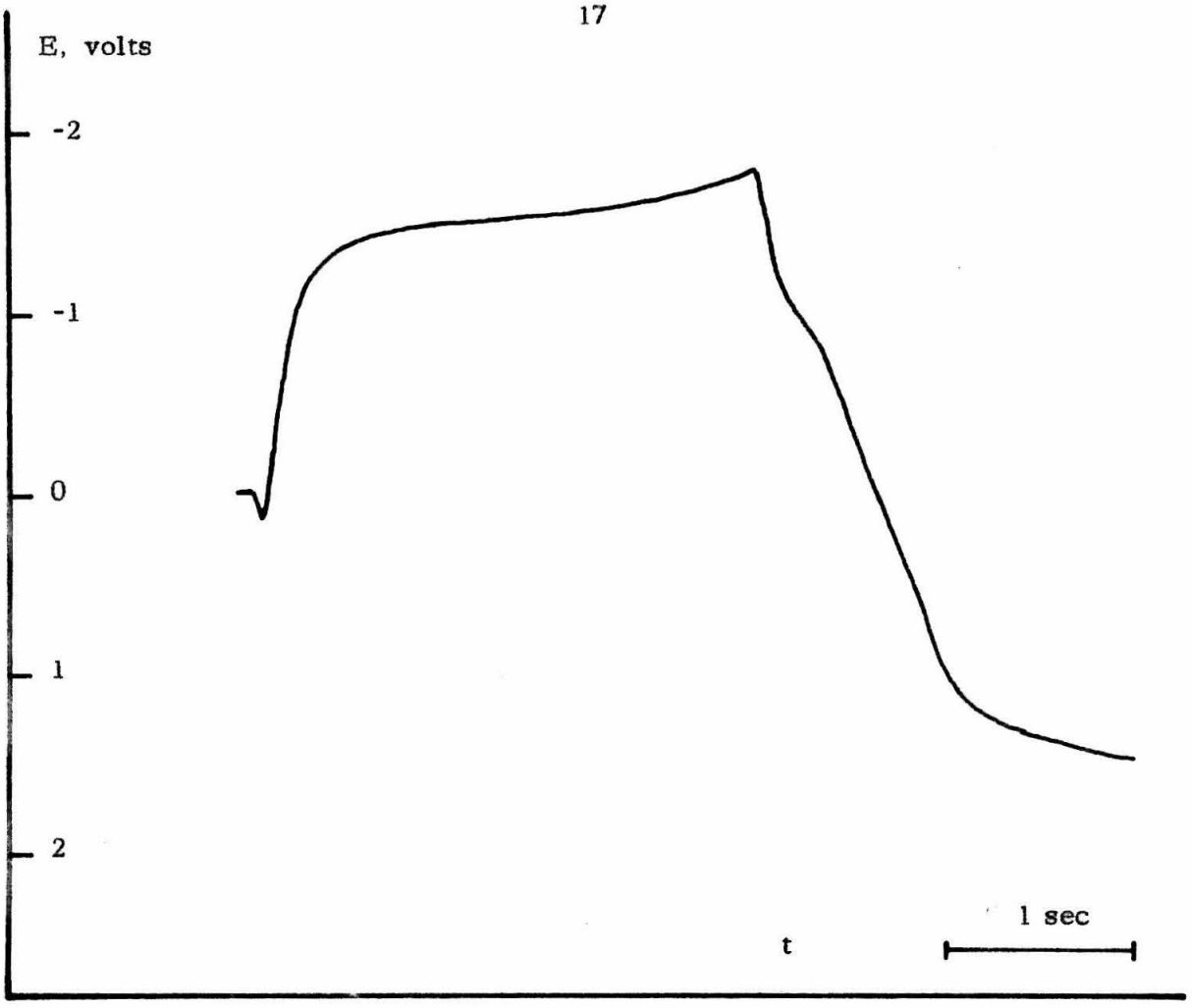

Solution Composition 0.20 M $(C_2H_5)_4NClO_4$, 0.06 M H_2O

Current Density 0.47 ma/cm^2

CURRENT-REVERSE CHRONOPOTENTIOGRAM

FOR OXIDE FILM REDUCTION

FIG. I-7

A typical reduction wave for dissolved oxygen in a 0.2 M solution of tetraethylammonium perchlorate in acetonitrile is reproduced in Figure I-8. Data for a series of measurements are given in table I-2.

TABLE I-2

OXYGEN REDUCTION WAVE

i	τ	$i\tau^{1/2}$
ma/cm^2	sec	$\frac{ma\text{-}sec^{1/2}}{cm^2}$
.469	5.85	1.13
.985	1.32	1.13
2.3	0.22	1.1
4.5	0.060	1.2
9.1	0.015	1.2

These data apply to an electrode which has been anodized and cathodized several times at the background potentials, the last treatment before the measurement being cathodic. The oxygen reduction wave was sensitive to the electrode history, as it is in aqueous solution (21, 22). The above electrode pretreatment gave reproducible transition times and a chronopotentiometric wave of reproducible appearance, but its quarter-wave potential varied by several tenths of a volt. The constancy of $i\tau^{1/2}$ over a 400-fold range of transition times proves that the reduction is a typical diffusion-controlled process.

Current-reverse chronopotentiometry shows the formation of an oxidizable product in the reduction of oxygen. A typical chronopotentiogram is shown in Figure I-8 (curve 2). The transition time for the reverse wave is one third the duration of cathodic current, as predicted for an anodic reaction involving the same number of electrons as the cathodic reaction. Data are given in table I-3 for a wide range of current density and transition time. The potential of the reverse wave was not very reproducible and $E_{.22}$ varied from -1.0 to -0.4 V. The reverse wave was always well defined, though, with a sharp inflection at the transition time.

TABLE I-3

REVERSE-CURRENT WAVE FOR OXYGEN REDUCTION

i	t_1	τ_2	$\frac{\tau_2}{t_1}$
ma	Cathodic sec	Anodic sec	
.248	5.80	1.71	.291
.526	1.37	0.43	.31
1.2	0.24	0.07^5	.32
2.4	.050	.013	.38
4.8	$.012^5$	$.003^5$	.36

The most probable reaction for the reduction of oxygen is

$$O_2 + H_2O + 2e^- = HO_2^- + OH^- \qquad (1)$$

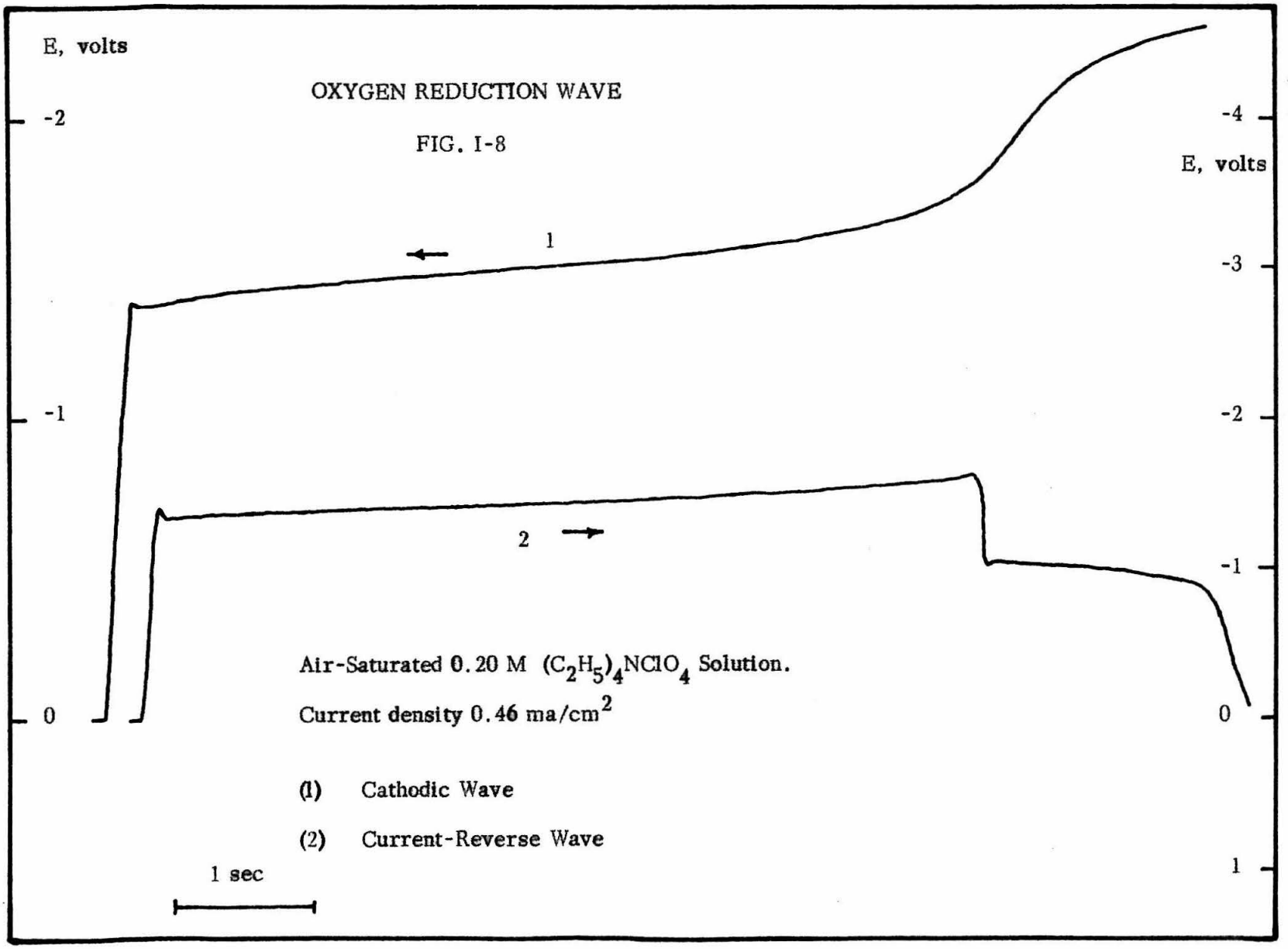
E, volts
OXYGEN REDUCTION WAVE
FIG. I-8
-2
-1
0
-4
-3
-2
-1
0
E, volts
1
2
Air-Saturated 0.20 M $(C_2H_5)_4NClO_4$ Solution.
Current density 0.46 ma/cm^2
(1) Cathodic Wave
(2) Current-Reverse Wave
1 sec
1

involving the traces of water present. This reaction is simply reversed in the reverse wave. If 30% H_2O_2 is added to the deaerated solution, no reduction wave can be detected but an anodic wave appears at about +1.5 V. This shows that hydrogen peroxide, if formed, would not be further reduced. In the usual reactions of molecular oxygen the initial step generally leads to the formation of peroxides. The discrepancy between the potentials of the anodic waves can be accounted for by the fact that in the reverse wave for oxygen reduction, OH^- ion is present, while in the wave for simple oxidation of H_2O_2, H^+ is present as a reaction product. The oxidation potential of H_2O_2 at platinum electrodes in aqueous solution is known to be pH-dependent (23).

An alternative explanation for the reverse-current wave is the oxidation of hydroxyl ion generated by the reaction

$$O_2 + 2H_2O + 4e^- = 4OH^- \qquad (2)$$

The potential at which the oxidation takes place appears too low to correspond to the oxidation of hydroxyl ion, though, being as much as 0.8 V more negative than the potential (-0.2 V, vide infra) for the reduction of hydrogen ion. This seems excessive even if the abnormally high activity of hydroxyl ion in acetonitrile is taken into account. (Kolthoff and Coetzee (7) found the potential for oxidizing mercury metal in the presence of hydroxyl ion to be 0.9 V more negative in acetonitrile than in water.) The difference between the equilibrium potentials for the two reactions must be larger than 0.8 V, probably by an appreciable amount, because of the overvoltages involved. (The irreproducibility mentioned above of the potential for the oxidation of the product of oxygen reduction indicates a significant overvoltage, since a reversible electrode process must occur at a reproducible potential.) This explanation of the reverse wave thus leads to the

unacceptable conclusion that the H_2/H^+ couple is far more oxidizing than the O_2/OH^- couple in acetonitrile solution.

The product formed by the reduction of oxygen at platinum electrodes in aqueous medium has not been established and the reduction mechanism is disputed (21, 22).

It is interesting that Popov and Geske (18) detected no reduction wave for oxygen at the rotating platinum electrode in an acetonitrile solution of lithium perchlorate. The cathodic background potential they reported (-3.3 V) is two volts more negative than the reduction potential for oxygen in tetraethylammonium perchlorate solution, so the effect of the supporting electrolyte is a drastic one. We have also found that oxygen is not reduced at platinum in sodium perchlorate solutions. The explanation probably rests in an augmented electric field at the electrode surface resulting from adsorption of tetraethylammonium ions on the negatively charged surface. Such double-layer effects have been studied extensively the past few years (24, 25).

Anodic Background Reaction

The anodic background reaction at a platinum electrode in acetonitrile solutions containing perchlorate supporting electrolyte was formulated by Schmidt and Noack (26) as follows:

$$ClO_4^- = ClO_4\cdot + e^- \quad (1)$$

$$ClO_4\cdot + CH_3CN = HClO_4 + \cdot CH_2CN \quad (2)$$

$$2\cdot CH_2CN = NCCH_2CH_2CN \quad (3)$$

Quantitative yield (99-101%) of acid was determined by potentiometric titration with diethylamine and succinonitrile was detected in the electrolysis mixture by conversion to pyrrole. No yield was given for the pyrrole. Billon (12) also reported a quantitative yield (94-98.5%) of acid, and was able to titrate diphenylguanidine coulometrically to an indicator endpoint in anhydrous acetonitrile containing sodium perchlorate as supporting electrolyte. Billon (27) found the current yield of succinonitrile less than 0.1% by vapor-phase chromatography, though. Unidentified peaks occurred just after that for acetonitrile. Streuli has reported the anodic coulometric titration of nitrogen bases in acetonitrile containing lithium perchlorate supporting electrolyte and 0.15 M water (28). He assumed that hydrogen ion was generated at the anode by oxidation of the water and used a glass electrode to determine the endpoint. Maki and Geske (29) studied the anodic background reaction for a solution of lithium perchlorate in anhydrous acetonitrile by performing the electrolysis in the cavity of an electron spin resonance spectrometer. They obtained a spectrum which was tentatively attributed to the perchlorate free radical. Their results were confirmed by Billon (27).

Figure I-9 shows a typical current-reverse chronopotentiogram for the anodic background reaction products in 0.2 M tetraethylammonium perchlorate solution. A long wave at -0.2 V is followed by two much shorter ill-defined waves at about -0.8 V and -1.3 V. Perchloric acid was reduced at -0.2 V in this solution and so the long wave can best be interpreted as representing the reduction of hydrogen ion. This agrees with the reports of hydrogen ion formation at the anode which are listed above. However, the yield of H^+ is less than quantitative. If a constant current efficiency η is assumed for hydrogen ion formation during

FIG. I-9

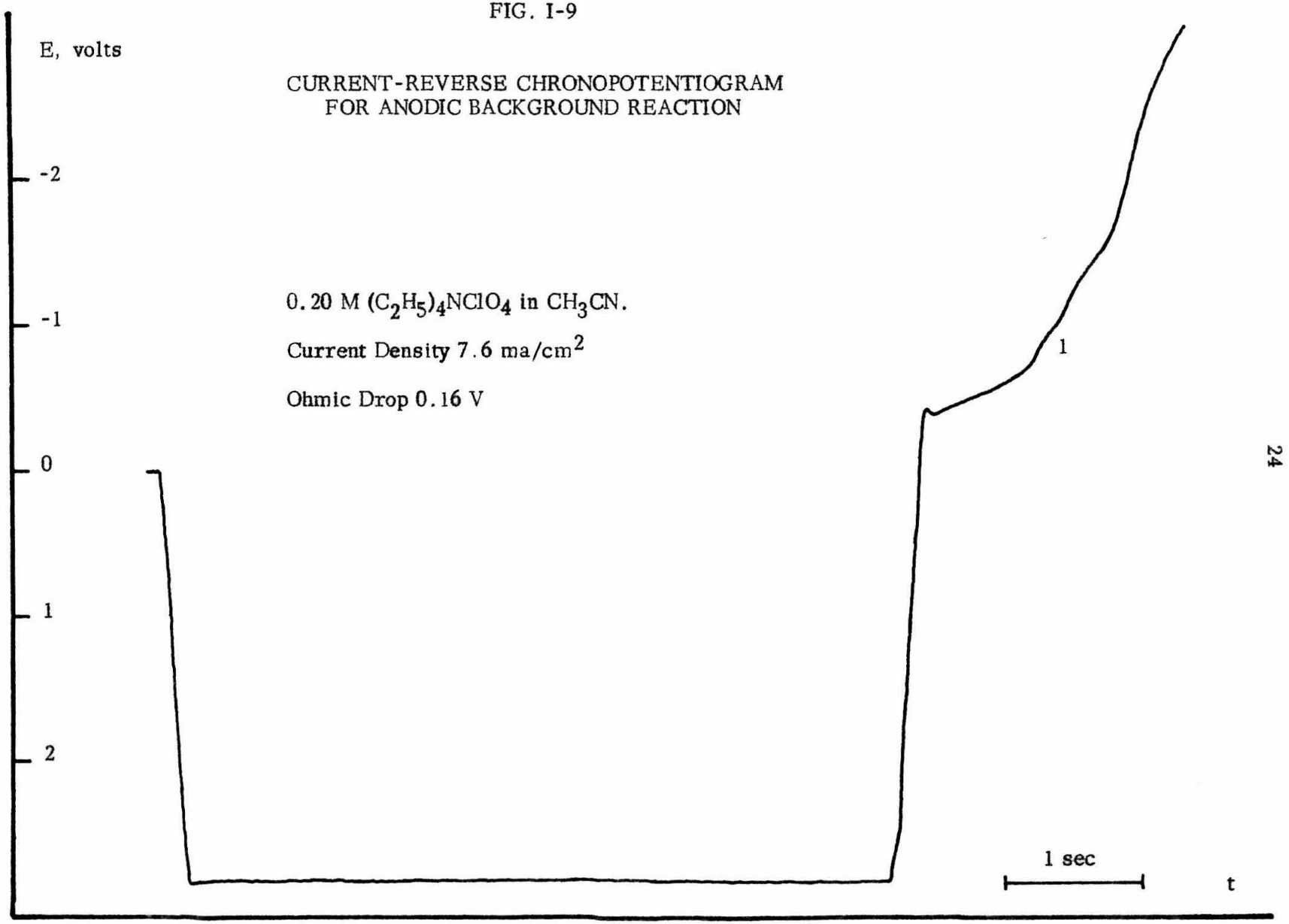
E, volts
CURRENT-REVERSE CHRONOPOTENTIOGRAM
FOR ANODIC BACKGROUND REACTION
-2
-1
0
1
2
0.20 M $(C_2H_5)_4NClO_4$ in CH_3CN.
Current Density 7.6 ma/cm^2
Ohmic Drop 0.16 V
1
1 sec
t

the interval of anodic current, η may be calculated from the cathodic transition time τ_2 and the duration of the anodic current t_1, using a modification of Delahay and Berzins' equation for the transition time in reverse-current chronopotentiometry (30):

$$\frac{1}{\eta} = \left(\frac{t_1}{\tau_2} + 1 \right)^{\frac{1}{2}} - 1 \qquad (4)$$

In the case of Figure I-9, $\eta = 0.66$. For quantitative generation of hydrogen ion $\frac{\tau_2}{t_1} = \frac{1}{3}$ according to theory, whereas in this case $\frac{\tau_2}{t_1} = \frac{1}{5.8}$. At higher current densities η tended to decrease. This result is in conflict with the reports of quantitative acid yield which were described above.

The ESR data of Maki and Geske (29) and of Billon (27) indicate that reaction 1 occurs to some extent, at least. Billon concluded from his ESR measurements that the "perchlorate radical" had a lifetime on the order of a minute. From the data of Maki and Geske one can deduce that the free radical they observed had at least a 2-sec lifetime, so short only if it were generated with 100% current efficiency. It is unlikely that the perchlorate radical should be so stable and the observed spectrum is more probably that of chlorine dioxide. The g-factor and coupling constant reported by Maki and Geske agree with those since reported by Cole (31) for chlorine dioxide. Nevertheless, the formation of oxides of chlorine suggests strongly the occurrence of reaction 1. The perchlorate radicals so produced could react with each other to form oxygen and oxides of chlorine.

In connection with reaction 3 of the Schmidt-Noack scheme, cognizance must be taken of the recent discovery that α-cyano free radicals in solution couple to form ketenimine to about the same extent as they couple to form dinitrile (32, 33, 34).

$$2 \quad \cdot CH_2CN \quad = \quad CH_2 = C = N - CH_2CN \qquad (5)$$

Of particular relevance is the fact that Eberson (34) found reaction 5 to predominate over reaction 3 by a 3 to 2 ratio for the cyanomethyl radicals generated by electrolytic oxidation of cyanoacetate at a platinum electrode in methanol. The electrochemical behavior of N-cyanomethylketenimine, the product of reaction 5, is therefore of interest. Besides its possible production in the anodic background reaction it could be formed as a side product in any electrode reaction in acetonitrile which generated free radicals capable of abstracting hydrogen atoms from the solvent, such as the Kolbe oxidation discussed in Part II of this thesis.

Dr. Chin-Hua S. Wu has generously furnished a sample of a closely related ketenimine, N-(1-cyanocyclohexyl)-pentamethyleneketenimine (m. p. 69-71° C) and its chronopotentiometric behavior in acetonitrile containing 0.2 M tetraethylammonium perchlorate has been investigated.

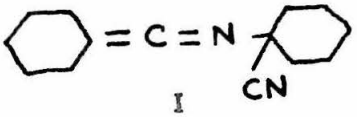

I

This compound is not reduced at the platinum electrode but yields a well-defined oxidizing wave at +1.0 V (0.01 M compound I, 0.2 M $(C_2H_5)_4NClO_4$, 1 ma/cm^2). The value of $i\tau^{1/2}/c$ was found constant at 170 ± 2 $\frac{\text{amp-cm-sec}^{1/2}}{\text{mole}}$ for two-fold

variation in current density. The products of its oxidation are also electroactive and Figure I-10 shows the two-step reverse-current wave for these products. The steps occur at -0.6 to -0.9 V and at -1.6 V. One might be tempted to identify them with the unidentified steps in the reverse-current chronopotentiogram for the anodic background reaction products (at -0.8 and -1.3 V).

These data and the data of previous workers cannot be reliably interpreted until an adequate analysis has been performed of the anodic reaction products. It is particularly necessary to resolve the dispute between Schmidt and Noack (26) and Billon (27) over the formation of succinonitrile.

Cathodic Background Reaction

The cathodic background reaction at platinum electrodes in acetonitrile solutions of tetraalkylammonium salts has been discussed by Billon (27). Billon found that hydrogen gas was evolved at the cathode and that the background potential was quite sensitive to the water content of the solution, becoming more positive with increasing moisture. Two reaction sequences were suggested:

$$\text{A}\begin{cases} 2CH_3CN + 2e^- = H_2 + 2CH_2CN^- & (1) \\ CH_2CN^- + CH_3CN = CH_3\underset{CH_2CN}{\overset{}{C}}{=}N^- & (2) \end{cases}$$

$$\text{B}\begin{cases} 2H_2O + 2e^- = H_2 + 2OH^- & (3) \\ OH^- + CH_3CN = CH_2CN^- + H_2O & (4) \\ CH_2CN^- + CH_3CN = CH_3\underset{CH_2CN}{\overset{}{C}}{=}N^- & (5) \end{cases}$$

FIG. I-10

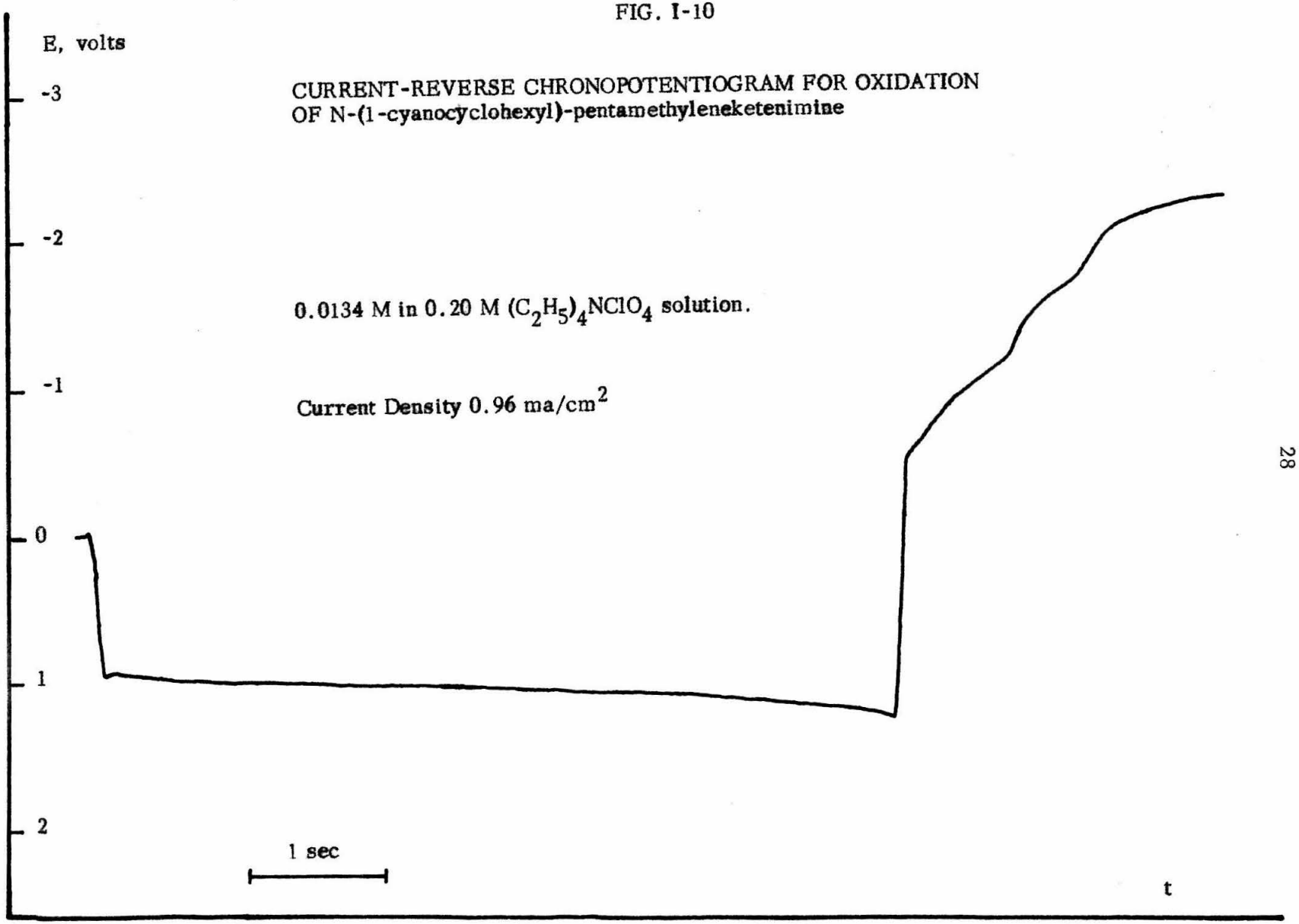
E, volts
-3
-2
-1
0
1
2
CURRENT-REVERSE CHRONOPOTENTIOGRAM FOR OXIDATION OF N-(1-cyanocyclohexyl)-pentamethyleneketenimine
0.0134 M in 0.20 M $(C_2H_5)_4NClO_4$ solution.
Current Density 0.96 ma/cm^2
1 sec
t

Reactions 2 and 5 correspond to the known base-catalyzed condensation of acetonitrile (35). Billon also mentioned the possibility of reducing the tetra-alkylammonium ion at the electrode.

The cathodic background reaction in solutions of lithium salts is the deposition of metallic lithium (18, 27). The background reaction in solutions of sodium salts is the deposition of sodium, which reacts rapidly with the acetonitrile (27).

A current-reverse chronopotentiogram for the cathodic background reaction products is shown in Figure I-11. The characteristics of this reverse chronopotentiogram were found to depend on the electrode history and the one reproduced here was selected as showing most clearly the four waves observed. Similar results were obtained when the current density was high enough (28 ma/cm^2) to eliminate any waves for the oxidation of the electrode surface or for products of the reduction of water. The alumina-treated spectral grade acetonitrile described in Part II of this thesis was used.

The first wave probably corresponds to the reduction of hydrogen gas. Billon (12) found hydrogen gas to be a product of the cathodic background reaction. Since base is generated by the reaction, the hydrogen should be oxidized at a much more negative potential than the value of 0.0 V observed in acidic medium (vide infra). Only the first wave fits this description. In oscillographic measurements with current reversal after 100 ms or less only this first wave appeared, corresponding probably to the simple reversal of reaction 1. Apparently some hydrogen gas is lost from solution in the measurements at longer transition times. The same phenomenon was observed by Mather (36) in reverse-current chronopotentiometric studies involving the

FIG. I-11

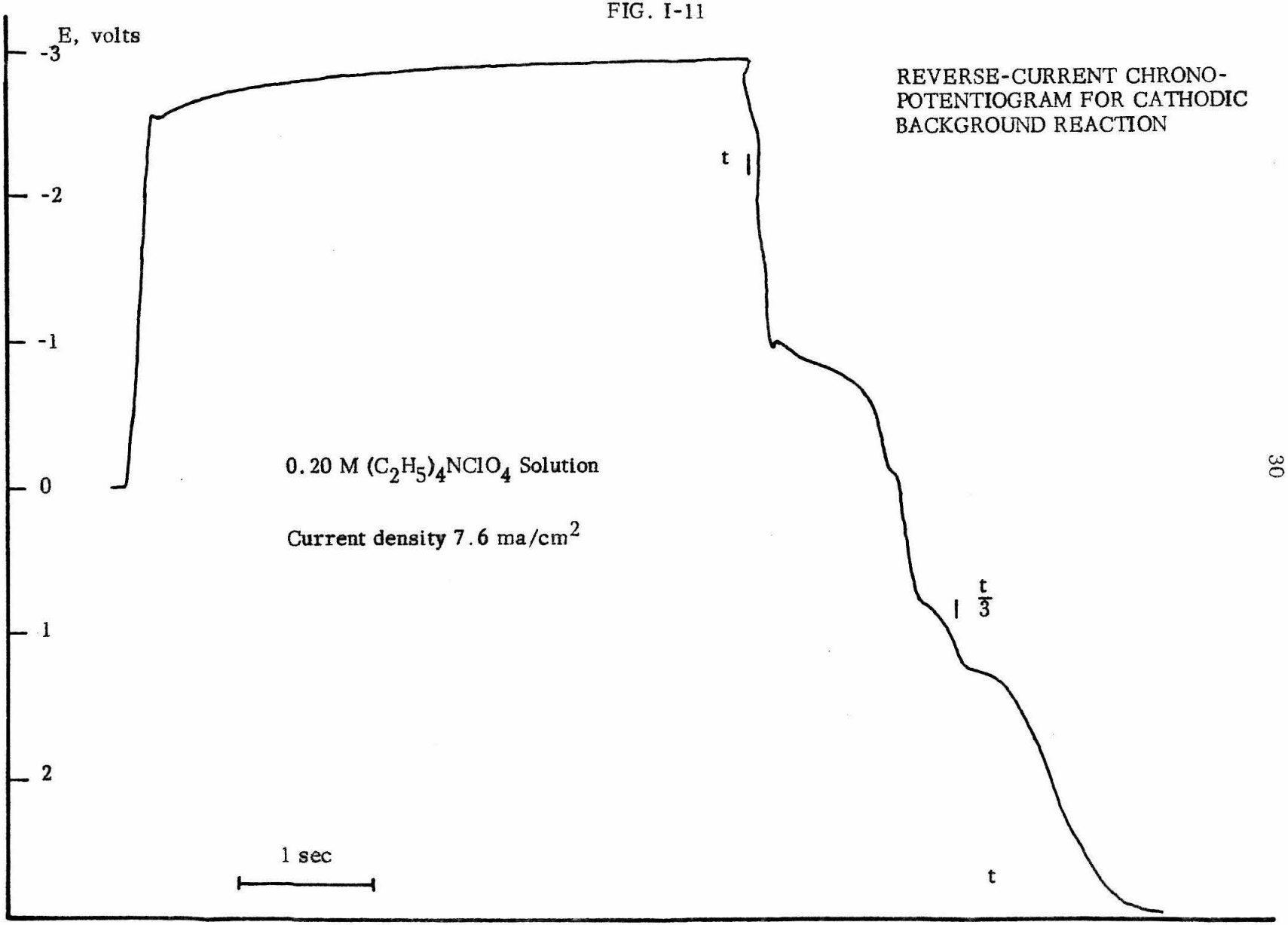

REVERSE-CURRENT CHRONO-POTENTIOGRAM FOR CATHODIC BACKGROUND REACTION

generation of hydrogen gas in acetic anhydride and was ascribed to the low solubility of hydrogen in acetic anhydride. The solubility of hydrogen in acetonitrile (about 10^{-3} M (37)) is also low. Reverse-current chronopotentiograms for the reduction of perchloric acid in acetonitrile solutions of tetraethylammonium perchlorate indicated loss of hydrogen, too; the figure cited above for the oxidation potential of hydrogen in acidic acetonitrile solution is the potential observed for the reverse wave. Thus in the measurements at very short transition times no hydrogen is lost from the solution and probably reaction 2 occurs to no great extent either, since the reactants and products would be expected to have different basicities and cause the oxidation of hydrogen to occur in two steps. In the measurements at longer transition times some hydrogen is lost from solution and then the excess cyanomethide ion and its condensation product with acetonitrile (reaction 2) are oxidized at the electrode. The occurrence of three waves indicates that one of these species reacts in two steps. This agrees with the fact that the total reverse wave is longer than 1/3 the duration of the cathodic current (fig. I-11), implying that more electrons are consumed in the anodic process than in the cathodic one.

If tetraethylammonium ion were reduced at the cathode an expected product is triethylamine. Amines have been produced by electrolytic reduction of quaternary ammonium salts in water and in liquid ammonia (38, 39). Triethylamine was found to give a well-defined oxidation wave at + 0.6 V in acetonitrile solutions of tetraethylammonium perchlorate. No such wave appears in the current-reverse chronopotentiogram for the cathodic background. The cathodic background reaction does not therefore appear to be the reduction of tetraethylammonium ion.

In conclusion, the chronopotentiometric data are consistent with reaction scheme A or B of Billon (27) and inconsistent with the reduction of tetraethylammonium ion. Of the two reaction sequences A and B, sequence A seems more likely since acetonitrile is too weak an acid to expect reaction 4 to go far enough fast enough to regenerate the water necessary to support the reaction. An alternative scheme which is consistent with the known facts and which would account for the sensitivity of the background potential to moisture content is

$$2H_2O + 2e^- = H_2 + 2OH^- \quad (6)$$

$$2OH^- + 2e^- = H_2 + 2O^{-2} \quad (7)$$

$$O^{-2} + CH_3CN = OH^- + CH_2CN^- \quad (8)$$

PART II

OXIDATION OF SUBSTITUTED ACETATES IN ACETONITRILE

Introduction

As early as 1834 Michael Faraday discovered that hydrocarbons were formed on passing an electric current through acetate solutions (40). Fifteen years later Hermann Kolbe conducted an investigation of the anodic oxidation of carboxylate salts that has given his name to the coupling reaction which, though only one of several competing processes in the oxidation, has been the one of greatest synthetic value. Since then the number of publications dealing with the anodic oxidation of carboxylate salts has run well into the hundreds. As the characteristics of free-radical reactions became established the carboxylate oxidation was found to fit well into this class and it is now widely accepted that the primary process is the discharge of the carboxylate anion to the neutral acyloxy radical, followed by or concomitant with decarboxylation to the alkyl radical (41). But important questions remain unanswered: Does decarboxylation follow or coincide with discharge? Are the reactive radicals adsorbed on the electrode or free in solution? Can the alkyl radicals be further oxidized electrolytically to carbonium ions? (The last question arises from the fact that an important side reaction leads to the formation of alcohols in aqueous solution and ethers in alcoholic solution, often with rearrangements typical of carbonium-ion reactions.) Direct answers to these questions can, in principle, be sought through the use of modern electrochemical techniques such as those reviewed by Vetter in a recent monograph (42). It is only necessary to find a solvent system that dissolves reactants and products and supports the flow of electric current without itself reacting at the anode.

We found that acetate ion could be oxidized in acetonitrile at potentials well below the potential at which the solvent itself was oxidized. This was discovered independently by Geske (43) who wrote, "These observations finally permit a rational systematic study of the 'Kolbe synthesis' . . . " With optimism akin to Geske's a chronopotentiometric study of the electro-oxidation of a series of substituted acetates was carried out in acetonitrile solution, after first verifying that ethane is the principal product of the oxidation of acetate. The optimism proved premature. Traces of water in the solution, which could not be eliminated, were found to interfere with measurement by reacting at the electrode when carboxylate anion was present though non-reactive otherwise. Only certain qualitative conclusions could be reached.

A further specific objective of this study, besides elucidating the mechanism of the Kolbe electrolysis, was the determination of substituent effects on the electrochemical transfer coefficient α for the reaction. Such a study has never been performed and would be of great significance since the various theoretical approaches to the electron-transfer process at electrodes in solution have led to different interpretations of the transfer coefficient. Thus Glasstone, Laidler and Eyring (44) interpret α as the fraction of the potential drop between electrode and solution which affects the activated complex; Randles (45) interprets α as an index of the symmetry of the potential barrier; Marcus (46) interprets α as related to the work required to transport the ion to the electrode before and after discharge; and Hush (47) interprets α as the fraction of time an electron spends on the ion as it resonates between ion and electrode in the activated complex. A study of substituent effects would place the meaning of the transfer coefficient on a firmer basis. Because of the interfering oxidation of water, only indicative results were achieved in the present investigation.

Analysis of Products from the Electrolytic Oxidation of Acetate Ion in Acetonitrile

To establish the principal reaction taking place and to make certain that acetonitrile serves as an inert solvent, an anode product analysis was undertaken for the electrolysis of a solution of tetrabutylammonium acetate in acetonitrile with tetraethylammonium perchlorate as the supporting electrolyte. This work has been published (48).

Experimental

Reagents. The tetrabutylammonium acetate used was in the form of double crystals containing 50 mole % acetic acid and was prepared by neutralizing aqueous tetrabutylammonium hydroxide with a large excess of acetic acid, evaporating to dryness at 60° C, and recrystallizing from benzene to obtain large white needles. These double crystals, unlike most tetraalkylammonium carboxylate salts, are not hygroscopic and are convenient to handle. Their melting range after several recrystallizations was 113-17° C, in agreement with the melting point of 116° reported for tetrabutylammonium acetate prepared by a similar procedure (49). If any loss of acetic acid took place below 113° C, it was not accompanied by a visible change. The composition of the crystals was determined by acidimetric titration of the acetate with perchloric acid in anhydrous acetic acid, by titration of the acetic acid with sodium hydroxide in aqueous solution, and by controlled-potential coulometric oxidation of the acetate in an acetonitrile solution. The controlled-potential coulometric analysis, in agreement with the

report of Geske (43), indicated that a one-electron oxidation of the acetate takes place. The acetic acid present did not interfere, since acetic acid is not oxidized below the anodic background potential in acetonitrile solutions of tetraethylammonium perchlorate. The anode potential was held at +1.4 volts vs. $Hg/Hg_2SO_4/K_2SO_4$ (sat. aq.) for the controlled-potential coulometric analysis.

Practical grade acetonitrile was purified by four or more distillations from phosphorus pentoxide, followed by one from potassium carbonate (50). It was stored in a siphon bottle fitted with a greaseless Teflon stopcock in the delivery tube and protected from the atmosphere with a drying tube. Tetraethylammonium perchlorate was prepared by the method of Kolthoff and Coetzee (7) and was recrystallized from water five times.

Apparatus and procedure. The products of the electrolytic oxidation of acetate in acetonitrile were identified by sweeping them from the anode compartment of the electrolysis cell with a stream of helium and analyzing the effluent gas by adsorption chromatography on silica gel. A current of 40.0 ma was provided by a constant-current source of Lingane's design (51) to a platinum gauze anode immersed in 20 ml of acetonitrile to which 0.5 gram of tetrabutylammonium acetate-acetic acid double crystals and 0.5 gram of tetraethylammonium perchlorate had been added. The electrolysis was carried out at room temperature.

The electrolysis cell is shown in Figure II-1. The anode was separated from the cathode by a salt bridge consisting of a 4- to 6-cm length of 6-mm (i.d.) Tygon tubing that had been rendered conductive by soaking it for several days in a solution of sodium perchlorate in acetonitrile and then passing current through it to draw more electrolyte into the polymer. The bridge resistance was of the order of 5 kilohms.

FIG. II-1

ELECTROLYSIS CELL

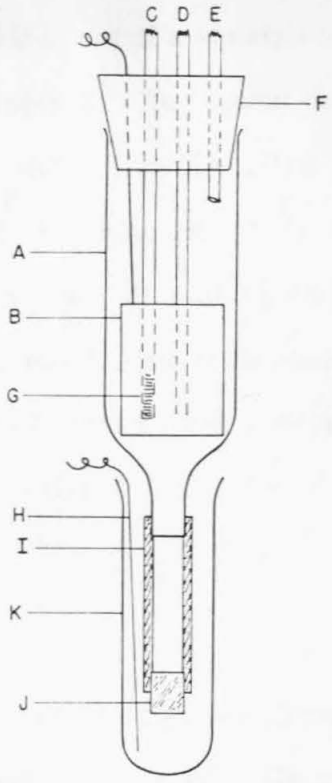

A. Anode compartment
B. Platinum gauze anode
C. Sat. aq. K_2SO_4 salt bridge to reference electrode
D. Helium inlet
E. Gas outlet
F. Cork sealed with epoxy resin
G. Agar-aq. K_2SO_4 gel
H. Cathode
I. Treated Tygon tubing
J. Solid glass plug
K. Cathode compartment

During the electrolysis helium was bubbled into the anode compartment at a constant rate (±2%) which was monitored by the pressure drop across a fritted-glass plug in the gas stream. Upon leaving the anode compartment, the gas stream was passed through a sulfuric acid bath to remove acetonitrile vapor and then to a sample-collection vessel. After the start of the electrolysis, 5 to 10 minutes were allowed for attainment of a steady state; gas samples were then collected at intervals and analyzed. Throughout the electrolysis the anode potential stayed between 1.3 and 1.5 volts vs. $Hg/Hg_2SO_4/K_2SO_4$ (sat. aq.), increasing with the depletion of acetate ion. In this potential range no appreciable oxidation of the solvent takes place: The background current in the absence of tetrabutylammonium acetate was 0.2 ma at an electrode potential of 1.5 volts and did not rise to 0.4 ma, or 1% of the current used in the electrolysis, until a potential of 1.7 volts was reached.

Results and Discussion

The products observed and their yields were: carbon dioxide, 91 ± 6%; ethane, 77 ± 3%; and methane, 3.7 ± 0.4%. The yields, based on theoretical yields of 1 mole per faraday for carbon dioxide and methane and 0.5 mole per faraday for ethane, were calculated from the helium flow rate, the per cent composition of the effluent gas, and the current. The limits of error are 95% fiducial limits, assuming normal distribution of the sample population about the true value. The random error is attributed partly to the gas analysis and partly to fluctuations in cell operation, due to slight variations in temperature and helium flow rate during the electrolysis, which changed the steady-state partition of CO_2, C_2H_6, and CH_4 between the solution and the gas. Fourteen

samples in all, from five different runs, were analyzed.

The principal reaction that occurs is a simple Kolbe coupling. The formation of ethane as the main product has been observed in the electrolytic oxidation of acetate under suitable conditions in such varied solvents as water (52), ethylene glycol (53), acetic acid (54, 55), methanol (56, 57, 55), ethanol (55), and even fused salts (41). Considerable evidence supports the hypothesis of a free-radical mechanism for this reaction (41).

$$CH_3COO^- = CH_3COO\cdot + e^- \quad (1)$$

$$CH_3COO\cdot = CH_3\cdot + CO_2 \quad (2)$$

$$2CH_3\cdot = C_2H_6 \quad (3)$$

Methane is a commonly observed side product in the electrolytic oxidation of acetate. Its formation in aqueous solution has been shown by deuterium tracer studies to involve attack by methyl radicals on acetic acid or acetate ion; ethanol and methanol are preferentially attacked if added to the electrolysis solution (58). Therefore, in the presence of a large preponderance of acetonitrile one might reasonably expect the acetonitrile to serve as the major source of hydrogen atoms. The following reaction is thus regarded as the probable origin of the observed methane:

$$CH_3\cdot + CH_3CN = CH_4 + \cdot CH_2CN \quad (4)$$

The free radical formed in this reaction could couple with other radicals present to form succinonitrile or propionitrile. No attempt was made to detect these.

The methane yield was not affected by adding enough glacial acetic acid to the electrolysis solution to raise the acetic acid concentration to 0.5 M. The initial concentration resulting from the acetic acid present in the tetrabutylammonium acetate crystals was 0.07 M.

It is not surprising that the measured yield of carbon dioxide is not 100% and that the sum of the yields of methane and ethane is not equal to the carbon dioxide yield, in view of the free-radical reaction mechanism. Simple free radicals, because of their instability, are notoriously nonselective in their attack on neighboring molecules. The literature shows that a number of side reactions could consume the radicals without resulting in the formation of the major products. Such side reactions could lead to the formation of esters (52, 54, 57, 59), diacyl peroxides and peroxy acids (60, 61, 62, 63), olefins (54, 56), and alkyl perchlorates (63). Furthermore, the chronopotentiometric data discussed later indicate concurrent oxidation of any water present as an impurity.

Chronopotentiometric Measurements

Experimental

Reagents. Acetonitrile purified by two different procedures was used. Some solutions were prepared from Matheson, Coleman, and Bell Practical Grade acetonitrile which had been washed with cold aqueous KOH, dried over anhydrous sodium carbonate, and distilled from P_2O_5 three times, the last time under nitrogen (64). Others were prepared from Matheson, Coleman, and Bell Spectroquality acetonitrile which had been passed through Merck chromatographic alumina (dried at 350° C) and collected under nitrogen. The product of both procedures contained 4 to 6 mM less water than the freshly opened spectral grade acetonitrile as determined by differential infrared absorption at 1.9 μ; this is the order of magnitude of the water concentration quoted by the manufacturer

for the spectral grade acetonitrile and both purification procedures may be presumed to yield a product containing at most two or three mM H_2O. Kolthoff and Coetzee have prepared acetonitrile by the first method and found a water content of less than 2 mM (7). Both preparations were found to contain no more than 0.3 mM acetic acid by titration with aqueous NaOH; the spectral grade acetonitrile contained substantially more before treatment with alumina. The spectral grade acetonitrile contained an unidentified impurity which formed an acid-soluble white precipitate with aqueous silver nitrate (acetate or cyanide?) but which was removed by the alumina. Acetonitrile purified by the first method showed strong absorption in the ultraviolet relative to spectral grade acetonitrile, which in turn showed somewhat stronger absorption than the material which had been passed through alumina. Thus the product of highest purity in the light of these tests was the spectral grade acetonitrile which had been passed through alumina. Duplicate measurements in both solvents failed to indicate any difference in their electrochemical behavior, however. The acetonitrile was stored in all cases in a siphon bottle protected by a drying tube, with delivery controlled by a greaseless Teflon stopcock.

Tetraethylammonium perchlorate was prepared as described in Part I of this thesis and dried over anhydrous magnesium perchlorate under oil-pump vacuum. The product contained less than 1 mole % water as indicated by the infrared absorption of its solution in acetonitrile. The dry product is easily obtained and stored, since the crystals are not wetted by water; a submerged crystal in a saturated solution may easily be set afloat with a pair of tweezers.

Linde High Purity Dry Nitrogen was, without further purification, used to deaerate the solutions.

Tetrabutylammonium salts were prepared by the exact neutralization of the appropriate acids in water or water-methanol solution with aqueous tetrabutylammonium hydroxide, using a Leeds and Northrup Model 7664 pH meter to detect the endpoint. Tetrabutylammonium hydroxide was prepared by recrystallizing Matheson, Coleman and Bell tetrabutylammonium iodide four times from benzene, treating with excess freshly precipitated silver oxide in water, filtering the solution and refiltering a week later to remove silver oxide which passes as a colloid through the first filtration. The acids used varied in purity, as listed:

Butyric, isobutyric, isovaleric, cyclopropanecarboxylic, and cyclohexanecarboxylic acids were purified by preparative scale gas chromatography, followed by simple vacuum distillation to remove any valve lubricant or column "bleeding" from the chromatograph. Trifluoroacetic acid was fractionally distilled using a 50 cm vacuum-jacketed packed column with reflux head. The calculated amount of water to form the water-trifluoroacetic acid azeotrope was added and the mixture then refractionated. Dichloroacetic acid was fractionated under vacuum using a 50 cm vacuum-jacketed packed column with reflux head. Cyanoacetic acid was recrystallized three times from an ether-chloroform mixture. Acetylglycine was recrystallized three times from water. Malonic and dimethylmalonic acids were washed with carbon tetrachloride and recrystallized once from ether in a Soxhlet extractor. The remaining acids were commercial reagent grade chemicals.

The solutions of tetrabutylammonium salts were dehydrated under vacuum to viscous liquids. Portions of liquid were then delivered to individual volumetric flasks of known weight and the flasks, together with their contents, dried for several days over phosphorus pentoxide under oil-pump vacuum.

After admitting air to the system through a drying tube filled with anhydrous magnesium perchlorate the flasks were quickly stoppered and weighed. Acetonitrile and tetraethylammonium perchlorate were delivered directly to these flasks, which were stored in a desiccator until used. A crystalline material was formed upon drying the salt except in the case of methoxyacetate, dichloroacetate, and ethoxyacetate which formed clear viscid liquids. The concentration of carboxylate anion in the solutions was determined by acidimetric titration with perchloric acid in anhydrous acetic acid (65). Comparison of titration results with the weight of tetrabutylammonium salt indicated that the water content of the salt corresponded in most cases roughly to the monohydrate. Solutions were made up to contain 0.20 M $(C_2H_5)_4NClO_4$ and about 0.01 M carboxylate salt.

Attempts to prepare the tetrabutylammonium salts of chloroacetic, bromoacetic, diphenylacetic, and triphenylacetic acids by this procedure failed. The chloroacetate and bromoacetate underwent nearly complete hydrolysis to the halide (recognized by its chronopotentiometric behavior) and polyglycollide (recognized by its melting point) despite reported preparation of the chloroacetate by a nearly identical method (66). Tetrabutylammonium triphenylacetate formed a dark greenish-brown material upon dehydration. Tetrabutylammonium diphenylacetate also underwent decomposition, as indicated by changes in its chronopotentiometric behavior with storage time.

Apparatus and Procedure

The apparatus described in Part I was used, except that the Heathkit power supply was replaced by a Wenking potentiostat (Elektronishe Werkstatten, Gottingen, Germany). This controlled the voltage across a standard resistor

in series with the cell and hence the current through the cell. The silver nitrate electrode described in Part I was used for all measurements.

The electrode and the cell in which it was mounted were cleaned with potassium dichromate-sulfuric acid cleaning solution between measurements, rinsed with water and dried at 130° C. While measurements were being made for Tables II-1 and II-2, current was passed through the electrode only in the anodic direction to ensure a reproducible, thoroughly oxidized surface. The most reproducible results were obtained after recording a preliminary chronopotentiogram in which the potential was allowed to rise all the way to the anodic background. (A similar observation was made by Hoh, McEwen, and Kleinberg (4)). Runs on a given compound were nonconsecutive so that any permanent change in the electrode surface resulting from the reaction of some particular compound would have been detected. No such change in electrode properties survived the cleaning procedure. All measurements were performed at 25.0 ± 0.1° C.

Results

Smooth waves with well-defined transition times and no bumps or irregularities were obtained for salts of the following acids in deaerated solution: acetic, propionic, butyric, isobutyric, pivalic, isovaleric, t-butylacetic, methoxyacetic, trifluoroacetic, malonic (mono- and di-tetrabutylammonium salts), and dimethylmalonic (mono- and di-tetrabutylammonium salts). Data describing these waves are given in Table II-1. Transition times were found by the method of Kuwana (see Appendix) and the value of $n\alpha$ was obtained from the

TABLE II-1

CHRONOPOTENTIOMETRIC DATA
FOR SALTS OF SUBSTITUTED ACETATES
in CH_3CN, deaerated, 0.20 M $(C_2H_5)_4NClO_4$

Acid	Current Density ma/cm^2	Concentration mM	τ sec	$E_{1/4}$ volts	$n\alpha$
Acetic	1.632	11.51	6.43	1.252	.310
	1.660	11.51	6.31	1.244	.307
	1.651	11.51	6.05	1.250	.302
	1.629	11.82	6.63	1.256	.326
	1.614	11.82	6.95	1.244	.320
	1.617	11.82	6.75	1.246	.322
Propionic	1.448	10.77	6.94	1.202	.329
	1.448	10.77	6.75	1.198	.334
	1.432	10.77	6.76	1.214	.334
Butyric	1.350	9.66	6.38	1.253	.283
	1.350	9.66	6.16	1.257	.278
	1.388	9.66	5.80	1.250	.285
Isobutyric	1.353	10.05	6.17	1.125	.342
	1.350	10.05	6.21	1.124	.338
Pivalic	1.731	12.38	5.52	1.140	.320
	1.610	12.38	6.38	1.128	.321
	1.617	12.38	6.36	1.133	.305
Isovaleric	1.134	8.15	6.27	1.264	.229
	1.142	8.15	5.85	1.258	.228
	1.410	10.18	6.10	1.267	.232
	1.407	10.18	5.78	1.272	.230
T-butylacetic	1.412	9.80	5.27	1.280	.255
	1.210	9.80	7.21	1.271	.255
Methoxyacetic	1.399	10.08	5.81	1.141	.305
	1.399	10.08	5.99	1.139	.304
	1.372	10.08	6.10	1.144	.330

TABLE II-1

Acid	Current Density ma/cm^2	Concentration mM	τ sec	$E_{1/4}$ volts	$n\alpha$
Ethoxyacetic	1.312	9.50	5.12	1.193	.267
	1.283	9.50	5.88	1.173	.272
	1.300	9.50	5.65	1.195	.269
Malonic (di-$(C_4H_9)_4N$ salt)					
	.582	6.86	9.18	.983	.216
	.584	6.86	9.08	.981	.220
Dimethylmalonic (di-$(C_4H_9)_4N$ salt)					
	-	6.55	4.42	.865	.207
	.874	6.55	3.99	.865	.208
	.889	6.55	4.07	.832	.200
Trifluoroacetic	1.103	8.12 (a)	7.31	2.146	.193
	1.212	8.12 (a)	6.55	2.125	.174
	1.204	8.12 (a)	6.38	2.135	.176
Dimethylmalonic (mono - Bu_4N salt)					
	.524	7.56	7.39	1.836	(b)
	.529	7.56	7.13	1.848	(b)
	.520	7.56	7.35	1.825	(b)

(a) Calculated from weight of tetrabutylammonium trifluoroacetate used to prepare solution.

(b) The wave for tetrabutylammonium hydrogen malonate showed curvature at the quarter-wave point.

TABLE II-2

CHRONOPOTENTIOMETRIC DATA
FOR SALTS OF SUBSTITUTED ACETATES
in air-saturated 0.20 M $(C_2H_5)_4NClO_4$ in CH_3CN

Acid	τ sec	Concentration mM	$E_{1/4}$ volts	Current Density, ma/cm^2	$i\tau^{1/2}/C$ cm-sec$^{1/2}$ amp moles
Butyric	6.62	9.02	1.274	1.149	328
	6.70	9.02	1.266	1.149	329
	5.54	9.02	1.260	1.273	332
	6.10	9.66	1.254	1.350	345
	6.01	9.66	1.259	1.350	343
	5.62	9.66	1.244	1.388	340
Isobutyric	5.85	8.84	1.176	1.221	334
	5.87	8.84	1.178	1.210	331
	5.34	8.84	1.174	1.274	333
	5.96	9.70	1.150	1.353	340
	6.06	9.70	1.152	1.350	342
	6.00	9.70	1.153	1.350	341
Isovaleric	5.26	8.24	1.249	1.183	329
	5.29	8.24	1.245	1.183	330
	5.45	8.24	1.247	1.191	337
	5.45	8.15	1.247	1.134	325
	5.50	8.15	1.240	1.134	326
	5.78	8.15	1.239	1.142	337
	5.85	10.18	1.244	1.410	335
	5.81	10.18	1.246	1.407	333
Propionic	6.65	10.60	1.219	1.448	352
	6.43	10.60	1.219	1.448	346
	6.76	10.60	1.236	1.432	351
Pivalic	5.20	7.32	1.116	1.070	333
	5.16	7.32	1.123	1.070	332
	5.66	12.38	1.115	1.731	333
	6.53	12.38	1.104	1.610	333
	6.44	12.38	1.109	1.617	332
Acetic	6.20	11.51	1.265	1.632	353
	6.16	11.51	1.250	1.660	358
	5.72	11.51	1.256	1.651	343
	6.66	11.82	1.251	1.629	355
	6.80	11.82	1.249	1.614	356
	6.75	11.82	1.248	1.617	355

TABLE II-2

Acid	τ sec	Concentration mM	$E_{1/4}$ volts	Current Density, ma/cm^2	$i\tau^{1/2}/C$ $cm\text{-}sec^{1/2}$-amp moles
Acetylglycine	5.19	10.10	1.281	1.437	324
	5.15	9.83	1.268	1.410	325
Cyclopropanecarboxylic					
	7.60	8.74	1.287	1.100	347
	6.50	9.25	1.308	1.237	340
Cyclohexanecarboxylic					
	5.74	8.76	1.223	1.207	330
	5.65	7.56	1.214	1.028	323
Cyanoacetic	6.80	11.57	1.380	1.512	341
	6.79	10.82	1.442	1.410	339
	6.73	11.57	1.379	1.504	338
	7.00	11.57	1.382	1.504	344
T-butylacetic	6.29	7.82	1.246	1.070	343
	5.18	7.82	1.246	1.070	311
	5.71	7.82	1.236	1.070	327
	5.30	9.80	1.248	1.412	332
	7.15	9.80	1.242	1.210	330
Malonic (mono-$(C_4H_9)_4N$ salt)					
	5.83	9.30	1.728	1.412	366
	5.77	9.30	1.750	1.418	366
Ethoxyacetic	5.30	9.50	1.102	1.312	318
	6.04	9.50	1.106	1.283	332
	5.85	9.50	1.106	1.300	331
Trifluoroacetic	7.21	8.12 (a)	2.151	1.103	367
	6.35	8.12 (a)	2.137	1.212	378
	6.55	8.12 (a)	2.143	1.204	374
Malonic (di-$(C_4H_9)_4N$ salt)					
	7.07	6.86	.899	.582	226
	7.04	6.86	.890	.584	226
Dimethylmalonic (mono-$(C_4H_9)_4N$ salt)					
	7.39	7.56	1.774	.990	356
	7.11	7.56	1.780	1.000	353
	7.40	7.56	1.781	.983	353
Dimethylmalonic (di-$(C_4H_9)_4N$ salt)					
	3.80	6.55	.821	.874	260
	3.67	6.55	.829	.889	260

TABLE II-2

Acid	τ sec	Concentration mM	$E_{1/4}$ volts	Current Density ma/cm^2	$i\tau^{1/2}/C$ cm-sec$^{1/2}$-amp moles
Dichloroacetic	6.17	10.50	1.603	1.470	347
	6.76	10.50	1.600	1.399	346
	6.81	10.50	1.606	1.288	320
Glycolate	6.54	10.74	1.19	1.470	350
	7.71	10.74	1.20	1.392	360
	7.82	10.74	1.20	1.372	357
Methoxyacetate	5.76	10.08	1.078	1.399	333
	5.76	10.08	1.074	1.399	333
	6.08	10.08	1.075	1.372	335

(a) Concentration calculated from weight of tetrabutylammonium trifluoroacetate used to prepare solution.

quarter-wave slope and the transition time as described in the Appendix. Plots of E against log $\left[1-\left(\frac{t}{\tau}\right)^{1/2}\right]$ deviated somewhat from linearity, seriously in the cases of mono- and di-tetrabutylammonium malonate, mono-tetrabutylammonium dimethylmalonate, and trifluoroacetate (figs. II-2, II-3). Cyclopropanecarboxylate and cyclohexanecarboxylate gave smooth waves which did not yield linear plots of E against log $\left[1-\left(\frac{t}{\tau}\right)^{1/2}\right]$ and which occurred at increasingly anodic potentials for consecutive runs unless the electrode was cleaned by anodization at the background potential for a few seconds before each run. The remaining salts, and the above as well in solutions containing oxygen, gave waves of more or less irregular shape which are reproduced in Figures II-4 to II-15. Corresponding numerical data are collected in table II-2. Well-defined transition times were obtained for all salts listed in table II-2, unaffected by deaeration except for the slight increase due to evaporation of solvent.

Diffusion coefficients calculated from $\frac{i\tau^{1/2}}{C}$ are listed in decreasing order in table II-3. Constancy of $\frac{i\tau^{1/2}}{C}$ ($\pm 10\%$) over the current range from about 1.4 to 14 ma/cm^2 was verified from oscilloscope traces of the waves for acetate, dichloroacetate, methoxyacetate, cyclopropanecarboxylate, cyclohexanecarboxylate, trifluoroacetate, di-tetrabutylamonium dimethylmalonate, and aminoacetate and can be assumed for the remaining salts. This proves the reaction to be diffusion-controlled. The waves were not much affected by the addition of small amounts of water (fig. II-16) or changes in the concentration of supporting electrolyte (table II-4) but were quite sensitive to the presence of small amounts of the conjugate acid (fig. II-17).

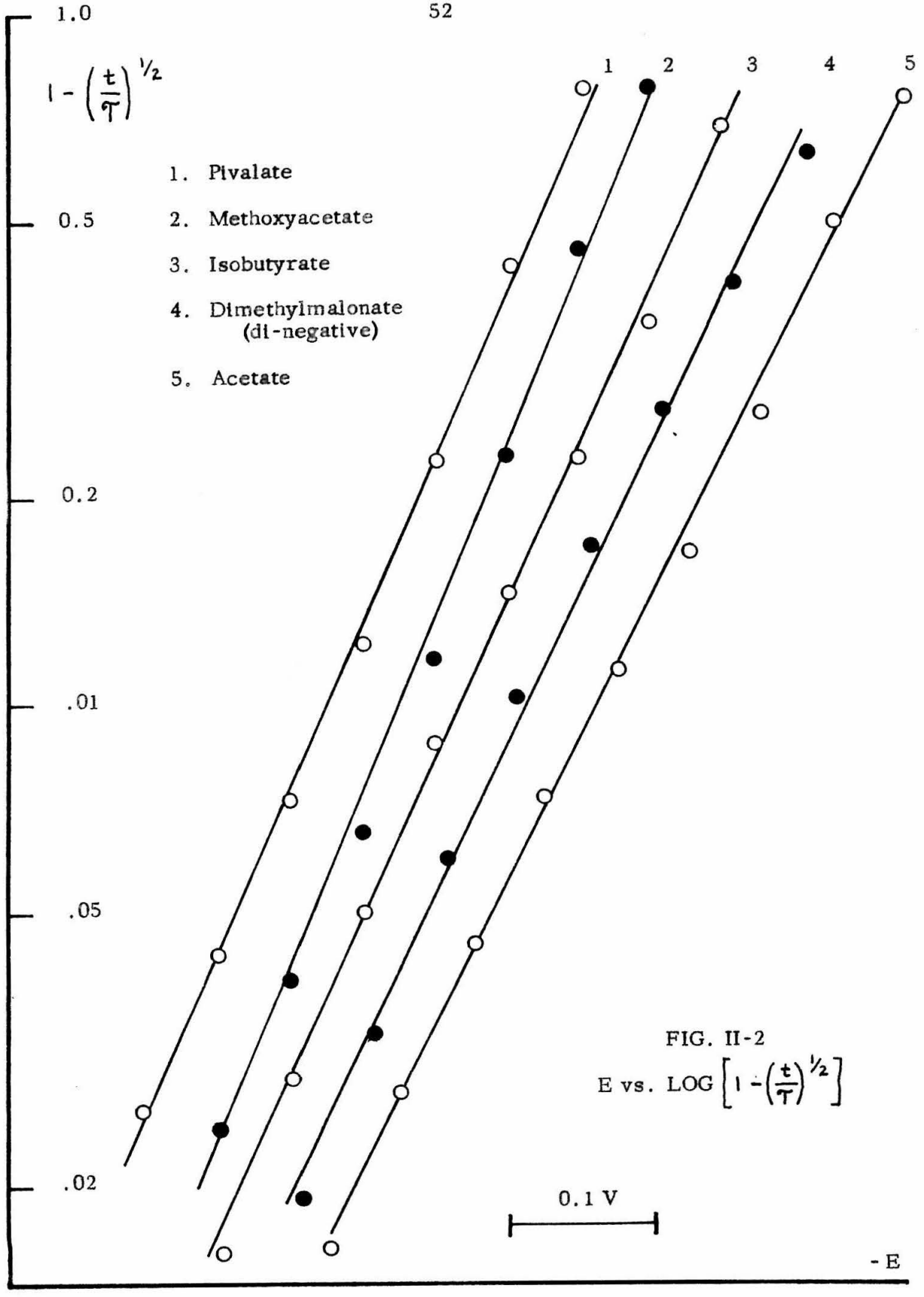

FIG. II-2

E vs. LOG $\left[1-\left(\frac{t}{\tau}\right)^{1/2}\right]$

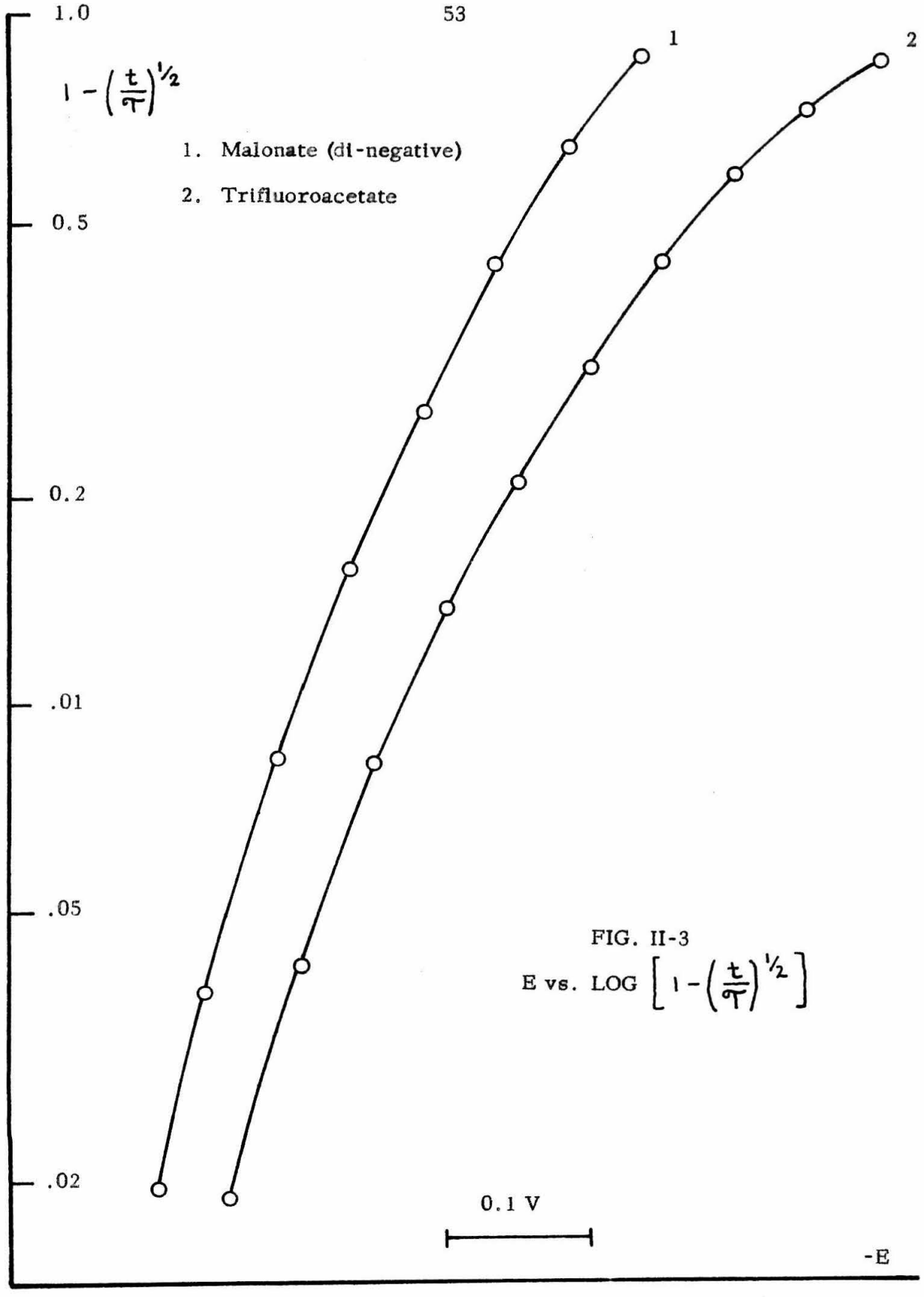

FIG. II-3

E vs. LOG $\left[1-\left(\frac{t}{\tau}\right)^{1/2}\right]$

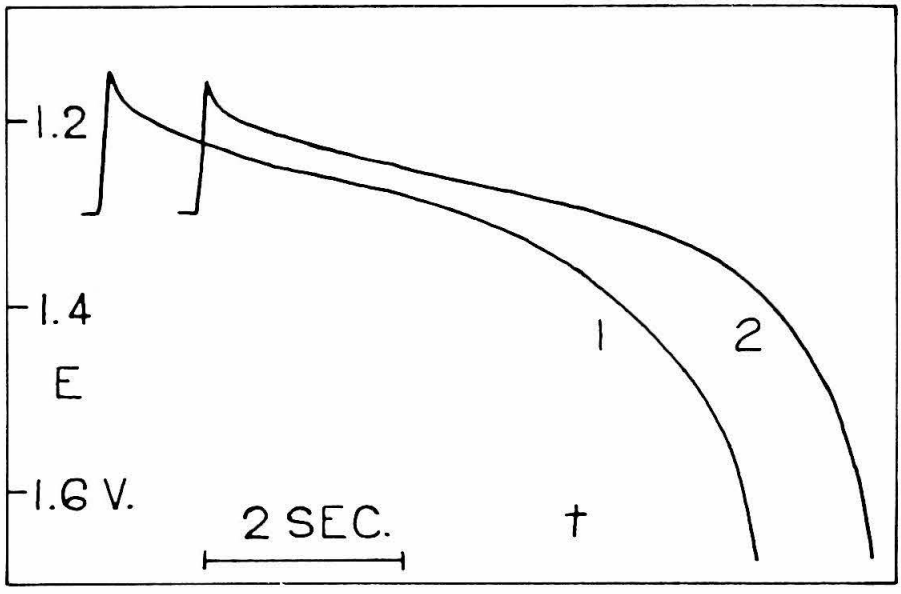

FIG. II-4

11.8 mM tetrabutylammonium acetate, 0.20 M tetraethylammonium perchlorate, 1.62 ma/cm^2 (1) air-saturated (2) deaerated

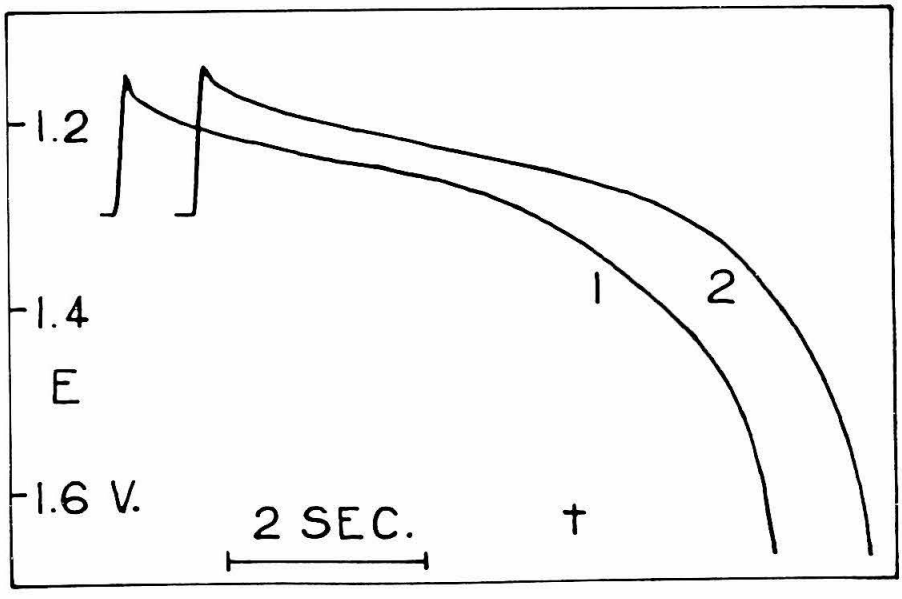

FIG. II-5

10.8 mM tetrabutylammonium propionate, 0.20 M tetraethylammonium perchlorate, 1.43 ma/cm^2 (1) air-saturated (2) deaerated

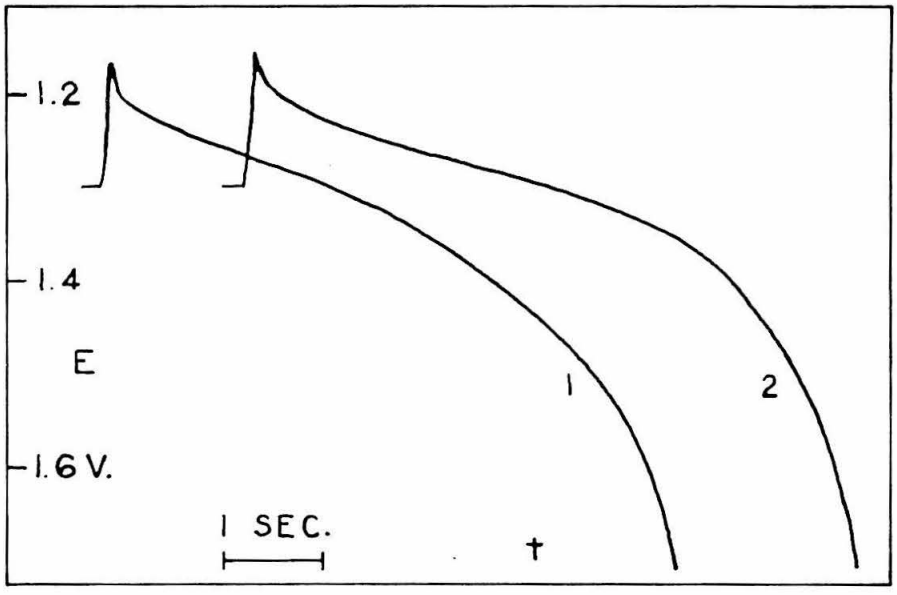

FIG. II-6

9.7 mM tetrabutylammonium butyrate, 0.20 M tetraethylammonium perchlorate, 1.35 ma/cm^2 (1) air-saturated (2) deaerated

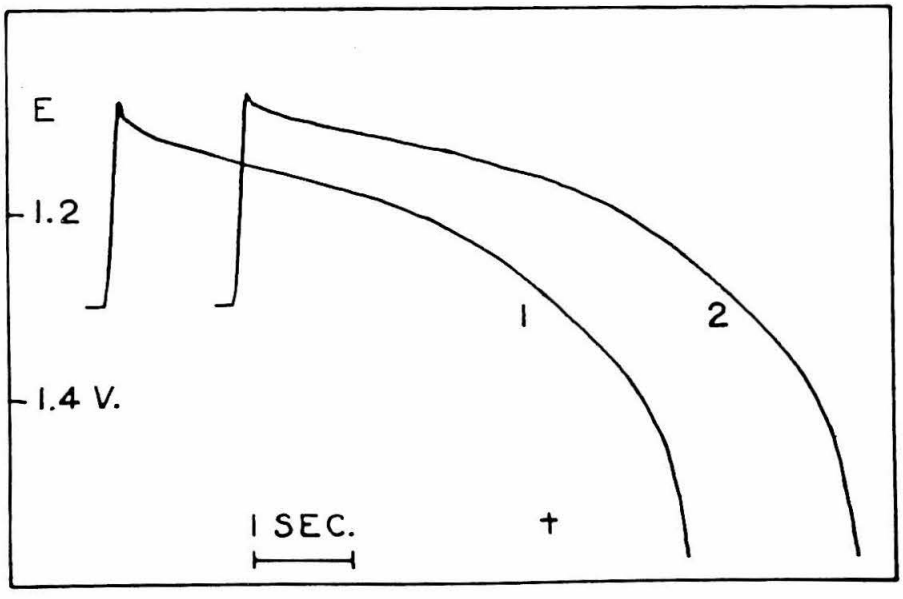

FIG. II-7

10.0 mM tetrabutylammonium isobutyrate, 0.20 M tetraethylammonium perchlorate, 1.35 ma/cm^2 (1) air-saturated (2) deaerated

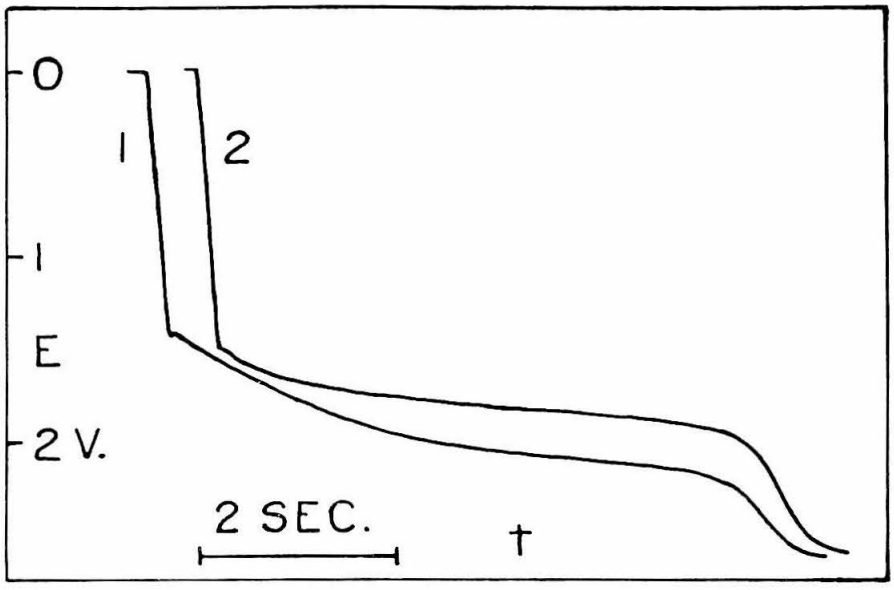

FIG. II-8

9.3 mM tetrabutylammonium hydrogen malonate, 0.20 M tetraethylammonium perchlorate. 1.42 ma/cm^2 (1) deaerated (2) air-saturated

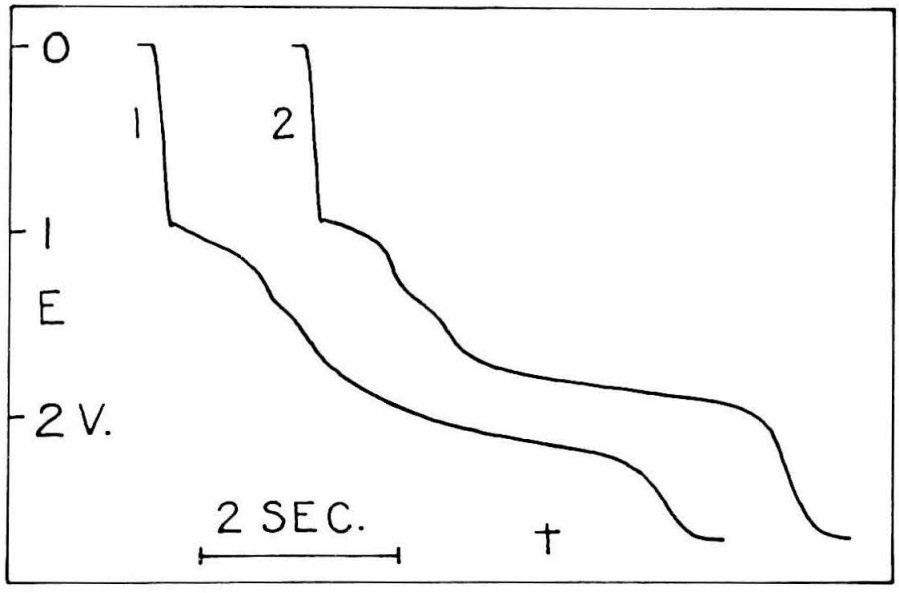

FIG. II-9

6.7 mM di-tetrabutylammonium malonate, 0.20 M tetraethylammonium perchlorate, 0.58 ma/cm^2 (1) deaerated (2) air-saturated

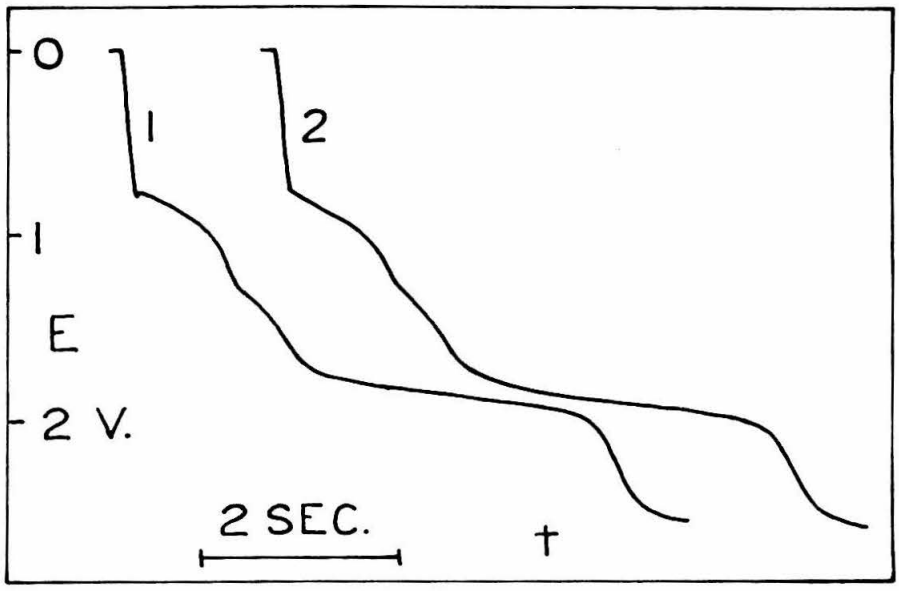

FIG. II-10

6.6 mM di-tetrabutylammonium dimethylmalonate, 0.20 M tetraethylammonium perchlorate, 0.98 ma/cm^2 (1) air-saturated (2) deaerated

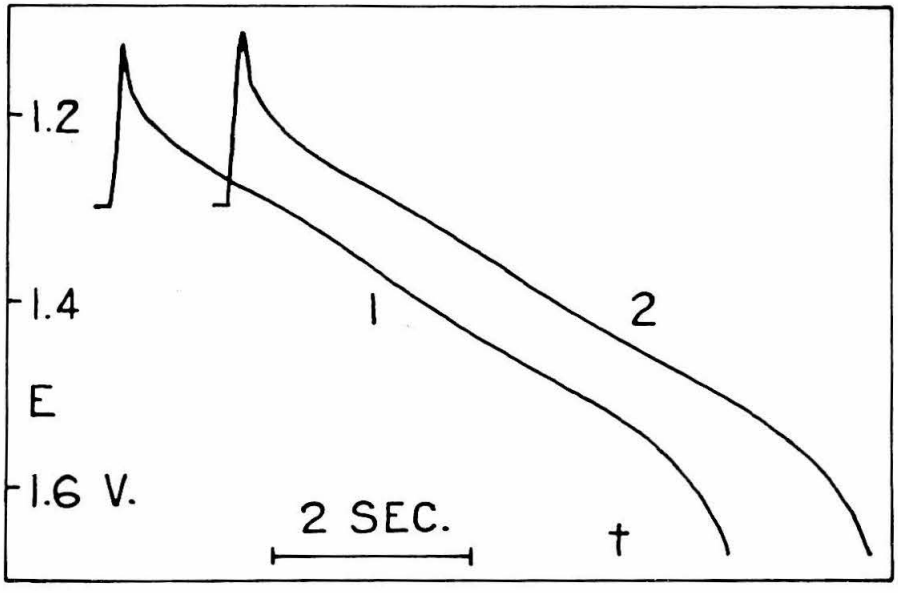

FIG. II-11

10.7 mM tetrabutylammonium glycolate, 0.20 M tetraethylammonium perchlorate, 1.47 ma/cm^2 (1) air-saturated (2) deaerated

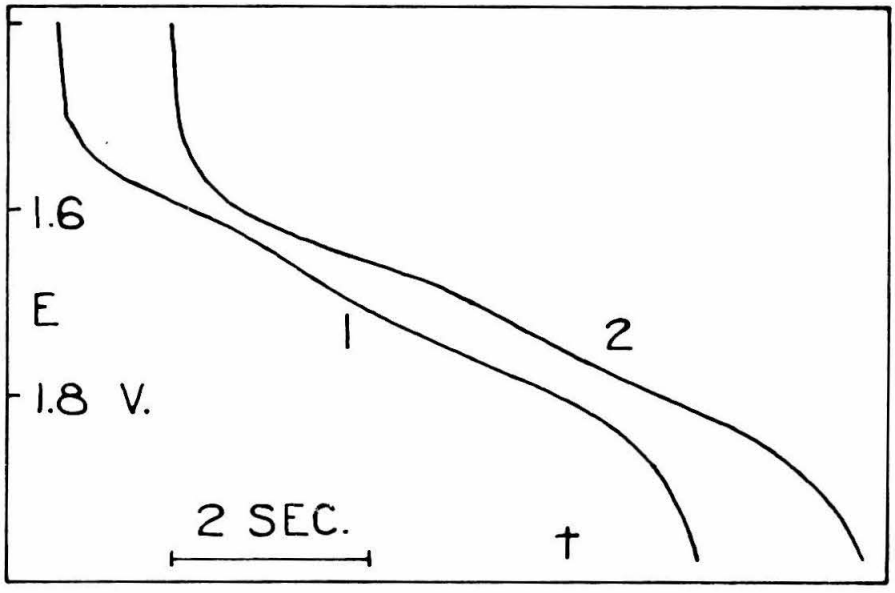

FIG. II-12

10.5 mM tetrabutylammonium dichloracetate, 0.20 M tetraethylammonium perchlorate, 1.29 ma/cm^2 (1) air-saturated (2) deaerated

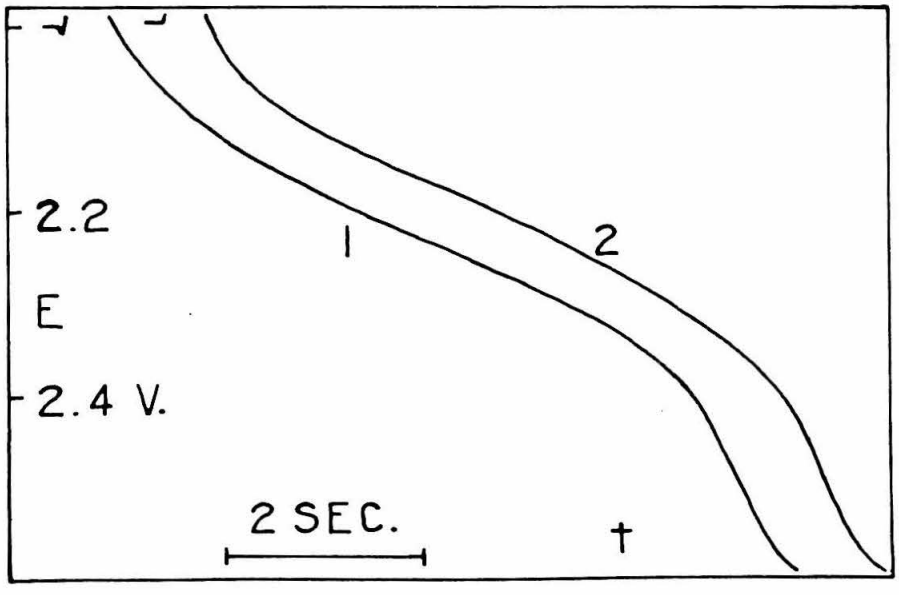

FIG. II-13

8.1 mM tetrabutylammonium trifluoroacetate, 0.20 M tetraethylammonium perchlorate, 1.20 ma/cm^2 (1) air-saturated (2) deaerated

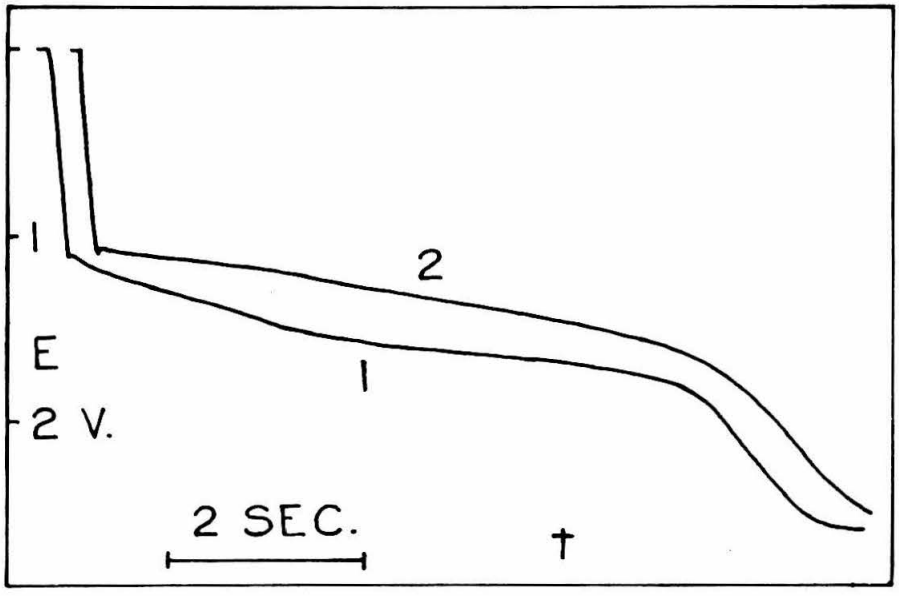

FIG. II-14

11.6 mM tetrabutylammonium cyanoacetate, 0.20 M tetraethylammonium perchlorate, 1.50 ma/cm^2 (1) air-saturated (2) deaerated

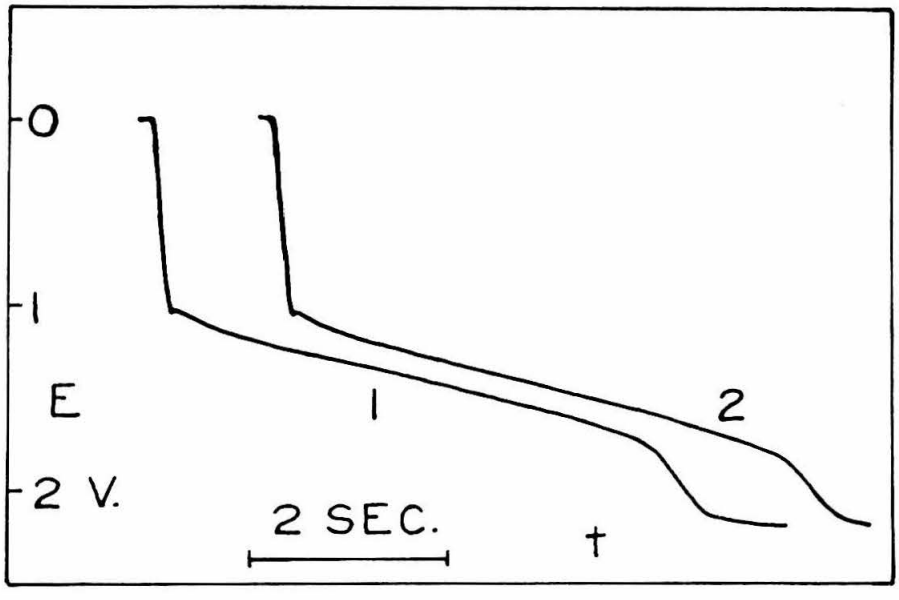

FIG. II-15

9.8 mM tetrabutylammonium aminoacetate, 0.20 M tetraethylammonium perchlorate, 1.41 ma/cm^2 (1) air-saturated (2) deaerated

TABLE II-3

IONIC DIFFUSION COEFFICIENTS
in 0.20 M $(C_2H_5)_4NClO_4$
in CH_3CN

Species	$i\tau^{1/2}/c$ $\frac{cm\text{-}sec^{1/2}\text{-}amp}{moles}$	Diffusion Coefficient D x 10^6 cm^2/sec
Trifluoroacetate	373	9.54
Hydrogen malonate	365	9.12
Glycolate	356	8.69
Hydrogen dimethylmalonate	354	8.59
Acetate	353	8.54
Propionate	350	8.40
Cyclopropanecarboxylate	344	8.11
Cyanoacetate	340	7.92
Dichloroacetate	338	7.83
Isobutyrate	337	7.78
Butyrate	336	7.74
Methoxyacetate	334	7.65
Trimethylacetate	333	7.60
Isovalerate	332	7.55
T-butylacetate	329	7.42
Ethoxyacetate	327	7.33
Cyclohexanecarboxylate	326	7.28
Aminoacetate	324	7.20

FIG. II-16

VARIATION OF $E_{1/4}$ WITH WATER CONTENT

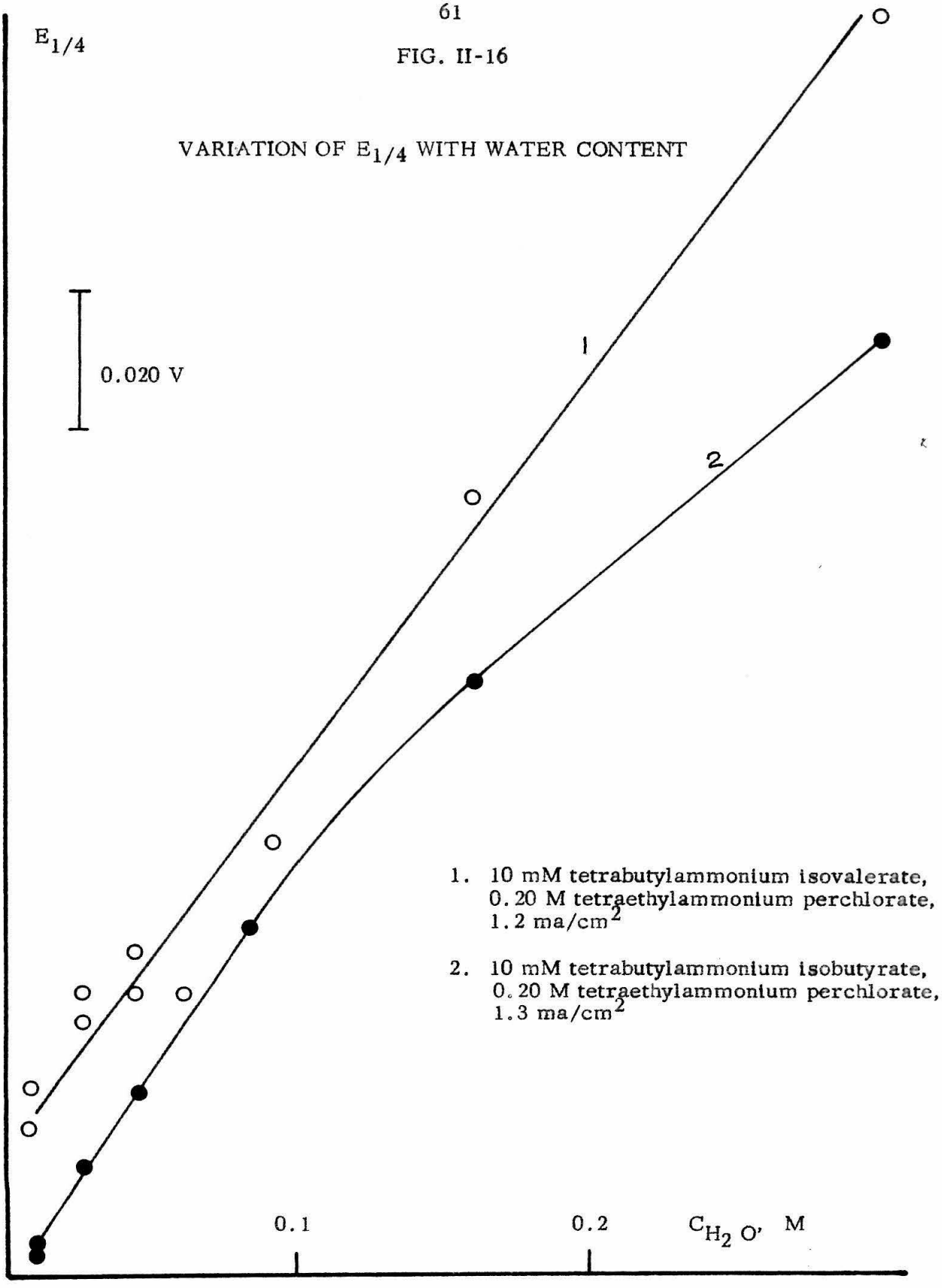

TABLE II-4

EFFECT OF SUPPORTING ELECTROLYTE CONCENTRATION

Concentration of $(C_2H_5)_4NClO_4$	12 mM tetrabutylammonium pivalate, 1.6 ma/cm^2		10 mM tetrabutylammonium isovalerate, 1.4 ma/cm^2	
	$E_{1/4}$	$n\alpha$	$E_{1/4}$	$n\alpha$
0.2 M	1.133	.305	1.281	.231
0.3	1.146	.314	1.292	.216
0.4	1.140	.304	1.295	.211

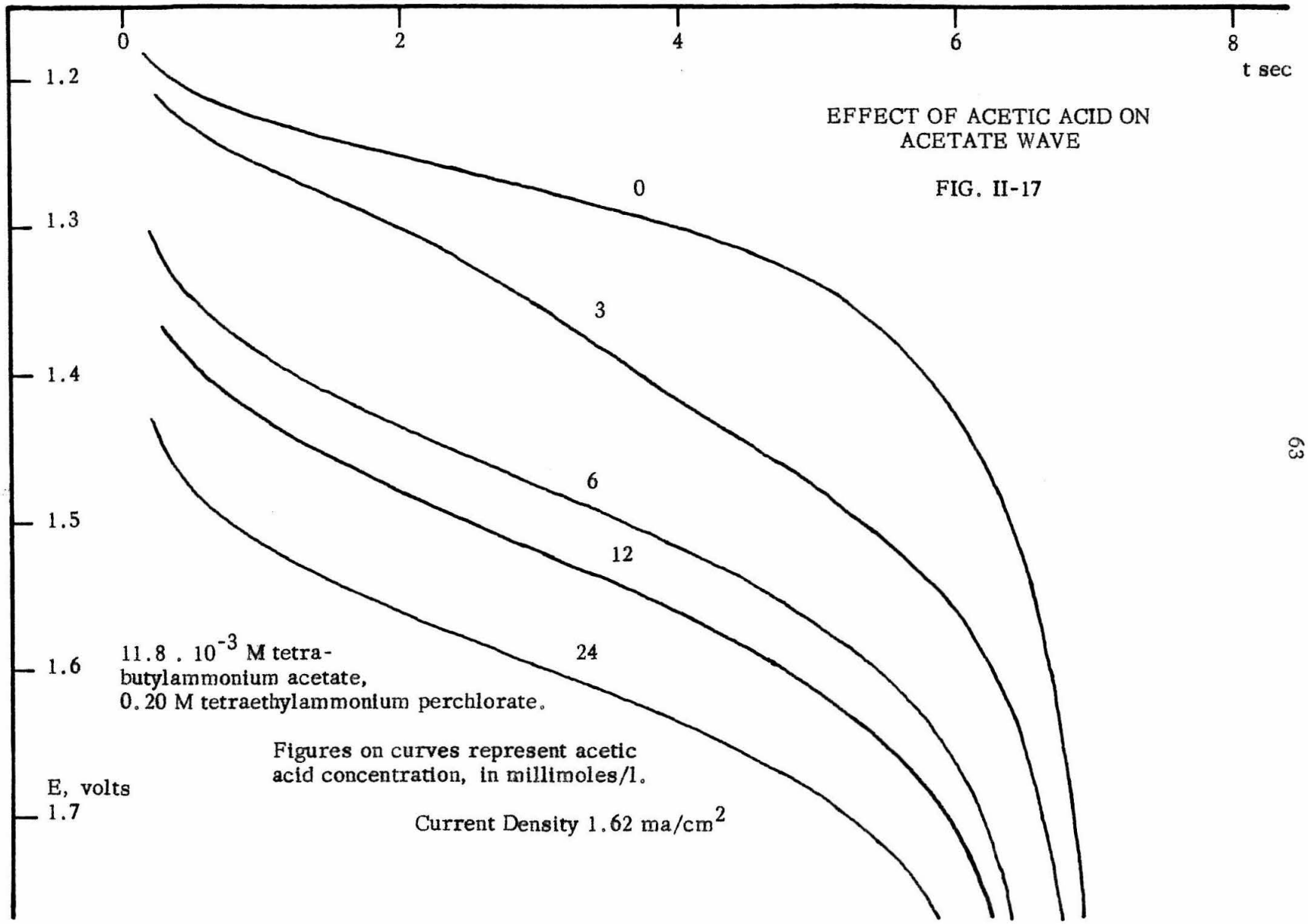

EFFECT OF ACETIC ACID ON ACETATE WAVE

FIG. II-17

Upon current reversal before the transition time, waves were found in the case of the following salts: acetate, cyclopropanecarboxylate, cyclohexanecarboxylate, acetylglycinate, methoxyacetate, cyanoacetate, trifluoroacetate, dichloroacetate, and tetrabutylammonium hydrogen malonate. Di-tetrabutylammonium malonate failed to show a reverse-current wave. No other salts were tested. The transition times and potentials for the reverse waves are listed in table II-5. There is clearly a tendency for the transition time τ_2 of the current-reverse wave to become longer relative to the duration t_1 of the anodic current as the current density increases and as t_1 becomes a smaller fraction of the anodic transition time τ_1. The data of table II-6 show the reverse-current wave to be diffusion controlled.

Discussion

The most striking feature of these results is the existence of the current-reverse wave, since the expected oxidation products of most of the carboxylates studied are not reducible at the electrode. The reverse-current data of table II-5 can best be explained by simultaneous carboxylate ion discharge

$$RCOO^- = R\cdot + CO_2 + e^- \qquad (5)$$

and oxidation of water introduced with the "dried" tetrabutylammonium carboxylate

$$2H_2O + 4RCOO^- = O_2 + 4RCOOH + 4e^- \qquad (6)$$

The effect of carboxylate ion on the ease with which water is oxidized is rather drastic for a simple pH effect (1.2 volts or more in some cases, which would

TABLE II-5

DATA FROM REVERSE-CURRENT CHRONOPOTENTIOGRAMS
(0.20 M tetraethylammonium perchlorate supporting electrolyte)

Salt	Concentration mM	Current Density ma/cm^2	t_1 sec	τ_2 sec	$\frac{\tau_2}{t_1}$	$E_{.22}$ volts	τ_1 sec	$\frac{t_1}{\tau_1}$
Acetate	12.95	.795	5.23	.75	.144	1.46	33.2	.16
	12.95	.795	6.30	.79	.125	1.47	33.2	.19
	12.95	.795	6.90	.95	.138	1.44	33.2	.21
	12.95	.795	6.02	.93	.154		33.2	.18
	12.95	.795	2.64	.72	.273		33.2	.08
	12.95	.795	1.93	.65	.337		33.2	.06
	12.95	6.8	.275	.040	.145		.30	.92
	12.95	.795	6.26	1.18	.189	1.38	33.2	.19
	12.95	.795	3.25	.87	.268	1.39	33.2	.10
	12.95	1.626	5.61	.45	.0803		7.90	.71
	12.95	1.626	2.26	.39	.173		7.90	.28
	12.95	13.6	.069	.011	.160		.080	.86
	12.95	13.6	.040	.010	.250		.080	.50
Methoxyacetate								
	8.89	.789	5.50	.75	.136	.98	14.2	.39
	8.89	.789	3.70	.78	.211	.94	14.2	.26
	8.89	13.6	.036	.014	.389		.048	.75
Trifluoroacetate								
	7.87	.795	5.32	1.35	.254	.59	13.7	.39
	7.87	.795	5.54	1.22	.220	.58	13.7	.40
	7.87	.795	4.73	1.20	.254	.58	13.7	.35
	7.87	.795	2.40	.64	.267	.65	13.7	.18
	7.87	.789	5.77	1.44	.250	.59	13.7	.42
	7.87	1.417	4.07	.72	.177		4.30	.95
	7.87	13.6	.045	.018	.400		.047	.96
Dichloroacetate								
	10.58	.799	5.55	2.4	.43	1.06	20.0	.28
	10.58	.799	4.47	1.7	.38	1.00	20.0	.22
	10.58	13.6	.052	.020	.384		.069	.75
Hydrogen Malonate								
	8.90	.795	4.81	1.38	.287	.76	16.7	.29
	8.90	.795	5.25	1.25	.238	.77	16.7	.31
	8.90	.795	5.97	1.60	.268	.77	16.7	.36
	8.90	1.210	6.07	1.58	.260	.79	7.20	.84
	8.90	1.210	6.50	1.60	.246	.77	7.20	.90
	8.90	1.210	5.38	1.29	.240	.77	7.20	.75
	8.90	1.210	6.69	1.50	.224	.76	7.20	.93

TABLE II-5

Salt	Concentration mM	Current Density ma/cm^2	t_1 sec	τ_2 sec	$\frac{\tau_2}{t_1}$	$E_{.22}$ volts	τ sec	$\frac{t_1}{\tau_1}$
Cyanoacetic	11.70	1.503	4.75	1.50	.316	1.25	7.00	.68
	11.70	1.503	5.25	1.31	.250	1.20	7.00	.75
	35.9	4.86	5.20	1.28	.246		6.30	.83
	35.9	4.86	4.96	1.25	.252	1.45	6.30	.79
	35.9	6.8	1.6	0.46	.288		3.2	.50
	35.9	6.8	1.2	.32	.266		3.2	.38
Cyclopropanecarboxylate								
	8.80	13.6	.040	.012	.33		.050	.80
	8.80	.586	5.34	.91	.170	1.58	26.6	.20
	8.80	.586	5.66	1.03	.182	1.59	26.6	.21
	8.80	.586	1.49	.56	.376	1.39	26.6	.06
	8.80	1.210	2.02	.31	.153		6.38	.22
	8.80	1.210	5.59	.42	.075		6.38	.88
	9.31	.580	4.57	1.01	.221		30.5	.15
	9.31	.580	5.65	.85	.150	1.78	30.5	.18
	9.31	.580	4.30	.85	.198	1.77	30.5	.14
Cyclohexanecarboxylate								
	9.30	.580	5.78	.111	.193	1.53	27.4	.21
	9.30	.580	2.29	.80	.350	1.40	27.4	.08
	9.30	1.095	4.91	1.03	.210		7.67	.64
	9.30	1.095	1.46	0.30	.206		7.67	.19
	9.30	13.6	.042	.08	.190		.050	.84
Aminoacetate								
	10.32	.790	5.00	.60	.120	1.04	29.4	.17
	10.32	.790	6.54	.73	.112		29.4	.22
	10.32	.790	1.62	.38	.234	1.10	29.4	.055
	10.32	1.207	6.98	.40	.0574		7.71	.91
	10.32	1.207	2.30	.30	.130		7.71	.30
	10.32	13.6	.036	.010	.278		.061	.59

TABLE II-6

TRANSITION TIME FOR REVERSE-CURRENT WAVE
36 mM tetrabutylammonium cyanoacetate
0.20 M tetraethylammonium perchlorate

Anodic Current ma	t_1 sec	Cat. Current ma	τ_2 sec	t_1/τ_2 (observed)	t_1/τ_2 (theoretical)*
6.8	1.2	6.8	.32	3.8	3
6.8	1.2	17	.084	14	11
6.8	1.2	33	.039	39	32
6.8	1.2	60	.011	110	90

* For diffusion control (5).

correspond to a change of 20 pH units if the reaction were reversible). It is likely that water associates directly with carboxylate ion to a significant extent and the species which reacts at the electrode to produce oxygen and acid may be the water-carboxylate complex. Similar hydrogen-bond complexes have been observed many times in acetonitrile solutions: between carboxylate anions and their conjugate acids (20, 67), between water and amines (68), between inorganic acids and their anions (69), and between nitrogen bases and their conjugate acids (20, 68). The current-reverse wave is thus attributed to the reduction of oxygen and of the acid formed in reaction 6.

$$2e^- + RCOOH + O_2 = RCOO^- + HO_2^- \quad (7)$$

$$2e^- + 2RCOOH = 2RCOO^- + H_2 \quad (8)$$

Since reduction of oxygen proceeds only to peroxide as discussed in Part I of this thesis, surplus acid remains which is directly reduced to elemental hydrogen. The oxygen reduction wave merges with the wave for the reduction of acid and distinct waves are not seen. Thus in Figure II-18 the first part (steep slope) of the reverse wave following cyanoacetate oxidation is due to oxygen reduction and the rest (flat slope) to cyanoacetic acid reduction. For comparison a chronopotentiogram is also shown for the reduction of cyanoacetic acid in a solution prepared from cyanoacetic acid and tetrabutylammonium acetate, containing tetraethylammonium perchlorate supporting electrolyte and saturated with air. Here too the oxygen and hydrogen waves merged (with suitable electrode pretreatment). The curve illustrated agrees in appearance and in potential with the reverse wave for cyanoacetate. It was also verified that the reverse waves for acetate and for hydrogen malonate occurred at the same potentials (± 0.2 V) as the reduction of the conjugate acids. The parallel between the

FIG. II-18

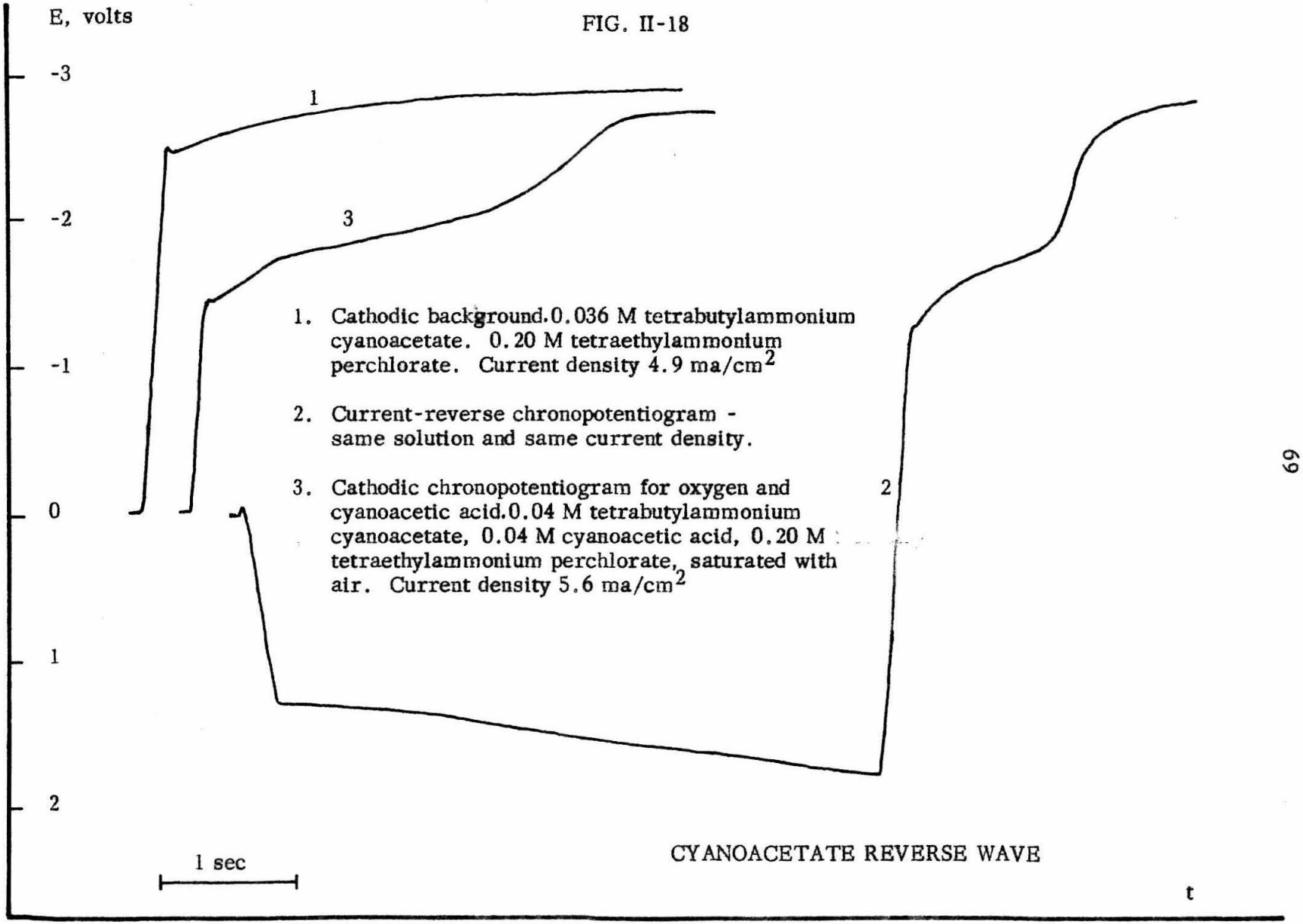

1. Cathodic background. 0.036 M tetrabutylammonium cyanoacetate. 0.20 M tetraethylammonium perchlorate. Current density 4.9 ma/cm^2

2. Current-reverse chronopotentiogram - same solution and same current density.

3. Cathodic chronopotentiogram for oxygen and cyanoacetic acid. 0.04 M tetrabutylammonium cyanoacetate, 0.04 M cyanoacetic acid, 0.20 M tetraethylammonium perchlorate, saturated with air. Current density 5.6 ma/cm^2

CYANOACETATE REVERSE WAVE

potential of the reverse wave and the basicity of the carboxylate ion can be seen clearly in table II-5. When the ratio of anodic to cathodic current was varied, the transition time of the reverse wave changed in the manner predicted for a diffusion-controlled process (table II-6), ruling out the possibility that the reverse wave could be due to an oxide (or other) film on the electrode surface. The cathodic wave vanished if the solution was stirred between the anodic and cathodic current pulses. No reverse wave was found for the first oxidation step of di-tetrabutylammonium malonate, alone among the carboxylates for which reverse waves were sought, as one would predict from the fact that the hydrogen malonate ion is not reduced before the cathodic background. These data point to the generation of hydrogen ion at the electrode, apparently by reaction 6. Oddly, though, the potential of the anodic wave is relatively insensitive to the water content of the solution, increasing with increasing amounts of water (fig. II-16).

The oxidation of water does not affect the anodic transition time since carboxylate anion is removed by reaction 6 as well as by reaction 5. The diffusion coefficients of table II-3, calculated from the transition time, show a distinct trend toward smaller values with increasing size and increasing basicity. The basicity of the anion presumably influences the diffusion coefficient by influencing the degree of solvation; evidently the strongest base is most highly solvated. Aminoacetate has the lowest diffusion coefficient in the list and trifluoroacetate the highest, reflecting the difference in base strength. Subordinate to the effect of base strength, the effect of increased ionic size within the series is quite clear.

The data of table II-5 show that oxidation of water occurs nearly to the exclusion of carboxylate ion discharge in the chronopotentiometric waves for the more difficultly oxidized salts (trifluoroacetate, hydrogen malonate, dichloroacetate). Oxidation of water was appreciable in all cases. It occurs principally in the first part of the wave as shown by the large value of the ratio $\frac{\tau_2}{t_1}$ when $\frac{t_1}{\tau_1}$ is small. It is more significant at high current densities and correspondingly short transition times. These facts are perhaps due to the generation of acid at the electrode surface which inhibits the further oxidation of water, or to inhibition of water oxidation by the simultaneous Kolbe reaction as observed in aqueous solution (55). The high yield of carbon dioxide which was found in the electrolysis of a tetrabutylammonium acetate-acetic acid solution in acetonitrile may be attributed in part to these factors, as well as to the low water content attained by using tetrabutylammonium acetate crystals containing acetic acid of crystallization in place of water-containing tetrabutylammonium acetate, and to the fact that much of the moisture present could have been consumed while the system was coming to steady state before measurement was begun.

The parameters of table II-1 describing the anodic chronopotentiometric waves for carboxylate salts in acetonitrile must be interpreted in terms of a mixed process, principally the oxidation of the carboxylate anion in the case of those waves which occur at lower potentials (alkyl-substituted acetates, alkoxyacetates) and principally the oxidation of water in the case of those waves which occur at higher potentials (dichloroacetate, hydrogen malonate, trifluoroacetate). The measured quarter-wave potentials and transfer coefficients for those salts which yielded linear plots of E vs. $\log \left[1 - \left(\frac{t}{\tau}\right)^{1/2}\right]$ reflect largely the discharge of the carboxylate anion and can be compared on a qualitative basis.

Substitution of successive methyl groups on the acetate ion make it progressively easier to oxidize (table II-7).

TABLE II-7

QUARTER-WAVE POTENTIALS
FOR SOME SUBSTITUTED ACETATES

	$E_{1/4}$ Air-Saturated Soln.	$E_{1/4}$ Deaerated Soln.
Acetate	1.26	1.25
Propionate	1.23	1.20
Isobutyrate	1.16	1.12
Pivalate	1.12	1.13
Butyrate	1.27	1.25
T-butylacetate	1.26	1.28
Methoxyacetate	1.10	1.14
Ethoxyacetate	1.15	1.18

This must be due in part to the electron-donating inductive effect of the methyl group, for inductive effects clearly operate to make trifluoroacetate, say, much more difficultly oxidized than acetate. But it could also be partly attributable to stabilization of the alkyl radical if decarboxylation occurs at the moment of discharge. An effect of the sort has been reported by Bartlett and Hiatt (70) in the decomposition of peresters, where decarboxylation follows rupture of the O-O bond in some cases and accompanies it in others. This interpretation finds support in the ease of oxidation of methoxyacetate and ethoxyacetate. Substitution of a single alkyl group larger than methyl into the acetate ion does not significantly affect its oxidation potential and one might suppose that here the inductive

and radical-stabilizing influence is counterbalanced by steric hindrance.

It is noteworthy that the transfer coefficient remained practically constant throughout the series of alkyl- and alkoxy-substituted acetates. This supports the viewpoint (45, 46, 47) that the rate-determining activation process in electron transfer at the electrode is reorganization of the solvation hull since this process would be relatively insensitive to substituent effects.

The slight distortion of the chronopotentiometric waves in oxygen-bearing solutions may be due to the supersaturation of the solution adjacent to the electrode with electrolytically produced oxygen and consequent accumulation of gas on the electrode surface or else to the reaction of dissolved oxygen with anodically generated radicals to form products which are adsorbed on the electrode surface. The oxidation of water is too irreversible for dissolved oxygen to influence it directly. The oxygen concentration at the electrode surface expected from reaction 6 was somewhat less than that present in air-saturated acetonitrile under the conditions of measurement.

The wave for tetrabutylammonium hydrogen malonate and the second wave for di-tetrabutylammonium malonate showed an exceptional sensitivity to the presence of oxygen for which no explanation can be offered (figs. II-8, II-9). The effect was definitely due to oxygen, for the passage of dried air through a solution which had been deaerated with nitrogen reversed the effect of deaeration. Dimethylmalonates did not show the same behavior.

The discovery of carboxylate-induced water oxidation at platinum electrodes in acetonitrile is of dismaying significance for the study of the Kolbe reaction in this solvent. To study the Kolbe discharge free from interference it will be necessary to prepare completely anhydrous solutions of the carboxylate ions in

acetonitrile. No acetates other than tetraalkylammonium acetates are known which are soluble in acetonitrile; tests showed that lithium, ammonium, guanidinium, mercuric, and silver acetates are all practically insoluble. (If silver or mercuric acetate were soluble it would be possible to remove the cation by electrolysis, replacing it with tetraalkylammonium ion by migration from a salt bridge.) Attempts were made to produce acetate by the direct electrolytic reduction of acetic acid at a platinum electrode in acetonitrile; the solution became discolored, indicating side reactions, and it appeared that this approach would not yield solutions of the purity required for reliable kinetic measurements. In principle anhydrous solutions of carboxylate salts could be prepared by the direct neutralization of the acid by a non-hydroxylic base in acetonitrile, but the neutralization must proceed to reasonable completion for the electrode process to be simple enough to interpret in an unambiguous fashion. It would be difficult to find a suitable base. Kilpatrick and Kilpatrick (71) found acetate ion to be a stronger base in acetonitrile than any of a series of (neutral) organic bases which they investigated. Because of the poor ability of acetonitrile to solvate ions, the reaction of neutral molecules to form ions in this solvent is inhibited. The fact that many organic bases can readily be oxidized at the anode compounds the problems. Another approach would be to suppress the oxidation of water by adding acid; Figure II-17 shows that this is hardly satisfactory since the excess acid also seems to influence the electrode process, probably by association with the carboxylate ion (see above). The use of heat to dry the tetrabutylammonium carboxylate salts was not attempted; several of the salts decomposed even when dried at room temperature (see above). Some of the salts could possibly be dried in this way, but probably not enough of them to

permit a systematic study of the kind attempted. A possibility which was not tried is the removal of water from the tetraalkylammonium salt solutions by distilling out the water — acetonitrile azeotrope.

PART III

OXIDATION OF SUBSTITUTED FERROCENES

Introduction

Oxidation potentials for substituted ferrocenes in acetonitrile have been measured chronopotentiometrically by Kuwana, Bublitz and Hoh (3) and by Hoh, McEwen and Kleinberg (4). Kuwana, Bublitz and Hoh correlated reversible quarter-wave potentials for substituted ferrocenes with the Taft σ^* constants for the substituents (72). Hoh, McEwen and Kleinberg correlated quarter-wave potentials with Taft σ^*, Hammett σ_m, and Hammett σ_p. They found all data to be correlated with Hammett σ_p and most of the data to be correlated with Taft σ^*. The correlation with Hammett σ_m was less satisfactory. Tirouflet and Boichard (73) reported half-wave potentials for the oxidation of a few substituted ferrocenes at a rotated platinum electrode in ethanol-water. Mason and Rosenblum (74) measured oxidation potentials for para-substituted phenylferrocenes by potentiometric titration in acetic acid-water. The measured potentials correlated with Hammett σ_p.

Chronopotentiometric quarter-wave potentials in acetonitrile have now been measured for a number of new compounds, permitting a re-evaluation of the $\rho\sigma$ correlation. Many of these are polysubstituted and the data provide a good test of the additivity of the substituent effects. A prediction by Kuwana, Bublitz and Hoh regarding the chronopotentiometric reversibility of bridged ferrocene compounds has been tested.

This work was done in collaboration with David Hall, in conjunction with a more exhaustive study of substituent effects in metallocene compounds on his part.

Experimental

Solutions of approximately 2 mM concentration in the ferrocene compound and 0.20 M in reagent grade anhydrous $NaClO_4$ (G. F. Smith Chemical Company) were prepared using spectral grade acetonitrile (Matheson, Coleman and Bell Company). The electrolysis cell was described in Part I of this thesis. The cracked-bead reference electrode described in Part I was used, except that 0.0100 M $AgClO_4$, 0.20 M $NaClO_4$ was used in place of silver nitrate solution. The current source was a Wenking potentiostat (Elektronische Werkstätten, Göttingen, Germany) which controlled the voltage across a standard resistor in series with the cell and hence the current through the cell. Chronopotentiograms were recorded on a Moseley X-Y-time recorder connected to the anode and to the reference electrode through two follower amplifiers of the DeFord type (13) constructed with George A. Philbrick Company plug-in amplifiers. The ohmic drop between anode and reference electrode was measured using a method described by Anson (14) and found to be only a few millivolts; due correction was made to the measured potentials. All measurements were performed at 25.0° C.

Preparation of the ferrocene compounds will be described elsewhere by D. Hall.

Results and discussion

The measured quarter-wave potentials are given in tables III-1 and III-2. Previously reported quarter-wave potentials in acetonitrile are given in table III-3. The data of Kuwana, Bublitz and Hoh, measured with respect to the saturated calomel electrode, were converted to our potential scale by subtracting 0.241 V. A correction of 0.269 V was subtracted from the data of Hoh, McEwen, and Kleinberg, also measured with respect to the saturated

TABLE III-1

OXIDATION POTENTIALS
FOR REVERSIBLY OXIDIZED FERROCENE DERIVATIVES

Substituent	$E_{1/4}$ 0.010 V.
1, 1'-$(C_2H_5OCONH)_2$ -	-.076
1, 1'-$(CH_3OCONH)_2$ -	-.074
CH_3OCONH -	-.007
CH_3CONH -	-.005
CH_3O -	.005
$HO(CH_2)_4$ -	.039
H_2NCH_2 -	.039 (b)
CH_3CHOH -	.062
H -	.063
$CH_3CH(OCH_3)$ -	.081
$CH_3CH(OCOCH_3)$ -	.140
3 - CH_3CO-1, 1'-$(CH_3)_2$ -	.211
1'-CH_3CO-1-CH_3OCONH -	.220
1'-CH_3CO-1-CH_3CONH -	.234
2-CH_3CO-1-CH_3CONH -	.313
1, 1' - Br_2 -	.380
NC -	.438
1'-CH_3CO-1-Br -	.469
1'-CH_3CO-1-Cl -	.490
1, 1'-$(CH_3CO)_2$ -	.551
1'-CH_3CO-1-CN -	.661 (a)

(a) Assumed reversible, but reversibility was not checked
(b) First of two waves

TABLE III-2

OXIDATION POTENTIALS
FOR IRREVERSIBLY OXIDIZED METALLOCENE COMPOUNDS

Compound	$E_{1/4}$ Volts	i ma/cm^2	$10^3 C$ moles/l
3-acetyl-1-1'-di(ethoxy-carbonylamino) ferrocene	.217	.15	1.6
3-acetyl-1-1'-trimethylene-ferrocene	.263	.26	1.9

TABLE III-3

OXIDATION POTENTIALS
FOR REVERSIBLY OXIDIZED FERROCENE DERIVATIVES

A. Data from Kuwana, Bublitz and Hoh (3)

Substituent	$E_{1/4}$
1, 1'-$(C_2H_5)_2$ -	-.047
C_2H_5 -	.004
CH_3CHOH -	.057
H -	.066
C_6H_5CHOH -	.077
CH_2=CH -	.084
HOOC -	.309
C_6H_5CO -	.330
CH_3CO -	.332
1, 1' -$(CH_3CO)_2$ -	.555

B. Data from Hoh, McEwen and Kleinberg (4)

Substituent	$E_{1/4}$
$(C_{10}H_{21})_2$ -	-.047
1, 1'-$(C_2H_5)_2$ -	-.045
$(C_8H_{17})_2$ -	-.041
1, 1' -$(CH_3)_2$ -	-.028
$CH_3CHC(CH_3)_3$ -	-.011
C_2H_5 -	.012
CH_3 -	.012
n-C_3H_7 -	.015

TABLE III-3

Substituent	$E_{1/4}$
i-C_3H_7 -	.017
sec-C_4H_9 -	.019
1, 1' -$(C_6H_5CH_2)_2$ -	.027
$C_6H_5(CH_2)_2$ -	.027
$CH_3CH_2CH(C_6H_5)$ -	.036
$C_6H_5CH_2$ -	.045
$CH_3CH(C_6H_5)$ -	.046
$CH_3CH = CH$ -	.047
$C_6H_5CH = CH$ -	.059
CH_3OCH_2 -	.071
H -	.072
$(CH_3)_3Si$ -	.077
Bis - $(CH_3)_3Si$ -	.077
C_6H_5 -	.097
1, 1' - $(C_6H_5)_2$ -	.101
$C_6H_5COCH_2$ -	.109
CH_3CO -	.318
$C_6H_5CH = CHCO$ -	.325
CHO -	.355
p-$CH_3OC_6H_4$ -	.054
p-ClC_6H_4 -	.118
p-BrC_6H_4 -	.127
p-$CH_3COC_6H_4$ -	.157
p-$NO_2C_6H_4$ -	.195

calomel electrode. These values were chosen to give best agreement between quarter-wave potentials measured by different investigators for identical compounds. The difference between the two correction factors above reflects the difference between quarter-wave potentials reported by the two groups for identical compounds and is probably due to differences in the liquid-junction potentials for their calomel electrodes. We chose the silver-silver perchlorate electrode only after experiencing difficulty with the saturated calomel electrode.

Figures III-1 and III-2 are plots of chronopotentiometric quarter-wave potentials against $\Sigma\sigma_p$ and $\Sigma\sigma_m$. All compounds are plotted for which reversible quarter-wave potentials and Hammett substituent constants are available. The substituent constants are those tabulated by McDaniel and Brown (75). For the urethanes, the σ_p and σ_m reported by Kaplan were used (76). The plot of $E_{1/4}$ vs. $\Sigma\sigma_p$ is fairly linear, in accordance with the findings of Hoh, McEwen, and Kleinberg (4), but those compounds (amides and urethanes) having nitrogen on the ring position deviate badly. Oxidation potentials for the nitrogen compounds have not been previously reported. Overall correlation with $\Sigma\sigma_m$ is poorer unless the compounds having oxygen, halogen, or nitrogen in the ring position are disregarded, in which case the correlation becomes exceedingly good. This suggests that these nucleophilic substituents can coordinate directly with the positive iron atom in the ferrocinium ion, stabilizing it and causing $E_{1/4}$ to deviate from the Hammett plot in the negative direction as in Figure III-2. The inductive and resonance effects of the substituents are better represented by σ_m than by σ_p but since the substituents capable of corrdinating with the iron happen to be electron donors by resonance, their effect on the oxidation potential correlates better with σ_p than with σ_m if the direct interaction is not taken into account. This fortuitous correlation with σ_p breaks down badly for the nitrogen compounds studied as seen in Figure III-1.

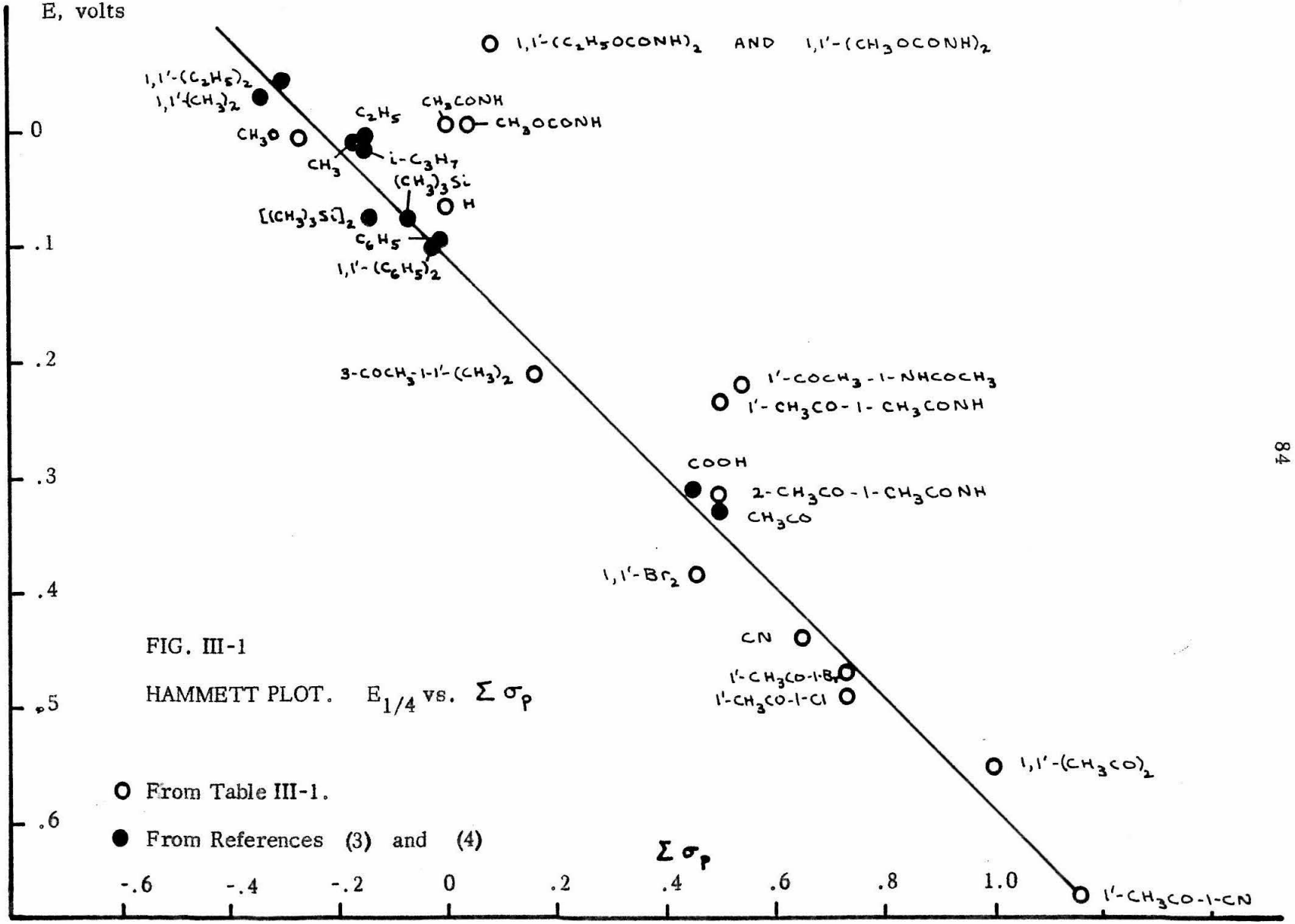

FIG. III-1

HAMMETT PLOT. $E_{1/4}$ vs. $\Sigma \sigma_p$

○ From Table III-1.

● From References (3) and (4)

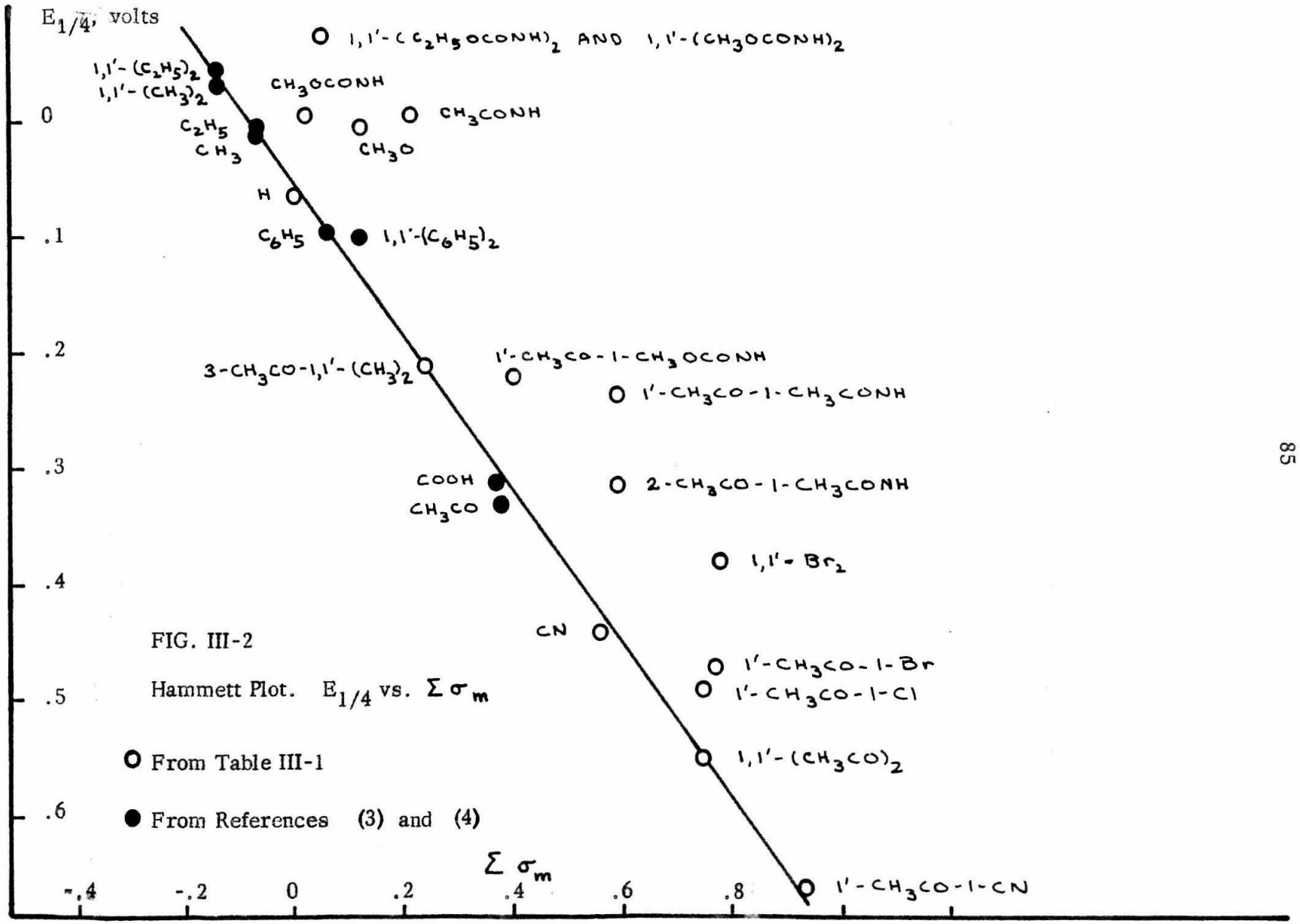

FIG. III-2

Hammett Plot. $E_{1/4}$ vs. $\Sigma \sigma_m$

O From Table III-1

● From References (3) and (4)

Equations of the regression lines for the two plots, eliminating substituents having oxygen, nitrogen, or halogen attached to the ring from the $\Sigma\sigma_m$ plot and eliminating substituents having nitrogen attached to the ring from the $\Sigma\sigma_p$ plot, are:

$$E_{1/4} = 0.663\,\Sigma\sigma_m + 0.055$$
$$E_{1/4} = 0.478\,\Sigma\sigma_p + 0.110 \qquad (1)$$

The correlation coefficients are 0.998 for the $\Sigma\sigma_m$ plot and 0.993 for the $\Sigma\sigma_p$ plot.

The deviations from the $\Sigma\sigma_m$ plot by compounds having substituents which interact with the iron are additive and independent of other substituents. The deviation caused by the methoxycarbonylamino group is thus 0.08 V for methoxycarbonylaminoferrocene, 0.08 V per methoxycarbonylamino group for 1, 1'-bis(methoxycarbonylamino)ferrocene, and 0.10 V for 1'-acetyl-1-methoxycarbonylaminoferrocene. The deviation caused by bromo-substitution is 0.09 V in 1'-acetyl-1-bromoferrocene and 0.09 V per bromine for 1, 1'-dibromoferrocene. The deviation caused by the N-acetylamino group is 0.20 V in N-acetylaminoferrocene and 0.20 V in 1'-acetyl-1-(N-acetylamino)ferrocene. These results can hardly be fortuitous and thus substantiate the foregoing argument.

Taking into account deviations due to direct interaction with the central iron, the subetituent effects were additive for the wide variety of polysubstituted ferrocenes studied with a single exception. The compound 2-acetyl-1-(N-acetylamino)ferrocene was oxidized at a potential 0.13 V more positive than predicted. Internal hydrogen bonding has been detected in the infrared spectrum of this compound (77) and apparently either the hydrogen bonding prevents the nitrogen from donating electrons as effectively to the positive iron or else the energy of hydrogen bonding is lost when the nitrogen coordinates with the iron. Since the

deviations due to direct interation with the iron are additive it would be possible to define a set of σ constants which would take this interaction into account.

The data of table III-1 indicate that nitrogen or oxygen in the α position cannot interact with the positive iron as they do on the ring position. Methylferrocenylcarbinol is slightly harder to oxidize than ethylferrocene and (aminomethyl)ferrocene is slightly harder to oxidize than methylferrocene, corresponding simply to the inductive effects of the hydroxyl and amino groups.

Hill and Richards (81, 82, 83, 84) have proposed a direct interaction between the iron atom in ferrocene and an alpha carbonium ion. Their case is based on stereochemical and kinetic data. They found, for example, that the hydrolysis (S_N1) of the exo isomer of α-acetoxy-1,2-tetramethyleneferrocene was faster by a factor of 2500 than the rate of hydrolysis of the endo isomer. An argument in terms of molecular orbital theory was presented for the feasibility of direct interaction and it was concluded that if the entire cyclopentadienyl ring were shifted slightly to bring the positive center closer to the iron atom, significant interaction could be expected. A similar shift in the position of the ring may be necessary to account for the interaction which is discussed here. If no distortion takes place on forming the positive ion from the neutral molecule, the Fe-Cl distance in the chloroferricinium ion may be estimated as 3.23 Å and the Fe-Br distance in the bromoferricinium ion is 3.37 Å using known covalent radii (85), the interatomic distance for ferrocene (86), and the assumption that the substituent is coplanar with the ring. For comparison, the iron-halogen distance is 2.48 Å in ferric chloride (87) and 2.63 Å in ferric bromide (88). The interatomic distances seem rather long for an interaction of the sort proposed here unless some distortion of the molecule occurs, such as the ring shift suggested by Hill and Richards.

The interaction proposed by Hill and Richards involves nucleophilic behavior on the part of the iron atom, while that proposed here involves electrophilic behavior. This is associated with a difference in electrical charge on the iron atom in the two cases. One can reasonably expect the positive charge borne by the iron atom in the ferricinium ion to greatly enhance its electrophilic properties.

Kuwana, Bublitz, and Hoh have suggested that the reversibility of the electrode reaction for hindered ferrocene derivatives might be connected with the free rotation of the cyclopentadienyl rings and that if the rings were tied together the process might become irreversible. We have found this to be the case for 3-acetyl-1,1'-trimethylene-ferrocene. No reverse wave at all was found, though, and the irreversibility appears due to decomposition of the product rather than slow electron transfer. The oxidation potential was only 0.052 V more positive than for the related unbridged compound, 3-acetyl-1,1'-dimethylferrocene. 3-acetyl-1,1'-bis(ethoxycarbonylamino)ferrocene was similarly irreversible, having no distinct reverse wave.

APPENDIX

INTERPRETATION OF TOTALLY IRREVERSIBLE CHRONOPOTENTIOMETRIC WAVES

Introduction

The simplest case in chronopotentiometry is the case of direct discharge of a single species under conditions of linear diffusion. If the discharge is totally reversible the theoretical potential-time curve, derived by Delahay and Berzins (30) and confirmed experimentally by Delahay and Mattax (78), is the following:

$$E = \frac{RT}{\alpha n_a F} \ln \frac{nFck}{i} + \frac{RT}{\alpha n_a F} \ln \left[1 - \left(\frac{t}{\tau}\right)^{1/2}\right] \qquad (1)$$

where E is the electrode potential, t the time measured from the beginning of the pulse of constant current, n the number of electrons involved in the overall electrode reaction, n_a the number of electrons involved in the rate-determining discharge process, k the rate constant, α the transfer coefficient, i the current density, c the bulk concentration of the species undergoing discharge, R the gas law constant, T the absolute temperature, and F Faraday's constant. τ is the "transition time", $\tau = \frac{\pi n^2 F^2 c^2 D}{2i}$, where D is the diffusion coefficient of the discharging species. The rate constant and transfer coefficient may be clearly obtained from the slope and E-intercept of a plot of E versus $\log\left[1-\left(\frac{t}{\tau}\right)^{1/2}\right]$. Delahay and Mattax (78, 79) used this method to obtain rate constants and transfer coefficients for several electrode reactions, but the method has largely been neglected as a means of measuring electrochemical kinetic parameters.

A difficulty in the use of this method is the determination of an accurate transition time. The transition time is not precisely defined in a typical chronopotentiogram (cf. fig. A-2) due to the capacitance of the double layer and

to the commencement of secondary reactions. Three empirical graphical procedures have been suggested for determination of the transition time from an experimental chronopotentiogram, but no published evidence indicates that any of these methods will yield the transition time best suited for calculation of rate parameters by the method described above. In the analytical use of chronopotentiometry the transition time can be chosen as the time required to attain a predetermined potential which is, within limits, arbitrary. This enables measurement of transition times with a precision of perhaps 1% but the measured transition time will differ from the "true" transition time, the transition time corresponding to theory, unless the correct "endpoint" potential is fortuitously chosen. The error is compensated in an analytical method based on comparison of chronopotentiograms obtained under similar conditions using known and unknown solutions of approximately equal concentrations, but unfortunately no such cancellation of errors can occur when the transition time is used to calculate kinetic parameters.

In this appendix new methods are presented for the interpretation of totally irreversible chronopotentiometric waves, and both new and old methods are checked against a least-squares fit of eq. (1) to the experimental data for the reduction of iodate ion at a mercury pool in aqueous sodium hydroxide solution.

Experimental

Reagents. The electrolysis solution (0.00420 M KIO_3, 0.890 M NaOH) was prepared from reagent grade chemicals and doubly distilled water, the first distillation being from basic permanganate. All glassware contacting the solution was cleaned with sulfuric acid-potassium dichromate cleaning solution. Comparison tests using all-glass equipment, including a glass electrolysis cell, showed that the solutions could be stored in polyethylene bottles without picking up any surface-active organic material which affected the measurements.

The mercury used was either technical grade mercury which had been treated in an "oxifier" and then agitated by air bubbles under a dilute solution of nitric acid and hydrogen peroxide for twelve hours, or Mallinckrodt triply distilled mercury. In either case it was forced through sintered glass directly into the electrolysis cell. No difference was found between the two preparations.

Apparatus. The measuring circuits were those described in Part II of this thesis. The electrolysis cell is illustrated in Figure A-1. A polyethylene vessel was used to avoid penetration of solution between the mercury and the wall of the vessel. When a glass vessel was tried, even if great care was used in delivering the solution to the cell to avoid wetting the walls below the mercury level, only the first chronopotentiogram was undistorted. (Waves of very irregular shape were obtained at high current densities using the glass cell; water was driven visibly between glass and mercury by the pulse of current.) Contact with the mercury pool was made by a platinum wire sealed in a glass tube which was covered with Teflon electrical spaghetti, also to avoid penetration of water between mercury and glass. The saturated calomel reference electrode was

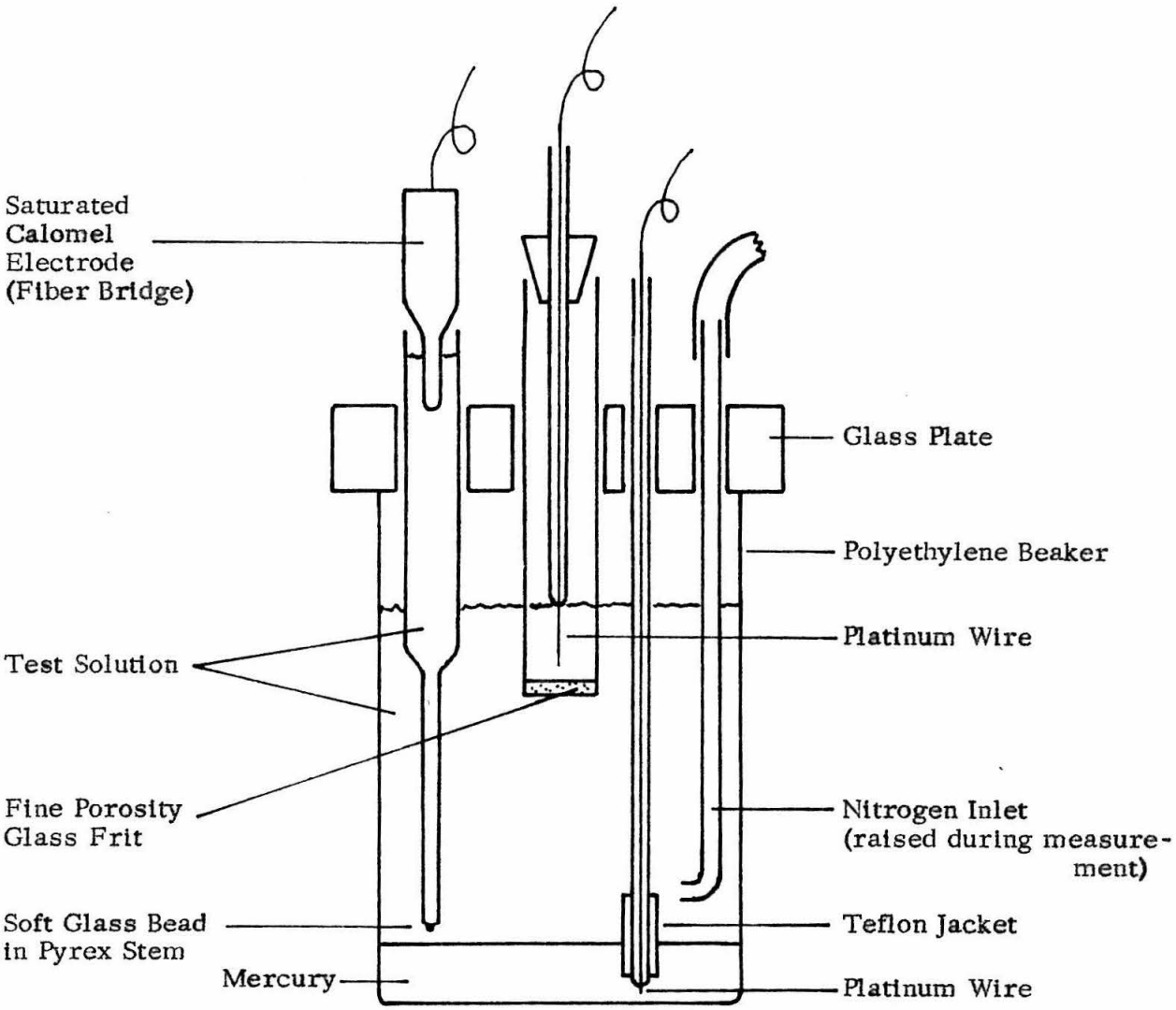

ELECTROLYSIS CELL

FIG. A-1

separated from the electrolysis cell by a salt bridge containing the same solution as in the cell. Ohmic drop between the mercury pool and the reference electrode was measured and found negligible.

Procedure. The solution was deaerated 20 min with Linde High Purity Dry Nitrogen (presaturated with water) and two chronopotentiograms were recorded.

Results and discussion

A typical chronopotentiogram is reproduced in Figure A-2 and points calculated from equation 1 are also plotted on the same coordinates using parameters which give the best least-squares fit. The least squares treatment was performed on a digital computer. The calculated points fit nearly the whole experimental curve within the accuracy of measurement. Table A-1 lists the least-squares parameters for a series of measurements.

Transition times calculated by the graphical methods of Delahay and Mattax (78) and of Reinmuth (80) are also listed in table A-1. The procedures are as follows.

Method of Delahay and Mattax (78) (fig. A-3). Tangent lines AC and BD are drawn to the linear portions of the wave preceding and following the potential pause. Two more lines, AB and CD, are drawn parallel to the time axis forming a trapezoid. A fifth line, EF, is drawn through points E and F lying one fourth of the distance from C to D and from A to B respectively. GH is drawn through the intersection of EF with the curve, parallel to time axis. The transition time then corresponds to the distance GH. Delahay and Mattax describe a method for handling

FIG. A-2

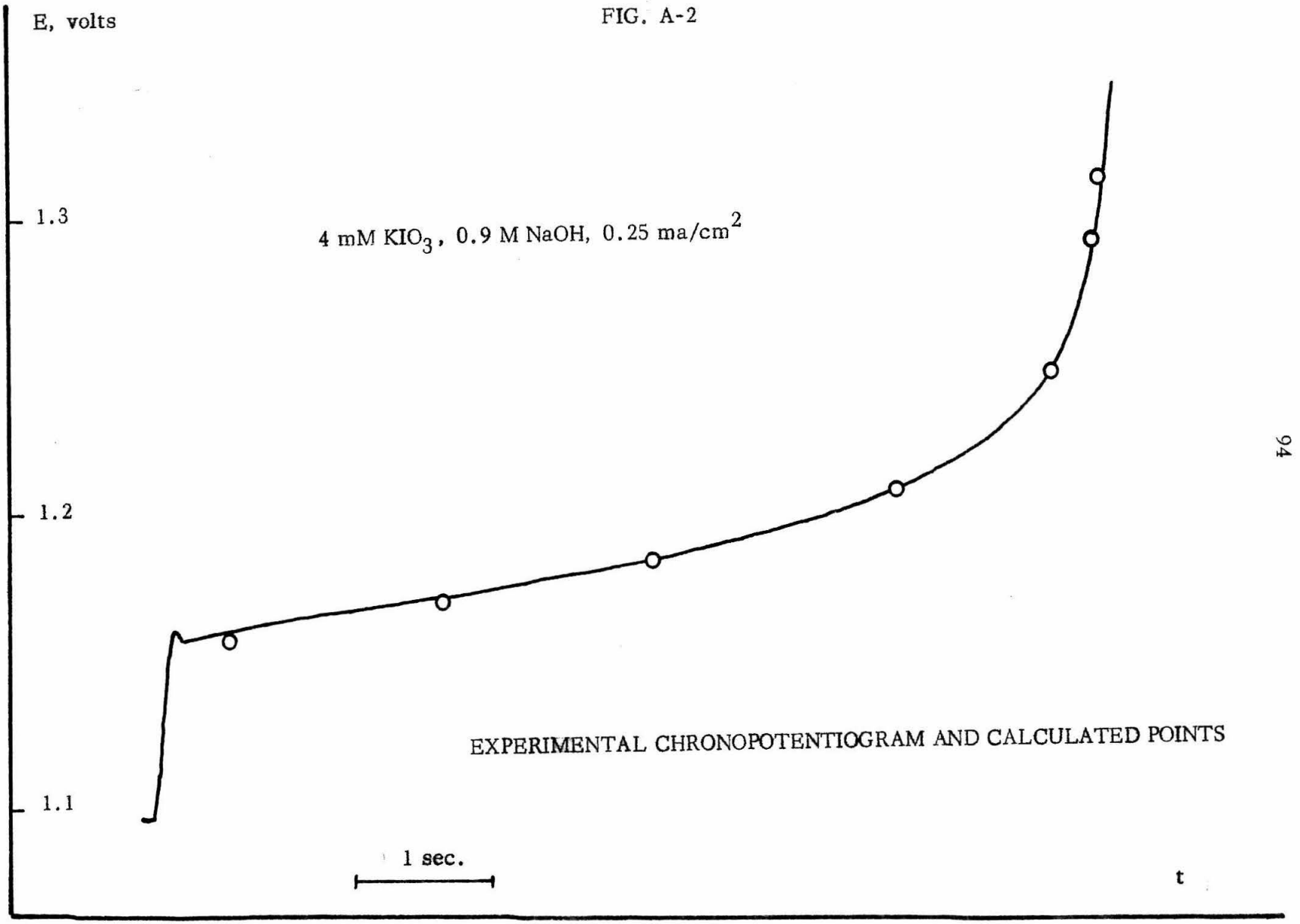

EXPERIMENTAL CHRONOPOTENTIOGRAM AND CALCULATED POINTS

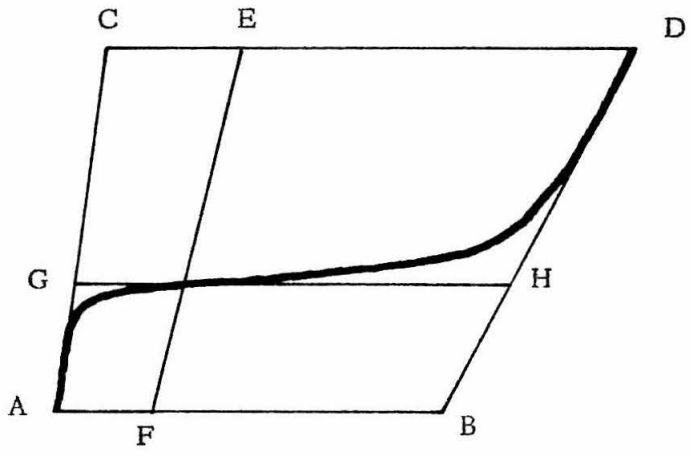

A. Method of Delahay and Mattax

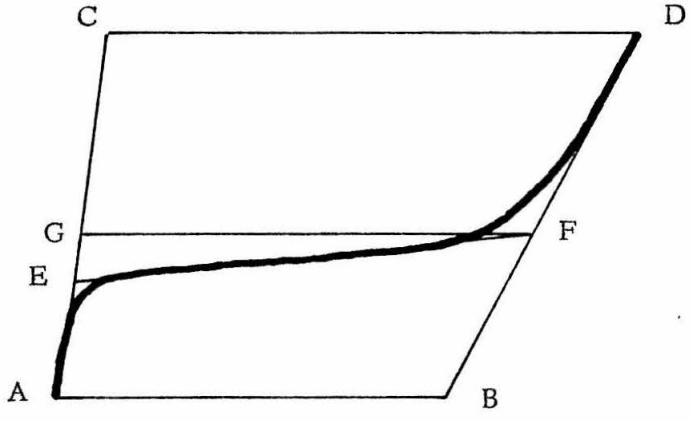

B. Method of Reinmuth

FIG. A-3

GRAPHICAL DETERMINATION OF TRANSITION TIME

TABLE A-1

INTERPRETATION OF CHRONOPOTENTIOMETRIC WAVES
BY VARIOUS METHODS

Least Squares			Delahay and Mattax	Reinmuth	Kuwana	Eq. 2		Eq. 3		Eq. 4
$E_{1/4}$	$n\alpha$	τ	τ	τ	τ	τ (a)	τ (b)	$n\alpha$ (a)	$n\alpha$ (b)	$n\alpha$ (c)
1.170	.899	6.83	6.64	6.69	6.79	6.83	6.79	.915	.957	1.00
1.172	.881	6.84	6.44	6.54	6.75	6.82	6.71	.936	.992	1.00
1.174	.917	6.81	6.61	6.67	6.82	6.80	6.71	.937	1.003	.99
1.176	.941	6.80	6.60	6.65	6.82	6.78	6.73	.948	.999	1.01
1.169	.900	6.94	6.75	6.80	6.96	6.91	7.01	.921	.943	.96
1.170	.934	6.86	6.69	6.74	6.88	6.87	6.86	.938	.937	.95
1.172	.904	6.62	6.39	6.45	6.65	6.60	6.54	.938	.975	1.00
1.173	.934	6.65	6.45	6.54	6.68	6.61	6.60	1.030	.989	1.04

(a) E_1 = 1.180 V, E_2 = 1.230 V, E_3 = 1.280 V

(b) E_1 = 1.170 V, E_2 = 1.210 V, E_3 = 1.250 V

(c) Least-squares τ was used in calculation

waves with very poorly defined potential breaks at the end of the potential pause, which we shall not consider here.

Method of Reinmuth (80) (fig. A-3). Tangent lines AC, BD, and EF are drawn to the linear portions of the wave preceding and following the potential pause and to the linear part of the wave near its inflection. A line, GF, is then drawn through the intersection of EF and BD, parallel to the time axis, and its length corresponds to the transition time.

Another graphical method is simply to lay a straightedge along the steep part of the curve and select the point at which the curve becomes straight as the transition time. (Though there is no theoretical reason for the curve to become linear, it generally does so.) This method has not appeared in print but since we believe it was first used by T. Kuwana it will be called the method of Kuwana. It gave the best results of the graphical methods (table A-1).

An algebraic method for calculating the transition time can be based on the equation

$$\tau^{1/2} = \frac{t_2 - t_1^{1/2} t_3^{1/2}}{2t_2^{1/2} - t_1^{1/2} - t_3^{1/2}} \qquad (2)$$

which follows exactly from equation 1. Here (t_1, E_1), (t_2, E_2), and (t_3, E_3) are points of the chronopotentiogram such that $E_3 - E_2 = E_2 - E_1$. The advantage of this method is that it is based on points from the central part of the curve where secondary effects (double layer capacity, secondary reactions) are unimportant. Best results are obtained if points fairly close to the steep regions are used, however, as table A-1 shows. Care must be taken in using this equation to carry enough significant figures since cancellation of errors between numerator and denominator occurs; if the times are known to three significant

figures, four significant figures must be carried through the calculation. Error analysis showed that the calculated value of τ is more sensitive to the errors in t_3 than in t_1, or t_2. For the data treated here, an error in t_3 (at E = 0.13) is multiplied by 1.5 in the calculated value of τ.

A similar equation may be derived for the transfer coefficient α in terms of three points (E_1, t_1), (E_2, t_2), (E_3, t_3) chosen so that $E_3 - E_2 = E_2 - E_1$.

$$n\alpha = \frac{RT}{F(E_1 - E_2)} \ln \frac{t_3^{1/2} - t_2^{1/2}}{t_2^{1/2} - t_1^{1/2}} \qquad (3)$$

Values of $n\alpha$ calculated from this equation are given in table A-1.

A graphical method for calculating the transfer coefficient can be based on the fact that the central part of a totally irreversible chronopotentiometric wave is nearly linear. It can be shown from eq. 1 that the wave has an inflection point at $t = \frac{\tau}{4}$ where the slope has the minimum value

$$\frac{dE}{dt} = \frac{2RT}{\alpha n F \tau} \qquad (4)$$

This slope can readily be found with a straightedge, since it is constant within 5% from 0.15τ to 0.38τ. Values of the transfer coefficient obtained from eq. 4 are listed in table A-1. This method requires that a value of τ be obtained independently.

A final means of interpreting a totally irreversible chronopotentiometric wave is to choose by trial and error the value of τ which results in the most linear plot of E against $\log\left[1 - \left(\frac{t}{\tau}\right)^{1/2}\right]$. Figure A-4 shows the sensitivity of the log plot to the assumed value of τ. Apparently τ can be determined this way to within several percent.

In all of the chronopotentiograms which were recorded the initial rise to the potential pause was too rapid for the recorder to follow. For this reason a vertical rise was assumed in the application of all methods for determining the transition time. (CA was drawn vertically, for example, in Figure A-3.) For the rest of the curve the rate of voltage change fell within the limits prescribed by the recorder manufacturer for 0.5% accuracy; lack of distortion was verified by monitoring the error signal from the recorder feedback amplifier. The rapid rise to the potential pause indicates negligible distortion over most of the wave from the effect of double-layer capacitance, since the ratio of charging current for the double layer to the total current during the potential pause is equal to the ratio of the slope of the curve during the potential pause to its slope preceding the potential pause. The ratio was less than 1% over most of the wave. If a large double-layer capacitance is present so that line CA cannot be drawn vertically in the methods of Figure A-3, its deviation from the vertical will tend to shorten the calculated transition time and counteract in part the opposite effect of the capacitance to lengthen the transition time. It does not simply undercompensate by a factor of approximately two as Reinmuth suggests, however, for the charging current during the potential pause is proportional to the rate of change of potential. It might be helpful to correct the current by subtracting the charging current estimated from the ratio of the slopes of AC and EF (fig. A-3B) but the simple eq. 1 no longer applies strictly and any effort to use it must involve some arbitrariness. It is desirable, when measuring kinetic parameters, to avoid conditions under which the charging current is significant.

We conclude from this example that the kinetic parameters for a totally irreversible chronopotentiometric wave can best be calculated by a least-squares procedure using a digital computer. The most reliable method of hand

calculation is the trial-and-error procedure exemplified in Figure A-4 but this is a tedious operation. As a rapid means of determining the parameters by hand, we suggest the graphical method of Kuwana for obtaining the transition time and the use of eq. 4 to obtain $n\alpha$. These are the fastest methods and seem to work as well as the previously reported graphical methods. Equation 4 has been applied to other sets of data with much more reproducible results than those in table A-1 (see Part II of this thesis), since a rather compressed voltage scale was used in recording the chronopotentiograms described in table A-1 and the slope of the wave was too small for most accurate measurement.

While conventional practice is to calculate the rate constant from the (extrapolated) potential at $t = 0$, it can just as well be calculated from the quarter-wave potential using the formula:

$$K = \frac{2i}{nFc} e^{-\frac{\alpha nF}{RT} E_{1/4}} \qquad (5)$$

This is the same formula as that used to calculate the rate constant from the potential at $t = 0$ except for a factor of 2 corresponding to the fact that when $t = \frac{\tau}{4}$ half of the reactant at the electrode surface has been consumed. The quarter-wave potential can be read directly from the chronopotentiogram. An advantage of calculating the rate constant from the quarter-wave potential and $n\alpha$ from the quarter-wave slope is that the calculations are based on the central part of the wave where the influence of the double-layer capacity and other secondary effects are at a minimum. The end portions of the wave must be used to determine the transition time, however, and an error in τ will also introduce errors into $E_{1/4}$ and $n\alpha$. On balance this procedure seems comparable in accuracy to those previously published and much simpler.

FIG. A-4

SENSITIVITY OF LOGARITHMIC PLOT
TO ASSUMED VALUE OF TRANSITION TIME

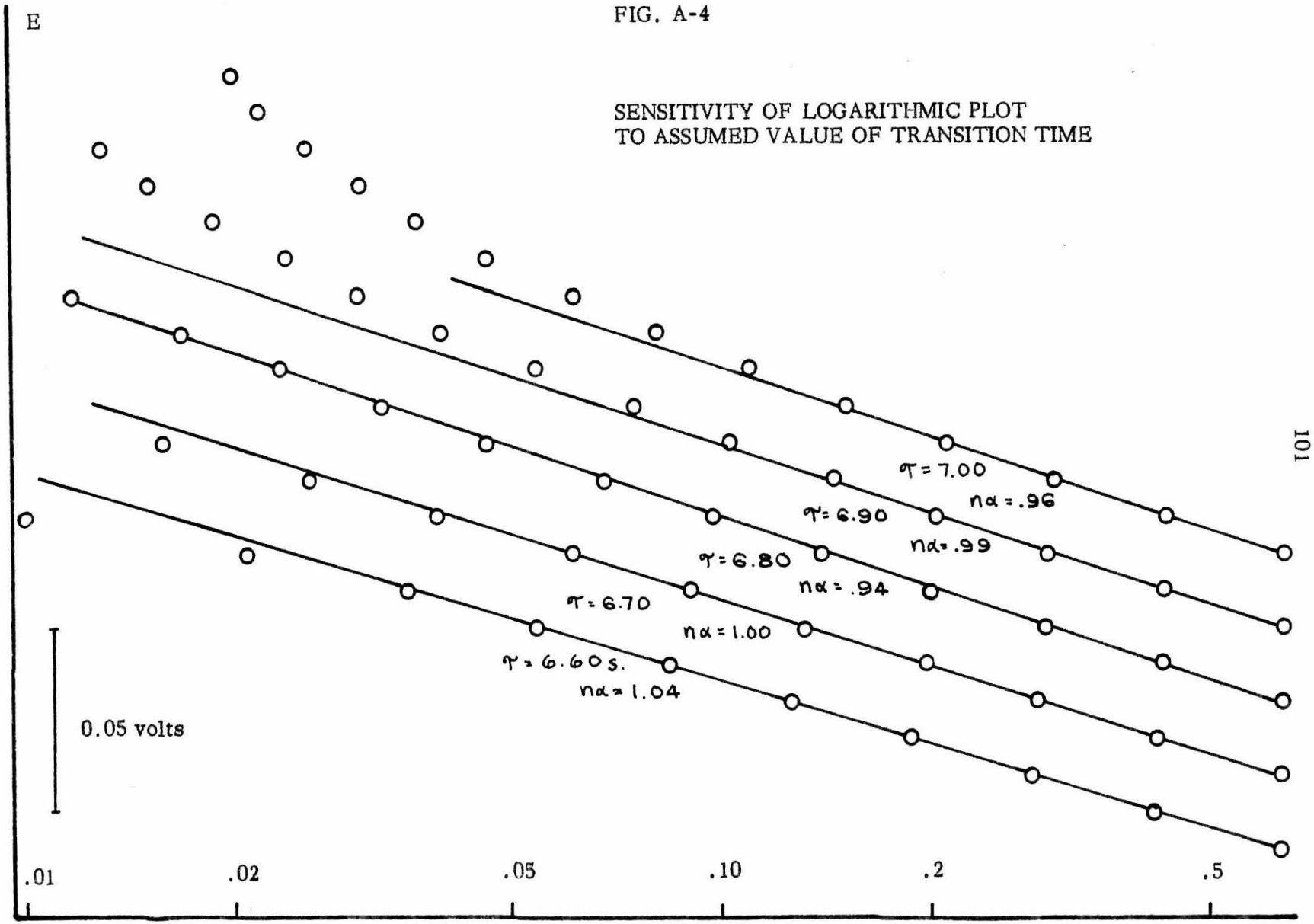

It should be remarked that the common practice of reporting rate constants based on the normal hydrogen electrode as reference voltage introduces an "irreversible" error into the data unless the quarter-wave potential is near zero. This results from the fact that the rate constant referred to zero potential (N. H. E.) has a large exponential factor $e^{\frac{\alpha n F}{RT} E_{1/4}}$ which causes the principal error in the calculated rate constant to be that arising from the error in α. After rounding off the calculated rate constant accordingly, it is impossible to recalculate the original quarter-wave potential from the reported constant to the accuracy with which it was originally measured. Thus information is permanently lost in the calculation. It is better to report a rate constant based on a non-zero reference potential which is near the quarter-wave potential, so that the exponential factor involving α is small.

Rate constants for the reduction of iodate in 1 M NaOH at a mercury electrode can be estimated from published graphical data. The value $k = 10^{-2.5}$ cm/sec at -1.150 V vs. SCE is obtained from the polarographic data of Gierst (24) for 0.9 M sodium hydroxide solution. Gierst reported $n\alpha = 0.67$. We calculate from the data of Delahay and Mattax (79) (measured chronopotentiometrically) that $k = 10^{0.0}$ (!), $n\alpha = 0.85$ for 1.0 M sodium hydroxide solution. The values calculated from the least-squares parameters of table A-1 are $k = 10^{-3.03}$ cm/sec, $n\alpha = 0.91$. The measured rate constant thus agrees moderately well with that reported by Gierst, and the measured transfer coefficient agrees with that reported by Delahay. The discrepancies between these three sets of data are nonetheless pronounced.

REFERENCES

1. Voorhies, J. D. and Furman, N. H., Anal. Chem. 31, (1959), 381-384.

2. Geske, D. H., J. Phys. Chem. 63, (1959), 1062-1070; and J. Am. Chem. Soc. 81, (1959), 4145-4147.

3. Kuwana, T., Bublitz, D. and Hoh, G. L. K., J. Am. Chem. Soc. 82, (1960), 5811-5817.

4. Hoh, G. L. K., McEwen, W. E. and Kleinberg, J., J. Am. Chem. Soc. 83, (1961), 3949-3953.

5. Delahay, P., New Instrumental Methods in Electrochemistry, Interscience Publishers, Inc., New York, (1954), pp. 179-216.

6. Rouse, T. O., Doctoral Dissertation, University of Minnesota, (1961).

7. Kolthoff, I. M. and Coetzee, J. F., J. Am. Chem. Soc. 79, (1957), 870-874, 1852-1858, 6110-6115.

8. Laitinen, H. A. and Kolthoff, I. M., J. Am. Chem. Soc. 61, (1939), 3344-3349.

9. von Stackelberg, M., Pilgram, M. and Toome, V., Z. Elektrochem. 57, (1953), 342-350.

10. Pleskov, V. A., Zhur. Fiz. Khim. 22 (1948), 351-561.

11. Popov, A. I. and Geske, D. H., J. Am. Chem. Soc. 79, (1957), 2074-2079.

12. Billon, J. P., J. Electronanal. Chem. 1, (1960), 486-501.

13. DeFord, D. D., Symposium on Electroanalytical Techniques, 133rd American Chemical Society Meeting, San Francisco, April, 1958.

14. Anson, F. C., Anal. Chem. 33, (1961), 939-942.

15. Anson, F. C. and Lingane, J. J., J. Am. Chem. Soc. 79, (1957), 4901-4904.

16. Vetter, K. J. and Berndt, D., Z. Elektrochem. 62, (1958), 378-386.

17. Laitinen, H. A. and Enke, C. G., J. Electrochem. Soc. 107, (1960), 773-781.

18. Popov, A. I. and Geske, D. H., J. Am. Chem. Soc. 80, (1958), 1340-1352.

19. Conway, B. E. and Dzieciuch, M., Proc. Chem. Soc., 1962, 121-122.

20. Romberg, E. and Cruse, K., Z. Elektrochem. 63, (1959), 404-418.

21. Lingane, J. J., J. Electroanal. Chem. 2, (1961), 297-309.

22. Sawyer, D. T. and Interrante, L. V., J. Electroanal. Chem. 2, (1961), 310-327.

23. Gerischer, R. and Gerischer, H., Z. Physik. Chem. N. F. 6, (1956), 178-200.

24. Gierst, L., Transactions of the Symposium on Electrode Processes, Philadelphia, (1959), Ed. by E. Yeager, John Wiley & Sons, Inc., New York, pp. 109-138.

25. Parsons, R., Advances in Electrochemistry and Electrochemical Engineering, Vol. I, Ed. by P. Delahay, Interscience Publishers, New York, (1961), pp. 1-64.

26. Schmidt, H. and Noack, J., Z. Anorg. Allgem. Chem. 296, (1958), 262-272.

27. Billon, J. P., Bull. Soc. Chim. France 1962, 863-871.

28. Streuli, C. A., Anal. Chem. 28, (1956), 916-917.

29. Maki, A. H. and Geske, D. H., J. Chem. Phys. 30, (1959), 1356-1357.

30. Berzins, T. and Delahay, P., J. Am. Chem. Soc. 75, (1953), 4205-4213.

31. Cole, T., Proc. Natl. Acad. Sci. U. S. 46, (1960), 506-509.

32. Talat-Erben, M. and Bywater, S., J. Am. Chem. Soc. 77, (1955), 3710-3711.

33. Wu, C. H. S., Hammond, G. S. and Wright, J. M., J. Am. Chem. Soc. 82, (1960), 5386-5394.

34. Eberson, L., J. Org. Chem. 27, (1962), 2329-2331.

35. Rodd, D. H., Chemistry of Carbon Compounds, Elsevier Publishing Company, Amsterdam, (1951), Vol. I, Part A, p. 606.

36. Mather, W. B., Doctoral Thesis, California Inst. of Tech., Pasadena, (1961), p. 39.

37. Vedel, J. and Tremillon, B., J. Electroanal. Chem. 1, (1959), 241-247.

38. Finkelstein, M., Petersen, R. C. and Ross, S. D., J. Am. Chem. Soc. 81, (1959), 2361-2364.

39. Schlubach, H., Ber. 53B, (1920), 1689-1693.

40. Faraday, M., Pogg. Ann. 33, (1834), 438.

41. Weedon, B. C. L., Quart. Revs. 6, (1952), 380.

42. Vetter, K. J., Elektrochemische Kinetik, Springer Verlag, Berlin, (1961).

43. Geske, D. H., J. Electroanal. Chem. 1, (1960), 502-503.

44. Glasstone, S., Laidler, K. J. and Eyring, H., The Theory of Rate Processes, McGraw-Hill, New York, (1941), pp. 575-7.

45. Randles, J. E. B., Trans. Faraday Soc. 48, (1952), 828.

46. Marcus, R. A., Can. J. Chem. 37, (1959), 155-63.

47. Hush, N., J. Chem. Phys. 28, (1958), 962.

48. Russell, C. D. and Anson, F. C., Anal. Chem. 33, (1961), 1282-1283.

49. Fuoss, R. M., Cox, N. L. and Kraus, C. A., Trans. Faraday Soc. 31, (1955), 749-761.

50. Muller, E., "Methoden de Organischen Chemie (Houben-Weyl)", Auflage 4, Band I, Teil 2, (1959), 828.

51. Lingane, J. J., Anal. Chem. 26, (1954), 1021-1022.

52. Kolbe, H., Ann. Chem. Liebigs 69, (1849), 257-294.

53. Glasstone, S. and Hickling, A., J. Chem. Soc. 1936, 820-827.

54. Hopfgartner, K., Monatsh. 32, (1911), 523-561.

55. Shukla, S. N. and Walker, O. J., Trans. Faraday Soc. 28, (1932), 457-462.

56. Fichter, F. and Meyer, R. E., Helv. Chim. Acta 16, (1933), 1408-1412.

57. Salauze, J., Compt. Rend. 180, (1925), 662.

58. Clusius, K. and Schanzer, W., Z. Physik. Chem. 192A, (1943), 273-291.

59. Petersen, J., Z. Physik. Chem. 33, (1900), 99-120.

60. Denina, E., Ferrero, G., de Paolini, F. S., Gazz. chim. ital. 68, (1938), 443.

61. Fichter, F. and Buess, H., Helv. Chim. Acta 18, (1935), 445-452.

62. Fichter, F. and Zumbrunn, R., Ibid. 10, (1927), 869-885.

63. Hallie, G., Rec. trav. chim. 57, (1938), 152-154.

64. Wawzonek, S. and Runner, M. E., J. Electrochem. Soc. 99, (1952), 457-459.

65. Markunas, P. C. and Riddick, J. A., Anal. Chem. 23, (1951), 337-9.

66. Thompson, W. E. and Krause, C. A., J. Am. Chem. Soc. 69, (1947), 1016-1020.

67. van der Heijde, H. B., Anal. Chim. Acta 16, (1957), 392-400.

68. Muney, W. S. and Coetzee, J. F., J. Phys. Chem. 66, (1962), 89-96.

69. Kolthoff, I. M., Bruckenstein, S. and Chantooni, M. K., Jr., J. Am. Chem. Soc. 83, (1961), 3927-3935.

70. Bartlett, P. D. and Hiatt, R. R., J. Am. Chem. Soc. 80, (1958), 1398-1405.

71. Kilpatrick and Kilpatrick, Chem. Revs. 13, (1933), 131-137.

72. Taft, R. W., Jr., Steric Effects in Organic Chemistry, Ed. by M. S. Newman, John Wiley and Sons, New York, (1956), pp. 556-675.

73. Tirouflet, J. and Bolchard, J., Compt. Rend. 250, (1960), 1861-1863.

74. Mason, J. G. and Rosenblum, J., J. Am. Chem. Soc. 82, (1960), 4206-4208.

75. McDaniel, D. H. and Brown, H. C., J. Org. Chem. 23, (1958), 420-427.

76. Kaplan, M., J. Chem. Eng. Data 6, (1961), 272-275.

77. Hall, D., unpublished.

78. Delahay, P. and Mattax, C. C., J. Am. Chem. Soc. 76, (1954), 874-878.

79. Delahay, P. and Mattax, C. C., J. Am. Chem. Soc. 76, (1954), 5314-5318.

80. Reinmuth, W. H., Anal. Chem. 33, (1961), 485-487.

81. Richards, J. H. and Hill, E. A., J. Am. Chem. Soc. 81, (1959), 3484-3485.

82. Hill, E. A. and Richards, J. H., J. Am. Chem. Soc. 83, (1961), 3840-3846.

83. Hill, E. A. and Richards, J. H., J. Am. Chem. Soc. 83, (1961), 4216-4221.

84. Hill, E. A., Doctoral Thesis, California Institute of Technology, Pasadena, (1961).

85. Pauling, L., The Nature of the Chemical Bond, Cornell University Press, Ithaca, 3rd Edition, (1960), p. 224.

86. Seibold, E. A. and Sutton, L. E., J. Chem. Phys. 23, (1955), 1967.

87. Wooster, N., Z. Kristallog. 38, (1932), 35-41.

88. Gregory, N. W., J. Am. Chem. Soc. 73, (1951), 472-473.

PROPOSITIONS

Proposition 1.

A. The Faradaic impedance is calculated for an electrochemical cell in which the electrodes are close enough for interaction between their diffusion layers. B. An equation is derived for the frequency distribution of the random electrical noise generated by an electrochemical cell under specified conditions.

(A)

In recent years the mathematical solutions of a great number of diffusion problems of interest in the study of electrochemical systems have appeared in the literature. A number of these have been collected in a monograph by Delahay (1). For the most part these treatments assume the anode and cathode to be far enough apart so that the diffusion processes occuring at the two electrodes do not interact. Oshida (2) has recently discussed the steady-state and transient response of an electrochemical system in which interaction does take place. This proposition will treat the alternating-current response of such a system.

It is known from the classical theory of alternating-current electrolysis (3) that a sinusoidal concentration disturbance at an electrode surface causes the propagation into the solution of damped sinusoidal concentration waves having the wavelength $2\pi\left(\frac{2D}{\omega}\right)^{\frac{1}{2}}$ and damping factor $\left(\frac{\omega}{2D}\right)^{\frac{1}{2}}$. It should therefore be expected that a weak resonance effect be observed when the diffusion wavelength equals the interelectrode distance; weak because the damping is large even at a distance of one wavelength. The detailed treatment which follows bears this out. With an electrode spacing of 0.1 mm the "resonant" frequency is about 10 cps for an ion with diffusion coefficient equal to 10^{-5}

NOMENCLATURE

C	concentration
C_R^0	concentration of species R before current flow
D	diffusion coefficient
F	Faraday's constant
j_0	exchange current
L	interelectrode distance
n	number of electrons transferred at electrode by reacting ion; as subscript, a running index
R	gas law constant
t	time
T	absolute temperature
x	distance from electrode surface
α	transfer coefficient
η	overvoltage
γ	$\left(\frac{\omega}{2D}\right)^{1/2}$
ω	angular frequency

cm^2/sec. When the interelectrode distance is appreciably larger than the diffusion wavelength the classical equations are valid; when the interelectrode distance is appreciably shorter than the diffusion wavelength a new limiting case obtains, in which the cell acts as a pure resistance of frequency-independent magnitude for small signal amplitudes.

The cell will be assumed to consist of a pair of inert parallel plane electrodes separated by an electrolyte solution containing an ionic species O, its reduced form R, and enough inert supporting electrolyte to permit neglecting migration of the reactive ions relative to their diffusion. (As Oshida points out, the presence or absence of supporting electrolyte is immaterial for sufficiently close electrode spacings and low applied voltages). The current density will be denoted by I. A sinusoidal current will be imposed on the cell:

$$I = a \cos \omega t \tag{1}$$

The diffusion equation

$$\frac{\partial C_o}{\partial t} = D_o \frac{\partial^2 C_o}{\partial x^2} \; ; \qquad \frac{\partial C_R}{\partial t} = D_R \frac{\partial^2 C_R}{\partial x^2} \tag{2}$$

must then be solved subject to the boundary conditions

$$\frac{I}{nF} = D_o \left.\frac{\partial C_o}{\partial x}\right|_{x=0} = -D_o \left.\frac{\partial C_o}{\partial x}\right|_{x=L} = -D_R \left.\frac{\partial C_R}{\partial x}\right|_{x=0} = D_R \left.\frac{\partial C_R}{\partial x}\right|_{x=L} \tag{3}$$

Two of these conditions may be replaced by the conditions

$$C_o\left(\frac{L}{2}, t\right) = C_o^o \; ; \quad C_R\left(\frac{L}{2}, t\right) = C_R^o \tag{4}$$

which follow from the symmetry of the problem. A "periodic-state" solution of the form

$$C_o(x,t) = C_o^\circ + A_o(x)\cos\omega t + B_o(x)\sin\omega t$$

$$C_R(x,t) = C_R^\circ + A_R(x)\cos\omega t + B_R(x)\sin\omega t \qquad (5)$$

will be sought.

Substitution of equation 5 into equation 2 yields

$$D_o\frac{d^2A_o}{dx^2}\cos\omega t + D_o\frac{d^2B_o}{dx^2}\sin\omega t = -A_o\omega\sin\omega t + B_o\omega\cos\omega t \qquad (6)$$

This must hold for all values of x and t; when t = $\frac{n\pi}{\omega}$ the sine terms drop out and

$$D_o\frac{d^2A_o}{dx^2} - \omega B_o = 0 \qquad (7)$$

Similarly

$$D_o\frac{d^2B_o}{dx^2} + \omega A_o = 0 \qquad (8)$$

The pair of equations 7 and 8 may be solved by routine methods for the solution of simultaneous homogeneous differential equations with constant coefficients to obtain

$$A_o(x) = \alpha e^{\nu_o x}\cos\nu_o x + \beta e^{\nu_o x}\sin\nu_o x + \gamma e^{-\nu_o x}\cos\nu_o x + \delta e^{-\nu_o x}\sin\nu_o x \qquad (9)$$

$$B_o(x) = \beta e^{\nu_o x}\cos\nu_o x - \alpha e^{\nu_o x}\sin\nu_o x - \delta e^{-\nu_o x}\cos\nu_o x + \gamma e^{-\nu_o x}\sin\nu_o x$$

where

$$\nu_o = \left(\frac{\omega}{2D_o}\right)^{1/2} \qquad (10)$$

and the remaining Greek letters represent constants of integration. Substitution of equation 9 into the boundary conditions gives

$$\alpha e^{\frac{\nu_o L}{2}}\cos\frac{\nu_o L}{2} + \beta e^{\frac{\nu_o L}{2}}\sin\frac{\nu_o L}{2} + \gamma e^{-\frac{\nu_o L}{2}}\cos\frac{\nu_o L}{2} + \delta e^{-\frac{\nu_o L}{2}}\sin\frac{\nu_o L}{2} = 0$$

$$\beta e^{\frac{\nu_o L}{2}}\cos\frac{\nu_o L}{2} - \alpha e^{\frac{\nu_o L}{2}}\sin\frac{\nu_o L}{2} - \delta e^{-\frac{\nu_o L}{2}}\cos\frac{\nu_o L}{2} + \delta e^{-\frac{\nu_o L}{2}}\sin\frac{\nu_o L}{2} = 0 \qquad (11)$$

$$\alpha + \beta + \delta - \gamma = \frac{a}{nFD_o\nu_o} \quad ; \quad \beta - \alpha + \gamma + \delta = 0$$

This set of equations can be solved for the integration constants, which with equation 9 yield

$$A_o(0) = -\frac{a}{2nFD_o\nu_o}\,\frac{\sin\frac{\nu_o L}{2}\cos\frac{\nu_o L}{2} + \sinh\frac{\nu_o L}{2}\cosh\frac{\nu_o L}{2}}{\cosh^2\frac{\nu_o L}{2}\cos^2\frac{\nu_o L}{2} + \sinh^2\frac{\nu_o L}{2}\sin^2\frac{\nu_o L}{2}}$$

$$B_o(0) = \frac{a}{2nFD_o\nu_o}\,\frac{\sinh\frac{\nu_o L}{2}\cosh\frac{\nu_o L}{2} - \sin\frac{\nu_o L}{2}\cos\frac{\nu_o L}{2}}{\cosh^2\frac{\nu_o L}{2}\cos^2\frac{\nu_o L}{2} + \sinh^2\frac{\nu_o L}{2}\sin^2\frac{\nu_o L}{2}} \qquad (12)$$

Similarly,

$$A_R(0) = \frac{a}{2nFD_R\nu_R}\,\frac{\sin\frac{\nu_R L}{2}\cos\frac{\nu_R L}{2} + \sinh\frac{\nu_R L}{2}\cosh\frac{\nu_R L}{2}}{\cosh^2\frac{\nu_R L}{2}\cos^2\frac{\nu_R L}{2} + \sinh^2\frac{\nu_R L}{2}\sin^2\frac{\nu_R L}{2}}$$

$$B_R(0) = \frac{a}{2nFD_R\nu_R}\,\frac{\sin\frac{\nu_R L}{2}\cos\frac{\nu_R L}{2} - \sinh\frac{\nu_R L}{2}\cosh\frac{\nu_R L}{2}}{\cosh^2\frac{\nu_R L}{2}\cos^2\frac{\nu_R L}{2} + \sinh^2\frac{\nu_R L}{2}\sin^2\frac{\nu_R L}{2}} \qquad (13)$$

Equations 12 and 13, together with the kinetic equation

$$I = j_o\left(\frac{C_R}{C_R^o}\,e^{\frac{\alpha nF}{RT}\eta} - \frac{C_o}{C_o^o}\,e^{-\frac{(1-\alpha)nF}{RT}\eta}\right) \qquad (14)$$

determine the voltage response of the electrode. To simplify the further treatment it will be assumed that the voltage variation is not more than a few millivolts so that the exponentials in equation 14 may be approximated by the first terms of their Maclaurin expansions. In this case the cell functions as a linear circuit element and the current-voltage relationship which is calculated on the basis of an imposed sinusoidal current is identical to that calculated on the basis of an imposed sinusoidal voltage. The cell voltage E becomes

$$E = \frac{2RT}{nF}\left(\frac{A_R}{C_R^o} - \frac{A_o}{C_o^o} + \frac{a}{j_o}\right)\cos\omega t + \left(\frac{B_R}{C_R^o} - \frac{B_o}{C_o^o}\right)\sin\omega t \qquad (15)$$

and the complex impedance of the cell is therefore

$$Z = \frac{2RT}{nF}\left[\frac{A_R}{aC_R^o} - \frac{A_o}{aC_o^o} + \frac{1}{j_o} + i\left(\frac{B_R}{aC_R^o} - \frac{B_o}{aC_o^o}\right)\right] \qquad (16)$$

(17)

At large values of $\sqrt{L}$ the classical formulas for Faradaic impedance are obtained as a limiting case and at small values of $\sqrt{L}$ the limiting relationship is

$$Z = \frac{2RT}{nF}\left[\frac{L}{2nF}\left(\frac{1}{D_o C_o} + \frac{1}{D_R C_R}\right) + \frac{1}{j_o}\right] \qquad (18)$$

where the impedance is purely resistive.

In this analysis, as in that of Oshida, the capacitance of the double layer was ignored. For the case of small-amplitude signals, however, the double layer effect can be simply represented by a suitable equivalent capacitance in parallel with the cell.

The above equations can also be applied to reversible electrode reactions, which correspond to the limit $j_o \to \infty$. This simply eliminates a term in equation 16. The same results can be obtained from the Nernst equation, together with equations 13 and 14.

B

The theory of random noise in the electrochemical cell involves a simple combination of Nyquist's (4) theory of random noise with the theory of Faradaic impedance in the electrochemical cell (3). The treatment which follows uses the basic arguments of these theories although the mathematical approach differs somewhat, particularly in the discussion of Faradaic impedance.

The method of calculating random thermal noise which will be applied to the case of the electrochemical cell is predicated upon the assumption (4) that

the fluctuating currents and voltages in a circuit may be analyzed by replacing each element by an identical but noiseless element in series with a random emf source characteristic of the element, and then applying Kirchoff's laws to the circuit so obtained. The circuit of Figure I may thus be replaced by that of Figure II. The noise voltages sources $e_A(t)$ and $e_R(t)$ are characteristic of the cell and of the resistor respectively. The first step in the analysis is that of finding the circuit properties of the electrochemical cell.

The voltage developed across the cell as a function of an arbitrary time-varying current passing through it will be derived from the conventional kinetic equation for an electrode reaction

$$I = j_o\left(\frac{C_o}{C_o^o} e^{-\frac{\alpha n}{\Phi}\eta} - \frac{C_R}{C_R^o} e^{\frac{(1-\alpha)n}{\Phi}\eta}\right) \tag{19}$$

and from Fick's law of diffusion

$$\nabla\cdot(D_o \nabla C_o) = \frac{\partial C_o}{\partial t} \quad ; \quad \nabla\cdot(D_R \nabla C_R) = \frac{\partial C_R}{\partial t} \tag{20}$$

In the above equations I is the "Faradaic" current passing through the electrode (distinct from that part of the current which serves only to charge the double-layer capacitance), α is the "transfer coefficient", j_0 is the "exchange current", η is the overpotential of the electrode (relative to its equilibrium potential), n is the number of electrons transferred to or from the electrode in the rate-determining step, c_0 is the concentration of the oxidized species taking part in the rate-determining step, c_R is the concentration of the reduced species participating in the rate-determining step, c_0^0 and c_R^0 are the initial concentrations to which j_0 and $\eta = 0$ refer, Φ is RT/F, and D_0 and D_R are the diffusivities of the oxidized and reduced species, respectively. Anodic overpotentials and cathodic currents are taken as positive. Coupling of the diffusion of one species to the concentration gradient of another is neglected.

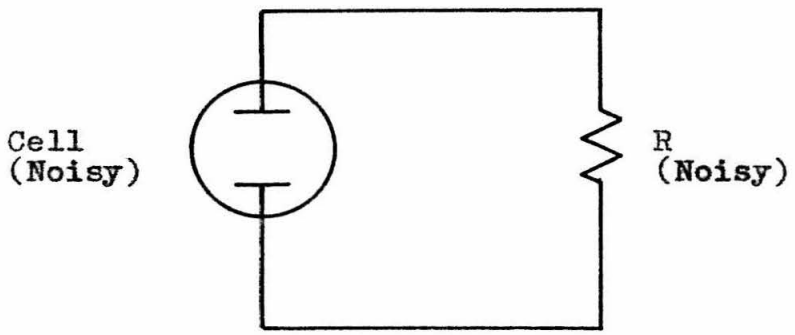

Figure I

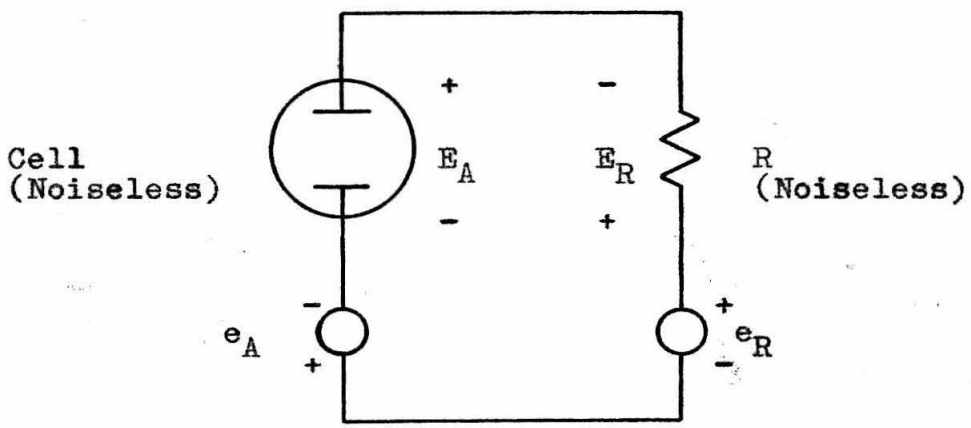

Figure II

The following simplifying restrictions will be made on the cell:

1. The two electrodes are identical and consist of plane surfaces. The cross-section of the vessel containing the electrolyte is identical in shape to the two electrodes at any point between them so that the geometry is one-dimensional.

2. The only reaction taking place at the electrode is the reaction $R = O + ne^-$. R and O do not react with any components of the solution.

3. An additional electrolyte besides R and O is present in the solution in much greater concentration than R and O, so that almost all of the current in the cell is carried by this electrolyte and diffusion rather than transference may be considered the sole mode of transport of R and O. This additional electrolyte does not react at the electrode.

Equation 19 will now be simplified by making approximations suitable for small overvoltages. If η is less than 0.2 mv the exponents $\frac{\alpha n}{\Phi}\eta$ and $\frac{(1-\alpha)n}{\Phi}\eta$ will be no greater than 0.01 at 25° C since α usually lies between 0.2 and 0.8 and n is usually either 1 or 2. The exponentials in equation 19 can then be closely represented by the first two terms of their Maclaurin expansions. Making this approximation and introducing the relative concentrations $c_0^r = c_0/c_0^0$ and $c_R^r = c_R/c_R^0$, we obtain

$$I = j_o \left(c_o^r - c_R^r - \frac{\alpha n}{\Phi}\eta c_o^r - \frac{(1-\alpha)n}{\Phi}\eta c_R^r\right) \tag{21}$$

For small currents c_0^r and c_R^r remain approximately unity, so that they may be replaced by 1 except where they occur as a difference. Then

$$I = j_o \left(c_o^r - c_R^r - \frac{n}{\Phi}\eta\right) \tag{22}$$

This small voltage-small current approximation will clearly apply to currents and voltages produced by thermal fluctuations.

The above approximations presuppose, of course, that the first-order terms $(c_0^r - c_R^r)$ and $(-\frac{n}{\mathfrak{F}}\eta)$ do not cancel each other out to leave only the second-order terms. It may be noted, however, that both terms will be functions of time. If developed in Fourier series, in order for one Fourier component of one term to cancel the corresponding component of the other term they would have to be not only equal in amplitude but 180° out of phase as well. It will later be shown that both $(c_0^r - c_R^r)$ and $(-\frac{n}{\mathfrak{F}}\eta)$ lead the current by phase angles between 90° and 180°, so that these terms will add rather than cancel (cf. equation 49 and equation 50).

An expression for $(c_0^r - C_R^r)$ will now be derived. Let an arbitrary current I (t) be imposed on the cell from time $t = -\theta$ to $t = \theta$. We wish to find $(c_0^r - c_R^r)$ as a function of time during this interval. First expand I (t) as a Fourier series in this interval:

$$I(t) = \sum_{n=1}^{\infty} a_n \cos \frac{\pi n}{\theta} t + \sum_{n=1}^{\infty} b_n \sin \frac{\pi n}{\theta} t \qquad (23)$$

assuming that there is no D-C component. The $(c_0^r - c_R^r)$ resulting from a single Fourier component of the current will first be found and these $(c_0^r - c_R^r)$ will then be superposed.

Within the body of fluid the diffusion equation 20 prevails. Assuming that the diffusivities are constant — which is a very good assumption in view of the minute concentration changes involved — the diffusion equations may be written for the one-dimensional case:

$$D_o \frac{\partial^2 C_o}{\partial x^2} = \frac{\partial C_o}{\partial t} \quad ; \quad D_R \frac{\partial^2 C_R}{\partial x^2} = \frac{\partial C_R}{\partial t} \qquad (24)$$

The boundary conditions are given by Faraday's Law.

$$I = -nFD_R \left.\frac{\partial C_R}{\partial x}\right|_{x=0} = nFD_o \left.\frac{\partial C_o}{\partial x}\right|_{x=0} = -nFD_R \left.\frac{\partial C_R}{\partial x}\right|_{x=L} = nFD_o \left.\frac{\partial C_o}{\partial x}\right|_{x=L} \quad (25)$$

where L is the distance between electrodes. If I(t) is a pure sinusoid

$$I = a\cos\omega t + b\sin\omega t \quad (26)$$

it is reasonable to look for a solution of the form

$$C_o(x,t) = C_o^\circ + A(x)\cos\omega t + B(x)\sin\omega t \quad (27)$$

(It is assumed that the interval of observation is long enough that the transient effects related to the initial condition of the cell can be neglected and only the steady-state — more properly "periodic-state" — solution of the differential equation need be considered.) Substituting equation 27 into equation 24 yields for component 0:

$$D_o \frac{d^2A}{dx^2}\cos\omega t + D_o \frac{d^2B}{dx^2}\sin\omega t = -A\sin\omega t + B\cos\omega t \quad (28)$$

This must hold at all values of x and t; when t = n the sine terms drop out and

$$D_o \frac{d^2A}{dx^2} - \omega B = 0 \quad (29)$$

Similarly

$$D_o \frac{d^2B}{dx^2} + \omega A = 0 \quad (30)$$

This pair of simultaneous linear differential equations may be solved by routine methods for A(x) and B(x). The results are

$$A(x) = \alpha e^{\nu x}\cos\nu x + \beta e^{\nu x}\sin\nu x + \gamma e^{-\nu x}\cos\nu x + \delta e^{-\nu x}\sin\nu x \quad (31)$$

and

$$B(x) = \beta e^{\nu x}\cos\nu x - \alpha e^{\nu x}\sin\nu x - \delta e^{-\nu x}\cos\nu x + \gamma e^{-\nu x}\sin\nu x \quad (32)$$

where

$$\nu = \left(\frac{\omega}{2D_o}\right)^{1/2} \quad (33)$$

and the remaining Greek letters represent constants of integration.

The boundary conditions must now be applied. Letting I(t) = a cos ωt + b sin ωt in equation 25,

$$\left.\frac{\partial c_o}{\partial x}\right|_{x=o} = \left.\frac{\partial c_o}{\partial x}\right|_{x=L} = \frac{a}{nFD_o}\cos\omega t + \frac{b}{nFD_o}\sin\omega t \quad (34)$$

To simplify the application of the boundary conditions it will be assumed that $\nu L \gg 1$ so that the concentration changes produced at one electrode will be damped out to a negligible magnitude by the time they have propagated the distance L to the other electrode. (This assumption will be quite good, for example, if $\omega > .01$ sec^{-1} and L=1mm, since diffusivities are ordinarily of the magnitude 1cm^2/day or less. If this assumption is not made, the distance L will enter into the equations in a complicated manner. See Part A for further discussion.) Then upon inserting the boundary conditions,

$$A(x) = \gamma e^{-\nu x}\cos\nu x + \delta e^{-\nu x}\sin\nu x - \gamma e^{\nu(x-L)}\cos\nu(L-x) - \delta e^{\nu(x-L)}\sin\nu(L-x) \quad (35)$$

$$B(x) = -\delta e^{-\nu x}\cos\nu x + \gamma e^{-\nu x}\sin\nu x + \delta e^{\nu(x-L)}\cos\nu(L-x) - \gamma e^{\nu(x-L)}\sin\nu(L-x) \quad (36)$$

in which

$$\delta = \frac{a+b}{2\nu_n FD_o} \tag{37}$$

and

$$\gamma = \frac{b-a}{2\nu_n FD_o} \tag{38}$$

Consider now the boundary conditions corresponding to an arbitrary I(t) expressed as the Fourier series of equation 23.

$$\left.\frac{\partial C_o}{\partial x}\right|_{x=0} = \left.\frac{\partial C_o}{\partial x}\right|_{x=L} = \frac{I(t)}{nFD_o} = \sum_{n=1}^{\infty}\left(\frac{a_n}{nFD_o}\cos\frac{\pi n}{\theta}t + \frac{b_n}{nFD_o}\sin\frac{\pi n}{\theta}t\right) \tag{39}$$

Since the diffusion equation 24 is linear, any finite number of solutions may be superposed to match a given set of boundary conditions. This will also be true for an infinite series of solutions if it is assumed that the operations of differentiation and summation can be interchanged for the particular series involved. Making this assumption the general solution for $c_0(x, t)$ may be written:

$$C_o(x,t) = C_o^o + \sum_{n=1}^{\infty} A_n(x)\cos\omega_n t + \sum_{n=1}^{\infty} B_n(x)\sin\omega_n t \tag{40}$$

where

$$\omega_n = \frac{\pi n}{\theta} \tag{41}$$

$$A_n(x) = \gamma_n e^{-\nu_n x}\cos\nu_n x + \delta_n e^{-\nu_n x}\sin\nu_n x - \gamma_n e^{\nu_n(x-L)}\cos\nu_n(L-x) - \delta_n e^{\nu_n(x-L)}\sin\nu_n(L-x) \tag{42}$$

$$B_n(x) = -\delta_n e^{-\nu_n x}\cos\nu_n x + \gamma_n e^{-\nu_n x}\sin\nu_n x + \delta_n e^{\nu_n(x-L)}\cos\nu_n(L-x) - \gamma_n e^{\nu_n(x-L)}\sin\nu_n(L-x) \tag{43}$$

$$\nu_n = \left(\frac{\omega_n}{2D_o}\right)^{1/2} \tag{44}$$

$$\delta_k = \frac{a_k + b_k}{2\nu_k n F D_o} \quad ; \quad \gamma_k = \frac{b_k - a_k}{2\nu_k n F D_o} \tag{45}$$

(Cf. equations 35 through 38.)

At the surface of one electrode, then

$$C_o(0,t) = C_o^o + \sum_{k=1}^{\infty} \gamma_k \cos\omega_k t - \sum_{k=1}^{\infty} \delta_k \sin\omega_k t \tag{46}$$

and

$$C_o^r(0,t) = 1 + \sum_{k=1}^{\infty} \frac{\gamma_k}{C_o^o} \cos\omega_k t - \sum_{k=1}^{\infty} \frac{\delta_k}{C_o^o} \sin\omega_k t \tag{47}$$

Similarly

$$C_R^r(0,t) = 1 - \sum_{k=1}^{\infty} \frac{\gamma_k D_o^{1/2}}{C_R^o D_R^{1/2}} \cos\omega_k t + \sum_{k=1}^{\infty} \frac{\delta_k D_o^{1/2}}{C_R^o D_R^{1/2}} \sin\omega_k t \tag{48}$$

so that

$$C_o^r - C_R^r = \sum_{k=1}^{\infty} \left\{ \gamma_k D_o^{1/2} \left(\frac{1}{C_o^o D_o^{1/2}} + \frac{1}{C_R^o D_R^{1/2}} \right) \cos\omega_k t - \delta_k D_o^{1/2} \left(\frac{1}{C_o^o D_o^{1/2}} + \frac{1}{C_R^o D_R^{1/2}} \right) \sin\omega_k t \right\} \tag{49}$$

Introducing equation 49 into equation 22 and setting $E_A = -2\eta$ (where E_A is the total voltage drop across the cell)

$$-\frac{j_o n}{2\Phi} E_A = \sum_{k=1}^{\infty} \left[j_o \gamma_k D_o^{1/2} \left(\frac{1}{C_o^o D_o^{1/2}} + \frac{1}{C_R^o D_R^{1/2}} \right) - a_k \right] \cos\omega_k t - \sum_{k=1}^{\infty} \left[j_o \delta_k D_o^{1/2} \left(\frac{1}{C_o^o D_o^{1/2}} + \frac{1}{C_R^o D_R^{1/2}} \right) + b_k \right] \sin\omega_k t \tag{50}$$

We now have the voltage across the cell as a function of the current flowing through it, for γ_k and δ_k are known in terms of I (t) through equation 45. This result is restricted to frequencies such that $\nu L \gg 1$ and such that the transient response of the cell which is associated with the frequencies under consideration takes place in a negligibly small fraction of the total period of observation.

The impedance presented by the electrode to a current component of frequency can readily be found from equation 50. If we write $Z = R \; iX$, then

$$R_\omega = \frac{2\Phi}{j_o n}\left\{\frac{j_o}{nF\sqrt{2\pi}}\left(\frac{1}{C_o^o D_o^{1/2}} + \frac{1}{C_R^o D_R^{1/2}}\right) + 1\right\} \tag{51}$$

$$X_\omega = -\frac{\Phi}{n^2 F}\sqrt{\frac{2}{\omega}}\left(\frac{1}{C_o^o D_o^{1/2}} + \frac{1}{C_R^o D_R^{1/2}}\right) \tag{52}$$

Equation 50 may now be written more concisely

$$E_A = Re \sum_{k=1}^{\infty} Z_k I_k e^{i\omega_k t} \tag{53}$$

where Z_k is the complex impedance corresponding to frequency ω_k and $I_k = a_k - ib_k$ is the complex representation of the current component of frequency ω_k.

The current I which actually involves charge transfer from electrolyte to electrode or vice versa is only a part of the total current passing through the electrode, since there is known to be a capacitative effect at the electrode surface. This "double-layer" capacitance will be assumed constant for small currents and voltages and denoted by the symbol C_D. If I denotes the total current,

$$I' = \frac{C_D}{2}\frac{dE_A}{dt} + Re \sum_{k=1}^{\infty} I_k e^{i\omega_k t} \tag{54}$$

remembering that there is a capacitance of C_D at <u>each</u> electrode. Assuming that the operations of differentiation and summation can be interchanged for the series involved,

$$I' = Re \sum_{k=1}^{\infty} I'_k e^{i\omega_k t} = Re \sum_{k=1}^{\infty} i\omega_k \frac{C_D}{2} Z_k I_k e^{i\omega_k t} + Re \sum_{k=1}^{\infty} I_k e^{i\omega_k t} \tag{55}$$

Equating corresponding coefficients

$$I_k' = i\omega_k \frac{C_D}{2} Z_k I_k + I_k \tag{56}$$

Solving for I_k and introducing it into equation 53,

$$E_A = Re \sum_{k=1}^{\infty} \frac{Z_k}{1 + i\omega_k \frac{C_D}{2} Z_k} I_k' e^{i\omega_k t} \tag{57}$$

Combining the complex constants of equation 57 into a single coefficient Z_n',

$$E_A = Re \sum_{n=1}^{\infty} Z_n' I_n' e^{i\omega_n t} \tag{58}$$

Note that Z_n' is simply the impedance of a parallel combination of $C_D/2$ and Z_n'. The real and imaginary parts of $Z_n' = R_n' + iX_n'$ are

$$R_n' = \frac{R_n}{\left(1 - \omega_n \frac{C_D}{2} X_n\right)^2 + \left(\omega_n \frac{C_D}{2} R_n\right)^2} \tag{59}$$

$$X_n' = -\frac{\omega_n \frac{C_D}{2}\left(R_\omega^2 + X_\omega^2\right) - X_\omega}{\left(1 - \omega_n \frac{C_D}{2} X_n\right)^2 + \left(\omega_n \frac{C_D}{2} R_n\right)^2} \tag{60}$$

The description of the circuit properties of the electrochemical cell given in equations 58 through 60 will now serve as the basis for a calculation of the noise generated by the electrode.

Consider the circuit of Figure II. Applying Kirchoff's voltage law,

$$E_A + E_R = e_A + e_R \tag{61}$$

$$Re \sum_{n=1}^{\infty} (Z_n' + R) I_n e^{i\omega_n t} = e_A + e_R \tag{62}$$

This may also be written as

$$\sum_{n=1}^{\infty} \{ [a_n (R_n' + R) - b_n X_n'] \cos\omega_n t + [b_n (R_n' + R) + a_n X_n'] \sin\omega_n t = e_A + e_R \tag{63}$$

If e_A and e_R are expanded as

$$e_A = \sum_{n=1}^{\infty} (c_n \cos \omega_n t + d_n \sin \omega_n t) \tag{64}$$

$$e_R = \sum_{n=1}^{\infty} (r_n \cos \omega_n t + s_n \sin \omega_n t) \tag{65}$$

and substituted into equation 63, we may equate corresponding coefficients to obtain

$$a_n(R_n' + R) - b_n X_n' = c_n + r_n \tag{66}$$

$$b_n(R_n' + R) + a_n X_n' = d_n + s_n \tag{67}$$

These two equations will be used later.

If the circuit is at thermal equilibrium there will be no net transfer of energy from the cell to the resistor during the interval of observation. The power generated in the cell by random fluctuations must therefore equal the power dissipated in the cell, and

$$\int_{-\theta}^{\theta} E_A I \, dt = \int_{-\theta}^{\theta} e_A I \, dt \tag{68}$$

Similarly

$$\int_{-\theta}^{\theta} E_R I \, dt = \int_{-\theta}^{\theta} e_R I \, dt \tag{69}$$

Now equation 58 may be written

$$E_A = \sum_{n=1}^{\infty} (a_n R_n' - b_n X_n') \cos \omega_n t + \sum_{n=1}^{\infty} (a_n X_n + b_n R_n') \sin \omega_n t \tag{70}$$

Then

$$\int_{-\theta}^{\theta} \left\{ \sum_{n=1}^{\infty} [(a_n R_n' - b_n X_n') \cos \omega_n t + (a_n X_n' + b_n R_n') \sin \omega_n t] \right\} \left\{ \sum_{n=1}^{\infty} (a_n \cos \omega_n t + b_n \sin \omega_n t) \right\} dt = \int_{-\theta}^{\theta} \left\{ \sum_{n=1}^{\infty} [c_n \cos \omega_n t + d_n \sin \omega_n t] \right\} \left\{ \sum_{n=1}^{\infty} a_n \cos \omega_n t + b_n \sin \omega_n t \right\} dt \tag{71}$$

Assuming that term-by-term multiplication of the above series is permissible and making use of the orthogonality properties of the sine and cosine functions

$$\sum_{n=1}^{\infty}(a_n^2+b_n^2)R_n' = \sum_{n=1}^{\infty} a_n c_n + b_n d_n \tag{72}$$

Similarly, from equation 69,

$$\sum_{n=1}^{\infty}(a_n^2+b_n^2)R = \sum_{n=1}^{\infty}(a_n r_n + b_n s_n) \tag{73}$$

Suppose now that at the start of the experiment ($t = -\theta$) a series combination of pure capacitance C and pure inductance L had been introduced into the circuit of Figure I, such that $\frac{1}{\sqrt{LC}} = \omega_k$ (This line of reasoning is due to Nyquist (4).) The "noise generators" e_A and e_R would have been unaffected by the addition according to the original hypothesis that they depend only upon the nature of the circuit element with which they are associated, so that the coefficients in equations 64 and 65 would have been the same. (It is necessary to consider the situation that would have resulted with the same e_A and e_R but different circuit rather than averaging over an ensemble of measurements, since the coefficients in equations 64 and 65 would simply average to zero.) In the limiting case, as $\frac{L}{C} \to \infty$ with ω_k constant, the only current that could flow would be one of frequency ω_k. The analysis leading to equations 66, 67, 72, and 73 is unchanged except that X_n' must be replaced by $X_n' + i\left(\omega_n C - \frac{1}{\omega_n L}\right)$ Since $a_n = b_n = 0$ unless $n = k$ and the terms associated with ω_k are unaffected by the presence of the L-C combination, equations 72 and 73 become

$$(a_k^2+b_k^2)R_k' = a_k c_k + b_k d_k \tag{74}$$

$$(a_k^2+b_k^2)R = a_k r_k + b_k s_k \tag{75}$$

This analysis of what would have occurred if, in the "experiment", an L-C bandpass filter had been present shows that in equations 72 and 73 the power dissipation terms for each frequency are individually equal.

$$(a_n^2 + b_n^2) R_n' = a_n c_n + b_n d_n \tag{76}$$

$$(a_n^2 + b_n^2) R = a_n r_n - b_n s_n \tag{77}$$

Equations 66, 67, 76, and 77 can be solved simultaneously to give

$$c_n = \frac{R_n}{R} r_n \quad ; \quad d_n = \frac{R_n}{R} s_n \tag{78}$$

If $R_n = R$, $c_n = r_n$, and $d_n = s_n$. This shows that the component at a given frequency of the noise generated by an electrochemical cell of the type considered is equal to that generated by a resistor having a resistance equal to the resistive component of the impedance which the cell presents to a sinusoidal current of the given frequency. Since the power spectrum G(f) of a resistor is given by the Nyquist equation,

$$G(f) = 4KTR'(f) \tag{79}$$

Using equation 59 and changing angular frequencies ω to frequencies f,

$$G(f) = \frac{4KTR_s}{(1 - \pi f C_D X_f)^2 (\pi f C_D R_f)^2} \tag{80}$$

The values of R_f and of X_f are given by equations 51 and 52.

Proposition 2

A. A circuit is proposed to correct for the background current in chronopotentiometry. B. A method is proposed for measuring ohmic drop in a three-electrode system.

(A)

In polarographic measurements it is customary to correct for the "background current" which flows when a blank run is made on the solvent and supporting electrolyte in the absence of the sample to be studied. No such correction can be made in chronopotentiometry because the background current influences the potential-time curve in a very complex manner. Even if the background current is assumed to arise solely from charging the electrical double layer at the electrode surface and the capacity of the double layer is assumed constant, the correction cannot be expressed analytically in closed form (1). A method has been proposed by Anson and Lingane (2) and another by Lingane (3) for correcting transition times to account for that component of the background current due to oxidation or reduction of the electrode surface. Neither method has firm theoretical justification.

A simple electrical circuit which automatically corrects for the background current in chronopotentiometric measurements is proposed here. Figure I is a block diagram of the proposed circuit. Two identical electrolysis cells are used, one filled with sample solution and the other with pure supporting electrolyte solution. The compensating circuit forces the working electrode of the reference cell to have the same potential as the working electrode of the sample cell, each relative to its own reference electrode. The current which flows in the reference cell is added to the current flowing in the sample cell, compensating

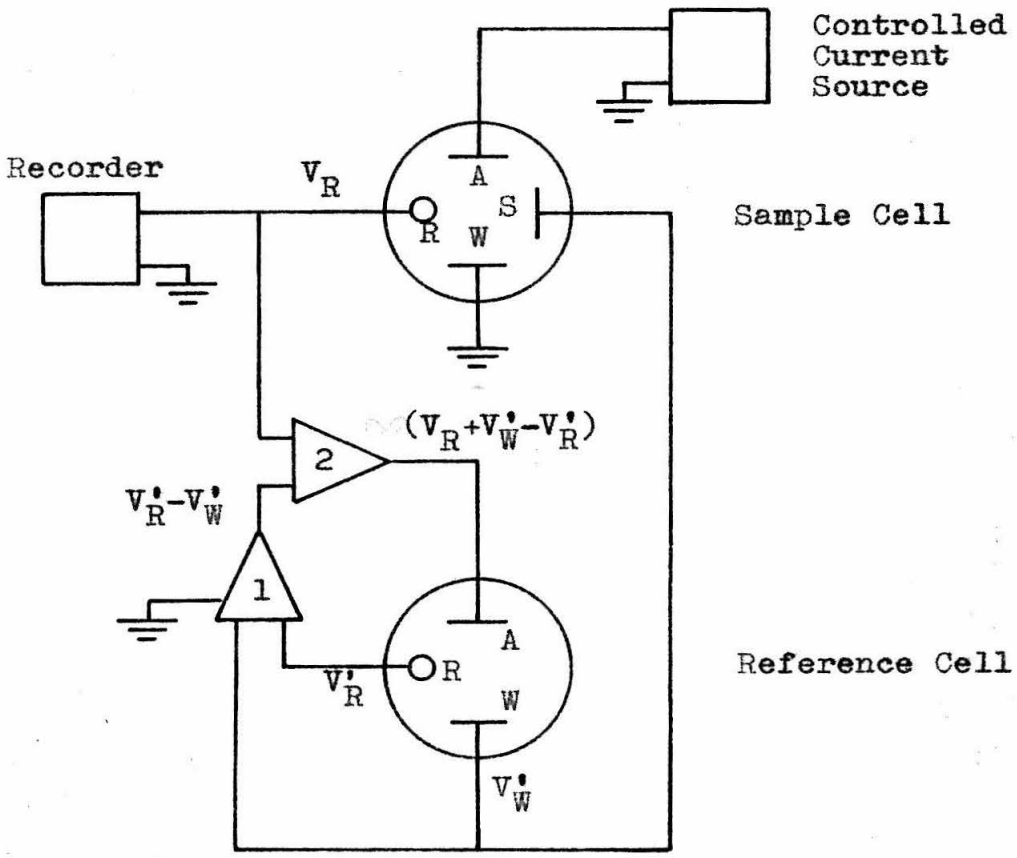

R Reference Electrode

W Working Electrode

A, S Auxiliary Electrodes

1. Analog Computer Subtracting Circuit
2. High Gain Operational Amplifier

Figure I

Block Diagram for Background

Compensating Circuit

for the background current. The circuit can be built from inexpensive, readily obtainable analog computer components.

To avoid oscillation it will be necessary to switch on the controlled current and the compensating circuit simultaneously.

(B)

A recurring problem in electrochemical measurements involving a three-electrode system of working electrode, reference electrode, and auxiliary electrode is the elimination of the ohmic potential drop between the working and reference electrodes which results from the potential field set up by the current flowing between the working electrode and the auxiliary electrode. The customary procedure is to minimize this ohmic drop by a cell design which places the reference electrode as close as possible to the surface of the working electrode, but it is often impossible to reduce it to a negligible level. In such cases an alternative approach is to measure the ohmic drop and correct for it. One must then measure the transfer function which relates the potential drop between reference and working electrodes to the current flowing between auxiliary and working electrodes. This has the dimensions of resistance and will be called the error resistance. The error resistance of a three-electrode system has been measured using a pulse method described by Anson (4) but not with great accuracy. A null-balance bridge technique for its measurement is described here.

The circuit (fig. II) is basically an A-C Wheatstone bridge with the electrolysis cell forming <u>two</u> arms of the bridge. The ratio ζ of the impedance between working and reference electrodes to the impedance between reference and

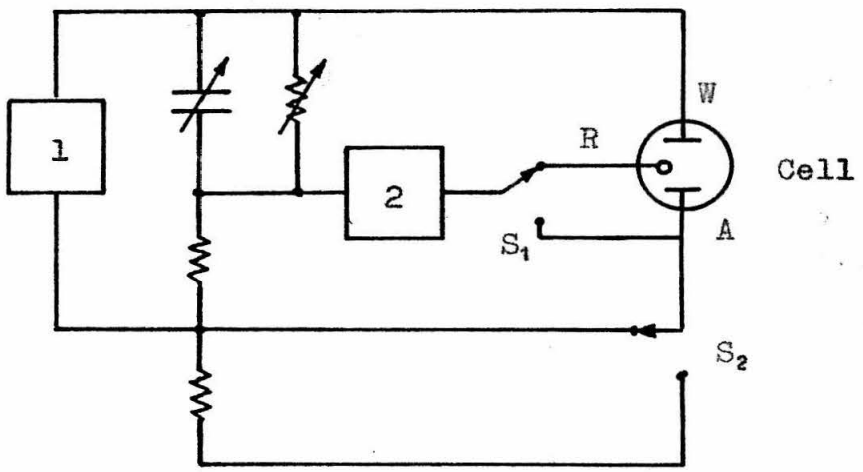

1. Oscillator
2. Null Detector

A Auxiliary Electrode

R Reference Electrode

W Working Electrode

Figure II

Bridge Circuit

auxiliary electrodes is measured by this circuit, being equal to the ratio of impedances of the other two arms of the bridge when balance is achieved. The circuit is then switched (switches S_1 and S_2) to a conventional bridge configuration and the impedance Z between working and auxiliary electrodes measured. The transfer function τ relating the potential drop between reference and working electrodes to the current flowing between auxiliary and working electrodes is then

$$\tau = \frac{\zeta Z}{1+\zeta} \tag{1}$$

The desired quantity is the component of this, ρ, which is due to the ohmic drop in the solution itself and allowance must be made for the impedance of the electrode-solution interface. Several means of doing this present themselves. If no species present in the solution reacts at the working electrode, the impedance of the electrode-solution interface is purely capacitive and ρ is simply the real component of τ. This can be made the case by performing the measurement with only supporting electrolyte present or by proper biasing of the working electrode using an external bias circuit. If a solution component is present which reacts reversibly enough at the working electrode, the interfacial impedance may be negligible. Finally, the interfacial impedance can be made negligibly small by operating the bridge at radio frequencies or by using platinized electrodes. The interfacial impedance for smooth electrodes is generally less than 1 ohm/cm^2 at frequencies above 50 kc.

Proposition 3.

It is proposed that the Taft substituent constant σ^* (1) could profitably be redefined in strict analogy with the definition of the Hammett substituent constants, on the basis of the dissociation constants of aliphatic carboxylic acids; that the reference substituent for which $\sigma^* = 0$ should be a long n-alkyl group; and that the substituent constant reported by Taft for the $-CH_2COOH$ group is incorrect due to neglect of a statistical factor.

Two schools of thought have developed about the Hammett substituent constants in recent years. One school, represented by Jaffe (2), prefers to interpret the σ constant as a constant chosen to represent best the effect of a given substituent on the course of a wide variety of reactions for which literature data are available. The other, represented by McDaniel and Brown (3), prefers the original definition of Hammett according to which σ represents the effect of the substituent on the ionization constant of benzoic acid. While the σ value conceived by Jaffe is perhaps a more fundamental constant than that originally defined by Hammett, the inexactness with which it can be calculated makes it unsuitable for studies such as those of Part III of the accompanying thesis in which deviations from the $\rho\sigma$ correlation are a source of information. The Taft constant can be discussed in the light of similar considerations.

Taft (1) found that the dissociation constants of most aliphatic carboxylic acids could be correlated well with the Taft constants as originally defined. Figure 1 illustrates the degree of correlation. A number of the σ^* values which Taft reports were actually calculated from dissociation constants rather than from his original definition. This close correlation between Taft σ^* and the pK_a for the correspondingly substituted aliphatic acid suggests that the value

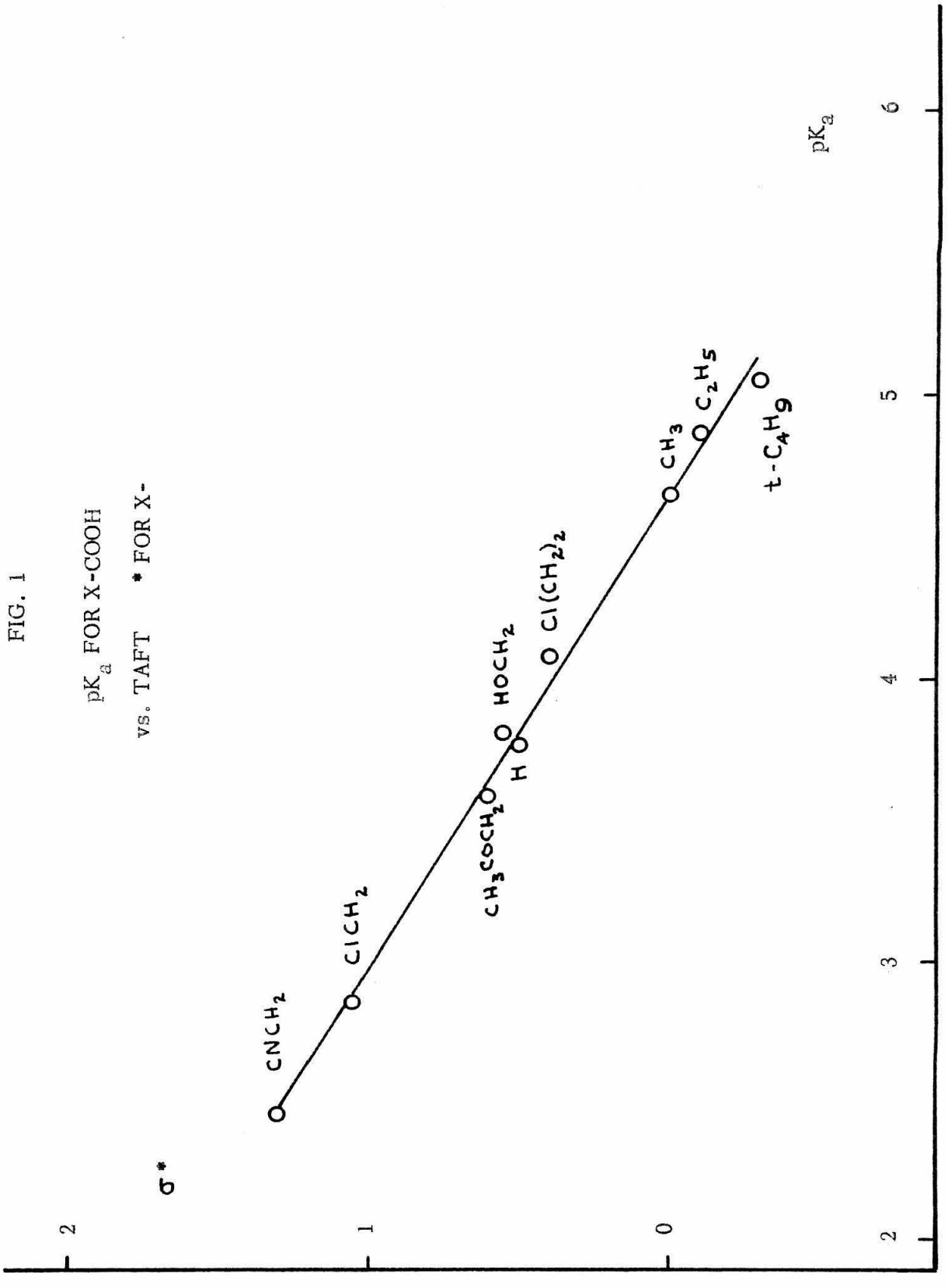

FIG. 1

pK$_a$ FOR X-COOH

VS. TAFT * FOR X-

of σ^* could be defined in terms of the measured pK_a. While the original definition involving comparison of the rates of acidic and basic ester hydrolysis is perhaps sounder theoretically, definition in terms of dissociation constants permits more accurate measurement and can lead therefore to more useful values of σ^*.

Taft reported that the dissociation constants of diethylacetic, diethylmalonic, and α,β -unsaturated acids are not correlated by the original σ^* constants. In the case of the unsaturated acids the deviation can be ascribed to resonance and it is probably best to calculate σ^* from the original definition. For the other two acids further study seems desirable.

The Taft constants tend to decrease by the factor 2.8 when a methylene group is interposed between the substituent and the reaction center (1). If this were strictly true the constant for a sufficiently long n-alkyl chain would be zero. Since this empirical property is a useful one, the choice of a sufficiently long n-alkyl group as the reference substituent for which $\sigma^* = 0$ is to be recommended. Taft chose the methyl group.

The value $\sigma^* = 1.05$ reported by Taft for the $-CH_2COOH$ group appears erroneous. It was calculated from the dissociation constant of malonic acid (1.40×10^{-3}), apparently omitting the statistical factor of 2 which arises from the fact that two equivalent acidic hydrogens are present. The correctly calculated value is 0.87.

Proposition 4

It is proposed that saturated lithium chlorate and lithium acetate solutions would be very interesting polarographic solvents.

The solubilities of lithium chlorate and lithium acetate in water are 314 g/100 ml (18° C) and 300 g/100 ml (15° C) respectively. Only 1.7 water molecules are present for each lithium ion in the saturated lithium chlorate solution and 2.5 water molecules per lithium ion in the saturated lithium acetate solution. One might expect these solutions to have properties similar to those of fused salts.

No diffuse double layer can be established in a medium of such high charge-carrier density; even in 1 M solution the Gouy-Chapman theory predicts a double layer thickness of only 3 A for a 1-1 electrolyte. Irregularities in polarographic waves attributable to the influence of the diffuse double layer (1), such as the minima in the chloroplatinite and peroxydisulfate waves, should be eliminated entirely.

Another interesting property of such solutions is the low chemical potential of the water present. It is likely that in some cases (such as the reduction of Ni^{+2}) (2) desolvation of an ion precedes its reaction at the electrode and such reactions should occur much more reversibly in saturated lithium chlorate solution.

The high viscosity and conductivity of these solutions will tend to suppress those polarographic maxima (3) which are attributable to electrokinetic phenomena.

All the effects described above would favor the use of these solutions in analytical work, where a reversible wave without maxima or minima is desired.

Propostion 5

It is proposed that the explanation given by Kuwana, Bublitz and Hoh (1) for the effect of pyridine on the oxidation potential of ferrocenecarboxylic acid in acetonitrile is incorrect, and another explanation is given.

According to Kuwana, Bublitz and Hoh (1) the chronopotentiometric quarter-wave potential for the oxidation of ferrocenecarboxylic acid in acetonitrile containing 0.2 M lithium perchlorate is +0.550 V vs. SCE. If 0.02 M pyridine is added, the quarter-wave potential becomes +0.430 V vs. SCE. They say:

> "The lower $E_{1/4}$ for the oxidation in the presence of pyridine may be explained on the basis of the acid (I) undergoing a chemical reaction
>
> $$\underset{\text{I}}{C_5H_5-Fe-C_5H_4-COOH} + C_5H_5N = \underset{\text{II}}{C_5H_5-Fe-C_5H_4-COO^-} + C_5H_5N^+-H \qquad (1)$$
>
> and the dissociated acid II undergoes the electrode reaction."

This explanation is refuted by the work of Kilpatrick and Kilpatrick (2). These authors published empirical correlations between acid strengths in acetonitrile and in water, from which the dissociation constant of ferrocenecarboxylic acid can be estimated as 10^{-10} and the dissociation constant for the pyridinium ion as 10^{0}. This rules out reaction 1 with a comfortable margin for error. Since reaction 1 involves formation of ions in a solvent which solvates them poorly, its equilibrium lies far to the left.

As the electrode reaction is reversible or nearly so, removal of the oxidation products can also lower the oxidation potential. The oxidized form of ferrocenecarboxylic acid will be a far stronger acid than ferrocenecarboxylic acid itself, and it is reasonable to expect the reaction

$$C_5H_5-Fe^+-C_5H_4-COOH + C_5H_5N = C_5H_5-Fe^+-C_5H_4-COO^- + C_5H_5N^+-H \qquad (2)$$

to occur, removing the oxidation product and lowering the oxidation potential.

Kuwana, Bublitz, and Hoh report that the value of $\frac{i_d\tau^{1/2}}{C}$ is unchanged upon adding pyridine. If reaction 1 is correct, this means that the diffusion coefficient of ferrocenecarboxylate ion must be within a few percent of that for ferrocenecarboxylic acid. (In order to account for the potential shift of 0.12 V reaction 1 would have to be nearly quantitative.) The structure of an organic molecule or ion has a pronounced effect on its diffusion coefficient, however, which is easily discernible in the chronopotentiometric data of Kuwana, Bublitz, and Hoh for substituted ferrocenes and in the data of Part II of this thesis for substituted acetates. It would be surprising indeed if the diffusion coefficient of ferrocenecarboxylate ion were not measureably different from that of ferrocenecarboxylic acid. According to the mechanism proposed here the species diffusing to the electrode surface both in the presence and absence of pyridine is ferrocenecarboxylic acid so that the same value of $\frac{i_d\tau^{1/2}}{C}$ is expected in both cases.

REFERENCES

Proposition 1

1. Delahay, P., New Instrumental Methods in Electrochemistry, Interscience Publishers, Inc., New York, (1954)

2. Oshida, J., Phys. Soc. Japan 15, (1960), 2288-2294.

3. Grahame, D. C., J. Electrochem. Soc. 99, (1952), 3700-3850.

4. Nyquist, H., Phys. Rev. 32, (1928), 110-113.

Proposition 2

1. Delahay, P. and Berzins, T., J. Am. Chem. Soc. 77, (1955), 6448-6453.

2. Anson, F. C. and Lingane, J. J., J. Am. Chem. Soc. 79, (1957), 1915-1020.

3. Lingane, J. J., J. Electroanal. Chem. 1, (1960), 379-395.

4. Anson, F. C., Anal. Chem. 33, (1961), 939-942.

Propostion 3

1. Taft, R. W., Jr., Steric Effects in Organic Chemistry, ed. by M. S. Newman, John Wiley and Sons, Inc., New York, (1956), pp. 556-675.

2. Jaffe, H. H., Chem. Revs. 53, (1953), 191-271.

3. McDaniel, D. H. and Brown, H. C., J. Org. Chem. 23, (1958), 420-427.

Proposition 4

1. Parsons, R., in Advances in Electrochemistry and Electrochemical Engineering, ed. by P. Delahay, Interscience Publishers, New York, (1961), Vol. I, pp. 1-64.

2. Gierst, L., in Transactions of the Symposium on Electrode Processes (Philadelphia, 1959), ed. by E. Yeager, John Wiley and Sons, Inc., New York, (1961), pp. 109-138.

3. Kolthoff, I. M. and Lingane, J. J., Polarography, Interscience Publishers, New York, (1952), Vol. I, pp. 169-179.

Proposition 5

1. Kuwana, T., Bublitz, D. and Hoh, G. L. K., J. Am. Chem. Soc. 82, (1960), 5811-5817.

2. Kilpatrick, M. Jr. and Kilpatrick, M., Chem. Revs. 13, (1953), 131-137.